Sustainable Forestry

EnPress Publisher

SF

1 2022
Volume 5
Issue 1
ISSN: 2578-2002

https://systems.enpress-publisher.com/index.php/SF

Editorial Board

Editors-in-Chief

Editorial Board Member

Volume 5 Issue 1 • 2022

Sustainable Forestry

EnPress Publisher

2022 | Volume 5 | Issue 1

Sustainable Forestry

https://systems.enpress-publisher.com/index.php/sf

Contents

Sustainable Forestry (2022) Volume 5 Issue 1
doi:10.24294/sf.v5i1.1615

ORIGINAL RESEARCH ARTICLE

Wave effect and shyness phenomenon in homogeneous forests of *Alnus acuminata*

Jesús Mao Estanislao Aguilar-Luna[1*], Noé Cabrera-Barbecho[1], Benjamín Barrios-Díaz[1], Juan Manuel Loeza-Corte[2]

[1] *Benemérita Universidad Autónoma de Puebla, Complejo Regional Norte, Tetela de Ocampo, Puebla, Mexico. E-mail: mao.aguilar@correo.buap.mx*

[2] *Universidad de la Cañada, Ingeniería en Agroindustrias, Teotitlán de Flores Magón, Oaxaca, Mexico.*

ABSTRACT

The wave effect and the shyness phenomenon in *Alnus acuminata* (Kunth) are crown parameters rarely studied, but important in the quality of the wood of standing trees, therefore, a morphometric modeling of the crowns of *Alnus acuminata* in homogeneous forests in the Sierra Norte de Puebla was carried out. In 20 rectangular sites of 1,000 m^2, the following were evaluated: total height (TA), normal diameter (ND), crown diameter (CD) and crown cover (CC). The Kruskal Wallis test was applied to data that did not meet the assumption of normality; for those that did, analysis of variance (ANOVA) was used, with Tukey mean comparison tests ($\alpha \leq 0.05$). The forest value index was 14.99, so its two-dimensional structure is normal based on DN, AT and CC. Its average slenderness index was 93.52, which makes the tree not very stable to mechanical damage. The life-space index was 38.92, which is high indicating that trees with low intraspecific competition developed better. At the canopy level, a pattern following an upward, oscillatory and constant wave effect was observed in groups of 10 trees. The shyness phenomenon showed an average crack opening of 27.39 cm between canopies, so this phenomenon is well defined for the species. It is concluded that in the crowns of *Alnus acuminata*, the wave effect is observed as a consequence of inequality in the acquisition of resources, and one way to minimize this inequality is through the phenomenon of botanical shyness.

Keywords: Aile; Homogeneous Forests; Forest Canopy; Slenderness; Living Space; Forest Value

ARTICLE INFO

Received: 11 January 2022
Accepted: 19 February 2022
Available online: 2 March 2022

1. Introduction

It is a pioneer species of fast growth and soft wood that, in the Sierra Norte de Puebla, is mainly used for the manufacture of spoons, handicrafts and musical instruments; but due to its extensive exploitation, the structure and composition of the forests where it is found has changed. The tops of the trees in close proximity form the canopy of a forest. This canopy plays an important role in the amount of photosynthetically active radiation it lets through to the understory[1]; it also influences branch mortality (autopoda), as well as stem size and shape[2].

Canopies, according to their social position within the stand or forest, can be: dominant, co-dominant, intermediate and suppressed[3]; their shape and dimension reflect a tree's vigor and interdimensional relationships (vertical space, competition, stability, vitality and productivity); as well as other little known (ripple effect and shyness phenomenon)[4], and architectural design, which delimits the spatial position of individuals within the neighborhood, to allow or not allow their coexistence within the canopy[5], which is reflected in the allometric relationships between different size attributes[6] and their adaptive significance with respect to their environment[7].

The ripple effect has been observed in some species such as: *Kochia scoparia* (L.) Schrad.[8]; *Pinus taeda* L.[9]; *Fagus sylvatica*, *Fraxinus excelsior*, *Carpinus betulus*, and *Tilia cordata*[10]; *Larix decidua* Mill.[11], because they extend their canopies beyond their assigned growing space; while others, yield part of that space to the dominant species, this effect can be described as a constant period wave[9,12].

Zeide[13], who is studying natural forests in the southern United States of America, observed that around a dominant tree there is usually a ring of suppressed trees; in turn, trees in the next concentric ring behave as dominant, and so on. The overall effect he described as a "density wave" that is damped with distance and propagates in all directions from the dominant trees. The spatial distribution of dominant and suppressed trees is not random, but can show great regularity; this has been demonstrated where the distribution of trees is very regular[14]. Therefore, the occurrence of spatial pattern in individual trees that are evenly spaced, can be analyzed by spectral analysis[15]. But, the development of spatial pattern not only occurs in trees that are evenly spaced, but every time they compete (for water, solar energy, nutrients and physical space), regardless of the planting regime[16,17].

Therefore, the phenomenon of shyness is observed in a certain group of trees (of the same species), which keep their crowns away from each other; to respect a distance that is known as "shyness crack". It is also known as "*canopyal sensagement*", "*crown shyness*" or "*shy canopies*". "Crown shyness was the term given by Australian biologist Maxwell Ralph Jacobs, he studied shyness patterns in eucalyptus and concluded that the shoots were sensitive to branch friction caused by wind, which caused clearings in the canopy[4].

In that sense, tree branches (of the same species) are damaged at the time of friction, so they choose to leave a space between the crowns and thus avoid tissue damage that could limit their growth[10]. In addition, trees have photoreceptors to benefit from a greater amount of available solar energy, thus leaving so-called "shy slots", which can measure between 10 cm and 50 cm, whose objective according to Binkley[16] is to avoid competition for solar energy, a limiting resource in the development and productivity of trees.

Whenever trees compete (inter and intra-specifically), they develop a hierarchy of dominance and suppression[18]. If competition for resources (water, solar energy, and nutrients) limits physical growing space, each individual tree should grow until its weight is proportional to the size of its immediate available space[14]. In the case of botanical shyness, this is only observed where there is intraspecific competition, even with dominance and suppression, since canopy opening acts as a defense and self-protection mechanism[16,19].

Some scientists believe that this phenomenon is due to an allelopathy (due to volatile organic compounds) that coordinate certain processes such as growth[20]. Another explanation is that it allows solar energy to better penetrate the forest and provide a selective evolutionary advantage against contagious diseases, as well as the spread of insects, whose larvae feed on leaves[18]. Thus, shy trees will be less likely to be infected by any disease or pest, despite being spatially in a dense distribution[4,21].

2. Objectives

The objective was to carry out a morphometric modeling of *Alnus acuminata* (Kunth) canopies (wave effect and shyness phenomenon) in homogeneous forests in the Sierra Norte de Puebla for which the following hypothesis was proposed: the behavior of *Alnus acuminata* canopies in intraspecific competition will allow a better understanding of the wave effect and shyness phenomenon as growth strategies within the vertical and horizontal gradient of the canopy, in different ecoregions of the Sierra Norte de Puebla.

3. Materials and methods

3.1 Study area

The Sierra Norte of Puebla is a region characterized by mountainous areas, is located northwest of the state, bordering Veracruz to the north, with

Hidalgo and Tlaxcala to the west. It is the second most inhabited region of the state of Puebla, due to the good natural and socio-cultural conditions. Its territorial extension is 5,903.5 km^2 and is made up of 65 municipalities[22].

Climates predominate: warm humid [A(C)f and A(C)m], warm sub-humid [A(C)w_0, A(C)w_1 and A(C)w_2], temperate humid [C(m) and C(f)], temperate sub-humid [C(w_0), C(w_1) and C(w_2)]. The mean annual temperature ranges from 12 °C to 18 °C, that of the coldest month ranges from 3 °C to 18 °C. The precipitation of the driest month is <40 mm; the percentage of winter precipitation, with respect to the annual precipitation, is <5 mm[23]. Frosts almost always occur with a frequency of 20 to 40 days per year; the maximum incidence of frosts is concentrated in the period from December to January.

The landscape is accompanied by fog in the highlands and humidity with rain throughout the year[22]. It is composed of mixed pine forests and pine-oak association, the outstanding species are: *Pinuspatula Schiede* ex Schltdl. Et Cham., *Pinus ayacahuite* Ehren., *Quercus rugosa* Née, *Abies religiosa* (Kunth) Schltd. and Cham., *Alnus acuminata* Kunth, *Cupressus lindleyi* Klotzsch ex Endl., *Taxodium mucronatum* Ten., and *Juniperus deppeana* Steud.[24].

3.2 Sampling sites

The sites were established in different ecoregions of the Sierra Norte de Puebla (**Table 1**). They were rectangular plots of 20 m × 50 m with a cluster sampling design. The criteria for delimiting the sites consisted of meeting the attributes homogeneity, density, purity, total height (AT), normal diameter (DN), crown diameter (DC) and crown cover (CC); in contemporary homogeneous forests without anthropic disturbance. A GPS (SOUTH S750-G2®) was used for positioning and location of the sites. ArcView software® was used to capture the location of the sites (**Figure 1**).

3.3 Tree sampling

The municipalities chosen for sampling cover 2,036 km^2, for this purpose a sampling intensity of 1% of the total municipalities was used[24]. The measurement was carried out in winter (form December 2017 to January and February 2018), because at this time the trees are leafless and their

Table 1. Geographical position of sampling sites in the Sierra Norte de Puebla

Site key	Municipality	Altitude	Latitude coordinates	Geographic longitude
1-Ch1	Chignahuapan 1	2,298	19°48′24″	98°01′47″
2-Ch2	Chignahuapan 2	2,300	19°48′30″	98°01′41″
3-Zt1	Zacatlán	2,071	19°54′38″	97°57′34″
4-Cu1	Cuautempan	1,499	19°54′53″	97°48′55″
5-Zo1	Tetela de Ocampo (Zontecomapan 1)	2,178	19°51′04″	97°43′59″
6-Zo2	Tetela de Ocampo (Zontecomapan 2)	2,164	19°51′05″	97°43′58″
7-Zo3	Tetela de Ocampo (Zontecomapan 3)	2,206	19°51′17″	97°44′12″
8-Zi1	Tetela de Ocampo (Zitlalcuautla 1)	2,287	19°44′18″	97°47′56″
9-Zi2	Tetela de Ocampo (Zitlalcuautla 2)	2,264	19°44′10″	97°47′58″
10-Zi3	Tetela de Ocampo (Zitlalcuautla 3)	2,319	19°44′03″	97°47′55″
11-Ca1	Tetela de Ocampo (Carreragco 1)	1,625	19°52′28″	97°40′46″
12-Ca2	Tetela de Ocampo (Carreragco 2)	1,696	19°52′25″	97°42′04″
13-Xo1	Xochitlán de Vicente Suárez 1	1,564	19°54′54″	97°38′27″
14-Xo2	Xochitlán de Vicente Suárez 2	1,544	19°54′57″	97°38′44″
15-Na1	Nauzontla	1,752	19°56′42″	97°35′26″
16-Zp1	Zacapoaxtla	2,104	19°53′01″	97°33′25″
17-Tq1	Tlatlauquitepec 1	2,069	19°49′30″	97°31′27″
18-Tq2	Tlatlauquitepec 2	2,158	19°49′20″	97°31′54″
19-Tq3	Tlatlauquitepec 3	2,122	19°49′17″	97°32′05″
20-Tq4	Tlatlauquitepec 4	2,111	19°49′05″	97°32′02″

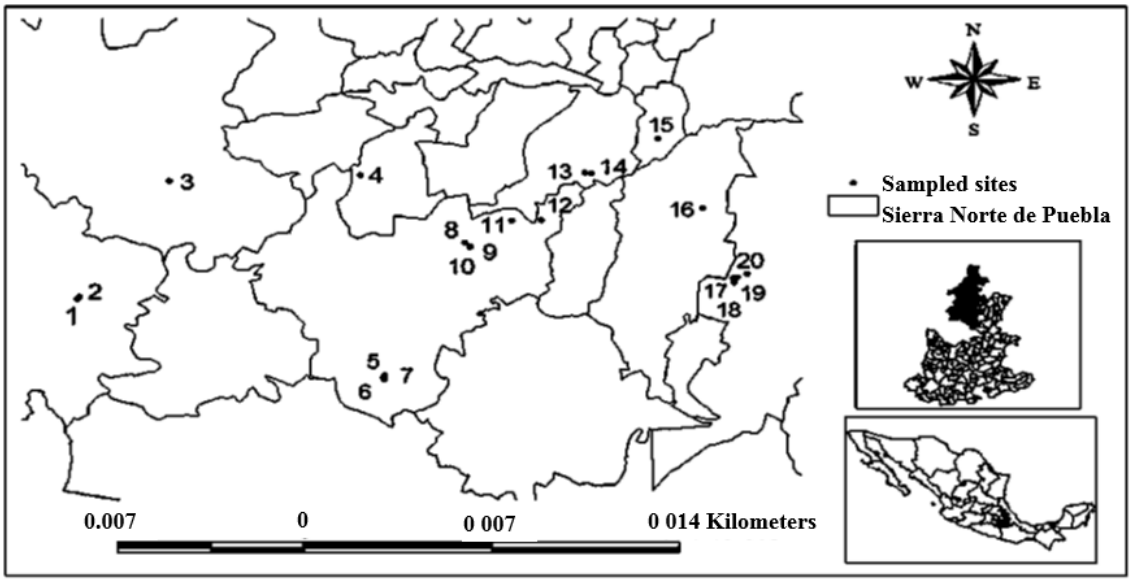

Figure 1. Positioning of sampled sites in the Sierra Norte de Puebla.

branching orders, the wave effect and the shyness phenomenon can be better observed. The classification of the trees, according to their DN was: brinzal (<5 cm); monte bravo (from 6 cm to 12 cm); vardascal (from 13 cm to 30 cm); alto latizal (from 31 cm to 50 cm) and fustal (>50 cm).

3.4 Response variables

Forest Value Index (FVI). It was determined by the sum of relative values of DN, AT and CC[25]. TA were measured with a Nikon Laser Forestry Pro® hypsometer/telemeter, crown measurements with a Stanley® tape measure, DN with a green laser forceps (800 mm Haglof®).

Slenderness index (SI). According to Serrada[17], it expresses the degree of stability of the forest stand, and was estimated with the following formula:

$$IE = \frac{AT}{DN} \times 100$$

In the equation: *AT* = total tree height; *DN* = normal diameter (1.30 m).

Living space index (LSI). It considers two basic indicators of the development or morphology of a tree, a consequence of the thickness in which it lives or has lived[17,27]. It was estimated with the following formula:

$$IEV = \frac{DC}{DN} \times 100$$

In the equation: *DC* = crown diameter; *DN* = normal diameter (1.30 m).

Wave effect (WE). Within each stand, we worked with groups of 10 trees (monopodic, without malformations, without the presence of pests or diseases and without fire or lightning damage). In close proximity, they were observed from above and below (the sampling system was selective and a non-destructive method was applied). Finally, the trend of the pattern that followed the wave effect and its possible changes or similarities with other sites were analyzed using the Multiple Optimization Model on Response Surfaces[27].

Shyness phenomenon (SP). To study the phenomenon of botanical shyness (crack opening), homogeneous stands of *Alnus acuminata* were analyzed, since in heterogeneous stands the species tend to intertwine their branches, making observations difficult due to interspecific competition. The crack opening between canopies was captured using aerial images from the understory with a Nikon B500® digital camera and from the canopy with a DJI Phantom 4 Pro® drone; a graduated rope between canopy and canopy was used as a reference measurement. Aperture sizes were defined as follows: N_0: absent crack opening; N_1: from 0 cm to 10 cm; N_2: from 11 cm to 30 cm; N_3: from 31 cm to 50 cm; N_4: >51 cm opening. To know the aperture sizes, we worked with Image Tool Portable software®, through which we transferred the images taken (which included an aperture with known dis-

tance) and proceeded to perform the conversion from pixels to centimeters.

3.5 Statistical analysis

The Kruskal Wallis test[27] was applied to data that did not meet the assumption of normality. For data that met the assumption of normality and homogeneity, analysis of variance (ANOVA) was used, with mean comparison tests by Tukey's method ($\alpha \leq 0.05$), independent for each sampling site. We worked with Minitab® 18 software[28].

4. Results

4.1 Forest value, slenderness and living space

Vertically, the forest structure of *Alnus acuminata* was represented by five developmental stages: brinzal, monte bravo, vardascal, alto latizal and fustal (**Figure 2(a)**). At no site were all five developmental stages observed at the same time; however, 60% of the population diameters had a DN >31 cm (forests with a high commercial value); while seedlings were scarce and only represented 2.32% of the total population (low regeneration per tall forest). Trees with DN >31 cm were found in sites: 2-Ch2, 3-Zt1, 5-Zo1, 11-Ca1 and 14-Xo2; while in the rest of the sites the predominant DN were from 6 cm to 30 cm, which represented 37.75% of the studied population. The DN >50 cm only represented 4.57% of the study population (2,474 trees).

The FVI was higher in site 2-Ch2, an ecoregion with cloud forests characterized by having trees with larger DN, TA and CC than in the other sites (**Table 2**). While the site with the lowest value was: 9-Zi2 (10.49), located in riparian zones, although it did not have the lowest DN, AT and CC in its individuals; but it did have a high natural regeneration (up to 327 trees-ha^{-1}) with a predominance in the sapling stage.

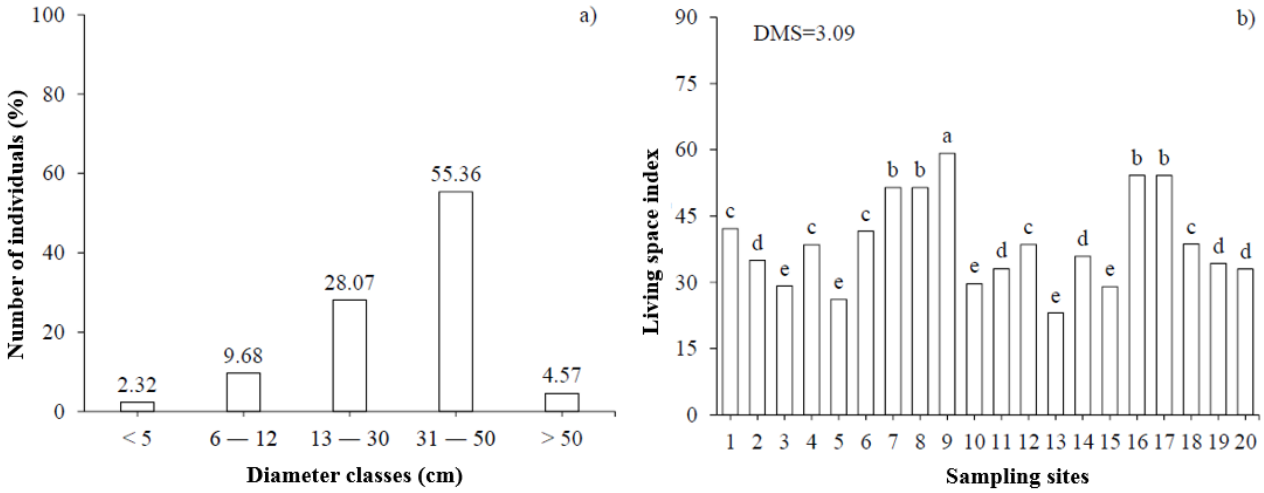

Figure 2. Developmental stages (n = 2,474 trees) (a), and IEV (b), in 20 sites sampled for *Alnus acuminata* in the Sierra Norte de Puebla.

Table 2. Forest value and height of *Alnus acuminata* in the Sierra Norte de Puebla

Site	Relative diameter (%)	Relative height (%)	Relative coverage (%)	Index of forest value	Leanness index
1-Ch1	4.42	4.05	4.26	12.73	81.35
2-Ch2	6.00	6.32	9.74	22.06	90.66
3-Zt1	6.84	5.38	9.15	21.37	72.74
4-Cu1	4.29	4.92	7.57	16.79	105.40
5-Zo1	6.02	5.72	3.60	15.33	82.61
6-Zo2	5.11	5.14	2.43	12.68	87.24
7-Zo3	3.69	5.64	4.34	13.67	141.11
8-Zi1	3.42	5.86	5.03	14.30	153.92
9-Zi2	3.93	3.90	2.66	10.49	86.85
10-Zi3	5.24	4.48	5.36	15.09	79.33
11-Ca1	6.78	5.05	7.71	19.54	63.75

Table 2. (*Continued*)

Site	Relative diameter (%)	Relative height (%)	Relative coverage (%)	Index of forest value	Leanness index
12-Ca2	3.30	3.83	5.82	12.95	100.09
13-Xo1	5.82	5.53	4.62	15.97	84.72
14-Xo2	6.59	5.65	2.71	14.96	78.30
15-Na1	5.73	5.17	3.81	14.70	83.05
16-Zp1	3.16	4.80	3.93	11.88	135.50
17-Tq1	4.42	5.28	4.11	13.80	107.91
18-Tq2	4.65	4.81	4.12	13.57	88.62
19-Tq3	5.53	4.23	3.26	13.02	70.70
20-Tq4	5.08	4.25	5.76	15.09	76.55
	100	100	100	300	$\mu = 93.52$

The majority of the sites had a tree stand that was not very stable to mechanical damage, the presence of strong winds or hurricane, since the mean EI between populations are statistically different ($\alpha \leq 0.05$); only sites 3-Zt1, 10-Zi3, 11-Ca1, 14-Xo2, 19-Tq3 and 20-Tq4, had normal EI (from 63.75 to 79.33).

The average EI for natural forests of *Alnus acuminata* in the Sierra Norte de Puebla was 93.52 (off-normal and close to critical); for each cm of tree diameter increase, there was an average increase of 93.52 cm in TA. The DN ranged from 11.65 cm to 25.23 cm on average for all sites, while the TA ranged from 12.43 m to 20.14 m (**Figure 3**).

It was at site 9-Zi2 (Tetela de Ocampo locality Zitlalcuautla) where *Alnus acuminata* trees developed with little competition (IEV = 59.17); while sites 3, 5, 10, 13 and 15 were those with the lowest IEV, that is, the sites with the highest inter- and intraspecific competition; to have an average of 38.92 in the Sierra Norte de Puebla (**Figure 2(b)**).

4.2 Wave effect and shyness phenomenon

The wave effect followed an oscillatory trend where one was dominant, four co-dominant, three intermediate and two suppressed, which is a generality for homogeneous *Alnus acuminata* forests in the Sierra Norte de Puebla (**Figure 4**).

Of 2,474 trees sampled, 247 were dominant, their large crowns were above the general level of the forest canopy, they received full vertical and partially lateral solar energy; 990 were codominant, their medium crowns were part of the general level of the canopy, they received full vertical and little lateral solar energy; 742 were intermediate, their small canopies extended below the canopy formed by the co-dominants, absorbed little solar energy vertically and none laterally; 495 were suppressed, their small canopies were located completely below the general canopy level, receiving no solar energy.

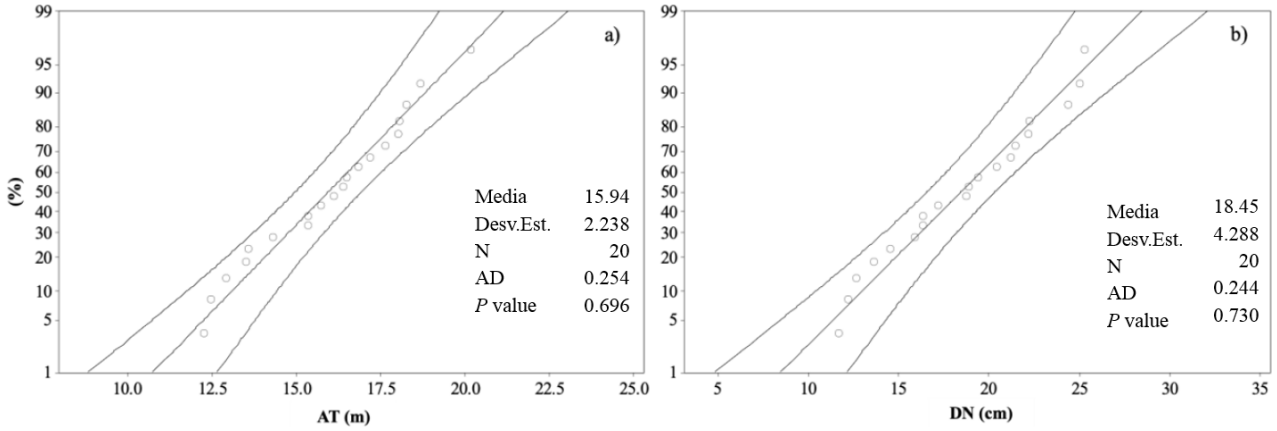

Figure 3. Normal probability with a 95% confidence index, for AT (a) and for DN (b), in trees of *Alnus acuminata* in the Sierra Norte de Puebla.

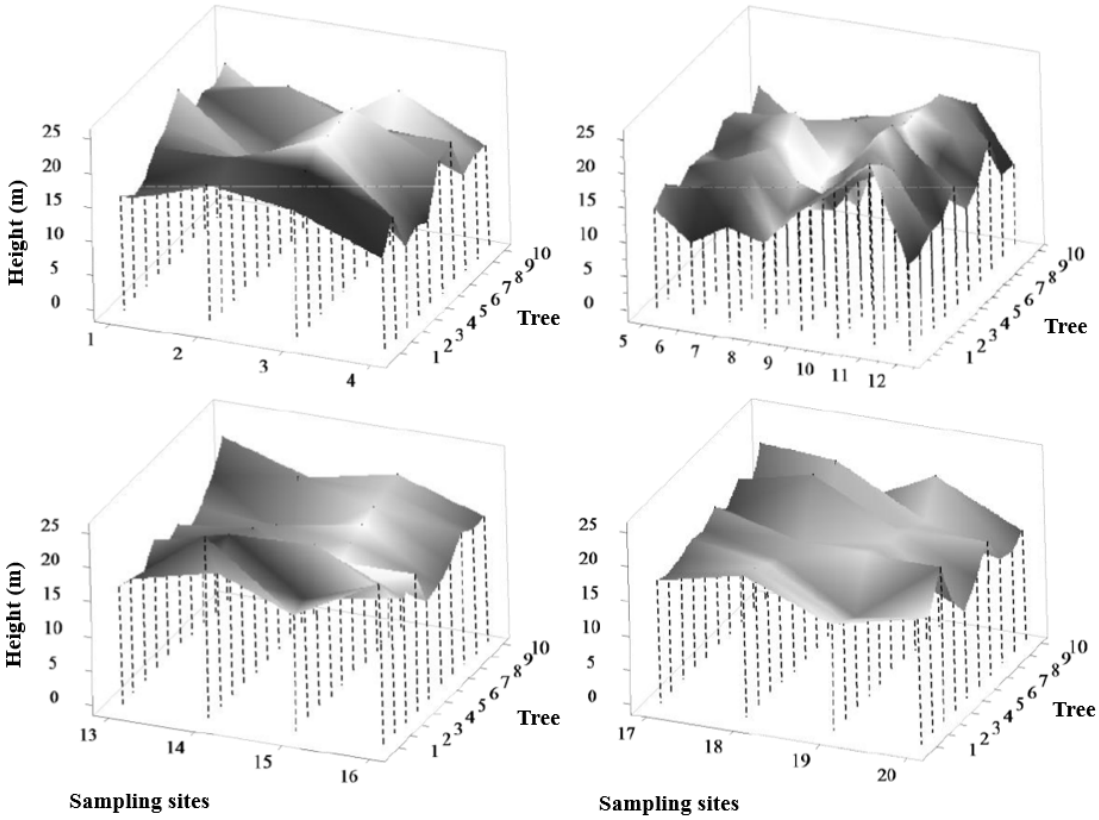

Figure 4. Response surface wave effect expressed for *Alnus acuminata* at sampling sites in the Sierra Norte de Puebla. From 1 to 4: Chignahuapan, Zacatlán and Cuautempan; from 5 to 12: Tetela de Ocampo; from 13 to 16: Xochitlán de Vicente Suárez, Nauzontla and Zacapoaxtla; from 17 to 20: Tlatlauquitepec.

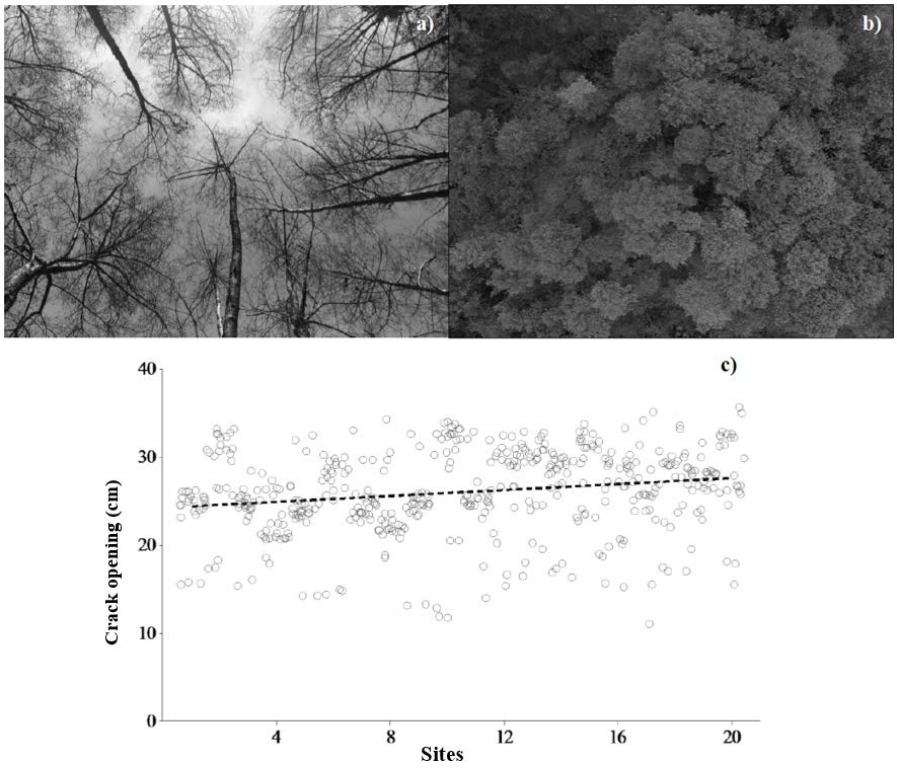

Figure 5. Crack opening (shyness phenomenon) in *Alnus acuminata* canopies in the Sierra Norte de Puebla; (**a**): canopies without autumn-winter foliage; (**b**): canopies with spring-summer foliage; (**c**): dispersion of opening sizes in canopies (n = 2,474).

The shyness phenomenon can be best observed at the time of the year when the trees are leafless (being a deciduous species) (**Figure 5(a)**); although the crack could be observed even with

well-developed foliage and independently of the canopy level, when including dominant, co-dominant, intermediate and suppressed trees (**Figure 5(b)**).

In 25% of the sites there was a crack opening >30 cm (the widest observed), in the sites: 2-Ch2, 10-Zi3, 13-Xo1, 15-Na1 and 20-Tq4. The other 75% of the sites had an opening between 20 cm and 30 cm, in the sites: 1- Ch1, 3-Zt1, 4-Cu1, 5-Zo1, 6-Zo2, 7-Zo3, 8-Zi1, 9-Zi2, 11- Ca1, 12-Ca2, 14-Xo2, 16-Zp1, 17-Tq1, 18-Tq2 and 19-Tq3. Throughout the Sierra Norte de Puebla, there was no broad distinction between sites for greater or lesser crack opening in *Alnus acuminata* canopies; having an average of 27.39 cm of observable opening between one canopy and another (**Figure 5(c)**).

5. Discussion

5.1 Forest value, slenderness and living space

The highest forest value for *Alnus acuminata* was presented in those sites of the Sierra Norte de Puebla, where there are cloud forests or mountain mesophyll forest, characterized by having a high concentration of fog especially at the canopy level. Although in all sites, a two- and three-dimensional spatial pattern was shown as a result of intraspecific competition, patterns that are repeated at the canopy level occur[8,9].

At the understory level, out of a sample of 2,474 trees, there were 495 suppressed trees, suggesting that young plants can adapt to a shaded environment; however, this species grows best in full sun[24]. The crown growth of *Alnus acuminata* is narrow, irregular and open, in individuals with less competition for physical space and solar energy (e.g. those located at the edges), although it can develop from the base; however, in homogeneous forests the trees reach a higher TA, with a proportion of stem free of branches and knots due to natural pruning[29].

Growth in DN and AT can increase only with an opening of the canopy, due to a higher photosynthetic rate[16]. Although this species can establish in gallery forests (along riverbanks), it is not a hydrophytic species, but rather a fast-growing, heliophilous, soft-wooded species that needs a lot of water for its development[29]. In the gallery forests of the Xaltatempa River, it can be found associated with *Ligustrum japonicum* Thunb., *Parathesis serrulata* (Sw.) Mez., *P. Patula*, *Platanus mexicana* Moric. and *Q. Rugpsa*, and have a high forest value, only inferior to *P. Mexicana*[30].

The vertical structure of *Alnus acuminata* is of great importance for its development in the homogeneous forests of the Sierra Norte de Puebla, where tall trees with relatively thin trunks develop (IE = 93.52); however, this IE places them outside the normal and close to the critical, since normal values are close to 70 and critical values are higher than 100[17]. In a comparative study with *Eucalyptus urophylla* S.T. Blake, in the warm-humid climate of Huimanguillo, Mexico, IE of 114 $cm \cdot cm^{-1}$, 118 $cm \cdot cm^{-1}$ and 122 $cm \cdot cm^{-1}$ were obtained[31]; similar results were obtained with *Eucalyptus nitens* H. Deane & Maiden, with an IE = 124[32]; with *Hieronyma alchorneoides* L., with an IE= 111 and with *Terminalia amazonia* (J.F. Gmel.) Exell, with an IE = 106[27].

Thus, by having a high slenderness value, the trees are not very stable to mechanical damage[33], it is assumed that they are thin and that care should be taken when applying strong thinning intensities[27,32]. Despite this, the average height (AT = 15.94 m) and average diameter (DN = 18.44 cm), suggest a low ratio (0.86), which is associated with conical trees, i.e., more slender[31]; which may be more resistant to strong winds, snow and hurricanes[34]. The presence of basal reiterations especially in suppressed trees is a direct consequence of a high population density (1,237 $trees \cdot ha^{-1}$) due to competition for solar energy and nutrients; since a deficit of solar energy over the canopy can produce a decrease in its yield[10].

The IEV expresses how many times the DC was greater than the DN, in relation to the occupation that the latter needs to develop without competition[12], this index grew as the tree thickens in diameter[27,33]. In homogeneous forests with *Alnus acuminata* in the Sierra Norte de Puebla, intraspecific competition was common, as variants in growth with dense-dependent effects were observed at the sites, subject to greater space for individual

development[35].

The absolute size of *Alnus acuminata* was a measure of its productive and reproductive potential, but this potential only manifests itself if it can prevent other adjacent trees from overlapping and shading it, which is why, for each group of 10 trees, only one was dominant. Minor AT, DC and CC in adjacent trees, can be more evident with time, and probably decisive in the final result of dominance and suppression[16]; even if the trees have almost the same height or with a difference of a few millimeters, this is decisive because when one leaf overlaps another, it photosynthesizes more[36]; which confers competitive advantages, since species with individuals taller than their neighbors can intercept more light[5].

These small differences in TA favored the formation of patterns in spaced gradients, which allowed the transmission of competition effects (inequality in resource acquisition) to occur as trees along the gradient began to interfere with their neighbors at different times. According to Ibáñez-Moreno *et al*.[12] from the competition among trees, a negative correlation can be predicted in the growth of neighboring trees, and an increase in the size of that tree with increasing physical space available.

5.2 Wave effect and shyness phenomenon

To determine the pattern of the wave effect in *Alnus acuminata*, it was useful to classify the canopy, which also served as a parameter to judge the vigor and maturity of the tree or the site, which may serve in the future to prescribe some cuts of different types (release, thinning, regeneration, etc.). The pattern that followed the wave effect in this species had an upward, oscillatory and constant movement in its canopy, which was presented in groups of 10 trees where only one was dominant; similar to the study of Liu *et al*.[11], who also stated that the diameter and propagation distance of the wave, can influence the propagation patterns.

This wave manifests a competition effect in which the degree of interference experienced by each individual depends on the degree of interference experienced by its neighbors[12]. Because trees cannot escape the interference effects of their neighbors by changing their position, the movement is restricted to the plasticity of the growth of the population of meristems present in different parts of the tree[8].

Another theory, advanced by Hallé[37], suggests that this phenomenon has genetic origins and that the configuration of the tree crowns is not random, but the product of a specific development program controlled by genes. The sites studied were incoetaneous due to the selective use of *Alnus acuminata* by local inhabitants for fuel and for making spoons and handicrafts, which gives rise to a regeneration of coppice by stands with different ages (between 10 years and 40 years). Natural (sexual) regeneration was very low (<5%), however, reiterations have maintained the vitality of the forest by producing asymmetric competition, which occurs whenever a branch or tree dies and leaves a physical space in the canopy that existing neighbors or newly recruited plants can invade, or whenever an individual acquires an advantage (dominance) over its neighbors[16].

However, the formation of hierarchies and spatial patterns in natural populations is uneven, because trees located at the edges, on the borders or without adjacent competition in any of the four cardinal points, have more space to develop and behave as dominant over their immediate neighbors, since this dominance frees neighbors from competition, which produces a periodic distribution of dominant and suppressed trees[36].

The phenomenon of shyness in *Alnus acuminata* was observed in all the sites sampled in the Sierra Norte de Puebla (with an average crack opening of 27.39 cm between crowns), which may be due to controlled endogenous development (in mature trees) to prevent the crowns from joining. With respect to this behavior, observable only in some tree species, several authors have expressed their opinion: Rudnicki *et al*.[19] demonstrated that this phenomenon in *Pinus contorta* Douglas was the result of crown abrasion caused by winds, since the crowns can collide hundreds of times per hour.

Smith and Long[38], studying age-related decline in forests, speculated that botanical shyness is

due to wind-induced canopy collisions that limit leaf area. Delagrange *et al*.[2], affirmed that, in temperate forests, the empty space around tree crowns (botanical shyness) is due to a disconnection of the crown due to internal factors; although there are other factors such as IE, site quality or spatial distribution of trees, which can also influence the presence of the phenomenon[10,17].

Shyness tends to increase in the best sites, because canopy size is related to site fertility[39,40]; which was observable in temperate forests with *Alnus acuminata*. The approach of Cabrelli *et al*.[1], through hemispheric photographs of the canopy, provides important functional relationships between wave effect and crack opening size; also, tree crowns subjected to wind influence and the resulting collisions can lead to branch breakage and foliage abrasion[19].

However, Smith and Long[38] concluded that the abrasion only represents a certain amount of foliage, proportional to that which begins to decline with crown closure. According to Hajek *et al*.[10] this phenomenon has also been observed (with variable crack openings) in *F. Sylvatica*, *F. Excelsior*, *C. Betulus* and *T. Cordata*; which has important implications for modeling forest dynamics and management.

6. Conclusions

In the homogeneous forests of the Sierra Norte de Puebla, *Alnus acuminata* is found at a high population density, with 1,237 tree·ha^{-1}, vertically represented by five developmental stages. Its average forest value was 14.99 and this was higher in ecoregions with cloud forests. The average slenderness index was 93.52, which makes the trees not very stable to mechanical damage by winds, hurricanes or snow; although their marked conicity protects them. The life space index was 38.92, which means that the trees develop better with little competition, but can sustain a high-density occupancy. In the canopy, an upward, oscillatory and constant wave effect pattern was observed, where for every 10 trees there can be one dominant, four co-dominant, three intermediate and two suppressed. The phenomenon of shyness could be observed, especially when the trees have no foliage, and was manifested with a crack of 27.39 cm on average, which prevents the crowns from joining each other and function as a growth strategy.

Conflict of interest

The authors declare that they have no conflict of interest.

References

1. Cabrelli D, Rebottaro S, Effron D. Characterization of forest canopy and light micro-environment in stands with management different, using hemispherical photography. Quebracho (Santiago del Estero) 2006; (13): 17–25.
2. Delagrange S, Messier C, Lechowicz MJ, *et al*. Physiological, morphological and allocational plasticity in understory deciduous trees: Importance of plant size and light availability. Tree Physiology 2004; 24(7): 775–784.
3. Tourn GM, Barthélémy D, Grosfeld J. Una aproximación a la arquitectura vegetal: Conceptos, objetivos y metodología (Spanish) [An approach to plant architecture: Concepts, objectives and methodology]. Boletín de la Sociedad Argentina de Botánica 1999; 34(1–2): 85–99.
4. Jacobs MR. Growth habits of the eucalypts. Australia: Forestry and Timber Bureau, Department of the Interior; 1995.
5. Báez-Hernández A, Herrera-Meza G, Vázquez-Torres M, *et al*. Allometric relationships of 19 mountain tropical rain forest tree species. Botanical Sciences 2016; 94(2): 209–220. doi: 10.17129/botsci.252.
6. Poorter L, McDonald I, Alarcón A, *et al*. The importance of wood traits and hydraulic conductance for the performance and life history strategies of 42 rainforest tree species. New Phytologist 2010; 185(2): 481–492. doi: 10.1111/j.1469-8137.2009.03092.x
7. Frankino WA, Zwaan BJ, Stern DL, *et al*. Natural selection and developmental constraints in the evolution of allometries. Science 2005; 307(5710): 718–720. doi: 10.1126/science.1105409.
8. Franco M, Harper JL. Competition and the formation of spatial pattern in spacing gradients: An example using Kochia scoparia. The Journal of Ecology 1988; 76(4): 959–974.
9. Zeide B. Fractal analysis of foliage distribution in loblolly pine crowns. Canadian Journal of Forest Research 2011; 28(1): 106–114. doi: 10.1139/cjfr-28-1-106.
10. Hajek P, Seidel D, Leuschner C. Mechanical abrasion, and not competition for light, is the dominant canopy interaction in a temperate mixed forest. Forest Ecology and Management 2015; 348: 108–

116. doi: 10.1016/j.foreco.2015.03.019.
11. Liu FL, Jiang F, Wang XP, *et al*. Stress wave propagation patterns in larch standing trees. Journal of Nanjing Forestry University (Natural Sciences Edition) 2017; 41(3): 133–139.
12. Ibáñez Moreno B, Ávila Castuera JM, Gómez Aparicio L, *et al*. Dinámicas de vecindad y regeneración del bosque (Spanish) [Neighborhood dynamics and forest regeneration]. Almoraima 2012; 43; 87–110.
13. Zeide B. Analysis of growth equations. Forest Science 1993; 39(3): 594–616. doi: 10.1093/forestscience/39.3.594.
14. Weiner J, Thomas SC. The nature of tree growth and the "age-related decline in forest productivity". Oikos 2001; 94(2): 374–376
15. Cao H, Chen Y, Tian Y, *et al*. Field investigation into wave attenuation in the mangrove environment of the South China Sea coast. Journal of Coastal Research 2016; 32(6): 1417–1427. doi: 10.2112⁄JCOASTRES-D-15-00124.1.
16. Binkley D. A hypothesis about the interaction of tree dominance and stand production through stand development. Forest Ecology and Management 2004; 190(2–3): 265–271. doi: 10.1016/j.foreco.2003.10.018.
17. Serrada HR. Apuntes de selvicultura (Spanish) [Forestry notes]. Madrid, España: Universidad Politécnica de Madrid. E.U.I. Técnica Forestal; 2008.
18. Farrior CE, Bohlman SA, Hubbell S, *et al*. Dominance of the suppressed: Power-law size structure in tropical forests. Science 2016; 351(6269): 155–157. doi: 10.1126/science.aad0592
19. Rudnicki M, Lieffers VJ, Silins U. Stand structure governs the crown collisions of lodgepole pine. Canadian Journal of Forest Research 2003; 33(7): 1238–1244. doi: 10.1139/x03-055.
20. Coley PD. Effects of plant growth rate and leaf lifetime on the amount and type of anti-herbivore defense. Oecologia 1988; 74(4): 531–536.
21. Goudie JW, Polsson KR, Ott PK. An empirical model of crown shyness for lodgepole pine (*Pinus contorta* var. *latifolia* [Engl.] Critch.) in British Columbia. Forest Ecology and Management 2009; 257(1): 321–331. doi: 10.1016/j.foreco.2008.09.005.
22. INEGI (Instituto Nacional de Estadística y Geografía). Perspectiva estadística puebla (Spanish) [Puebla statistical perspective]. Puebla, México: INEGI; 2014.
23. García E. Modificaciones al sistema de clasificación climática de Köppen (Spanish) [Modifications to the climate classification system of Köppen] [Internet]. Universidad Nacional Autónoma de México; 2004. Available from: http://www.publicaciones.igg.unam.mx/index.php/ig/catalog/view/83/82/251-1.
24. Comisión Nacional para el Conocimiento y Uso de la Biodiversidad [Conabio]. La Biodiversidad en puebla: Estudio de estado (Spanish) [Biodiversity in Puebla: State study]. México. Puebla, Mexico: Conabio, Gobierno del estado de Puebla, Benemérita Universidad Autónoma de Puebla; 2011.
25. Justavino FC, Hernández JIV, Alcalá VMC, *et al*. Estructura forestal de un bosque de mangles en el noreste del estado de Tabasco, México (Spanish) [Forest structure of a mangrove forest in the northeast of the state of Tabasco, Mexico]. Revista Mexicana de Ciencias Forestales 2001; 26(90): 73–102.
26. Arias-Aguilar DA. Morfometría del árbol en plantaciones forestales tropicales (Spanish) [Tree morphometry in tropical forest plantations]. Revista Forestal Mesoamericana Kurú 2005; 2(5): 19–32.
27. Montgomery DC. Dzsenoy analtszs of experiments (Spanish) [Design and analysis of experiments]. 2nd ed. Mexico: Limusa Wiley; 2006.
28. Minitab. Software para estadísticas de Minitab, Versión 18 en español para Windows (Spanish) [Minitab Statistical Software, Version 18 for Windows]. State College, Pennsylvania; 2018. Available from: https://www.minitab.com/es-mx/products/minitab//.
29. CATIE (Centro Agronómico Tropical de Investigación y Enseñanza). Jaúl: *Alnus acuminata* spp. Arguta (Schlechtendal) Furlow, multiple use tree species in central America. Turrialba, Costa Rica: CATIE; 1995.
30. Aguilar-Luna JME, Loeza-Corte JM, García-Villanueva E, *et al*. Arboreal vegetation structure and diversity in the gallery forest of the Xaltatempa river, Puebla, Mexico. Madera y Bosques 2018; 24(3): e2431616. doi: 10.21829⁄myb.2018.2431616.
31. Hernández-Ramos J, Santos-Posadas HM, Valdéz-Lazalde JR, *et al*. Estimación del volumen comercial en plantaciones de Eucalyptus urophylla con modelos de volumen total y de razón (Spanish) [Estimation of commercial volume in Eucalyptus urophylla plantations with total volume and ratio models]. Agrociencia 2017; 51(5): 561–580.
32. Díaz Bravo S, Espinosa M, Valenzuela L, *et al*. Effect of thinning on growth and some properties of wood of Eucalyptus nitens in a plantation of 15 years old. Maderas. Ciencia y tecnología 2012; 14(3): 373–388. doi: 10.4067/S0718-221X2012002005000009.
33. Nájera-Luna JA, Hernández-Hernández E. Morphometric relationships of a contemporary forest from the region of El Salto, Durango. Ra Ximhai 2008; 4(1): 69–81.
34. Wilson JS, Oliver CD. Stability and density management in Douglas-fir plantations. Canadian Journal of Forest Research 2000; 30(6): 910–920.
35. Vacchiano G, Derose RJ, Shaw JD, *et al*. A density management diagram for Norway spruce in the temperate European montane region. European Journal of Forest Research 2013; 132(3): 535–549.
36. Renshaw E, Ford ED. The description of spatial pattern using two-dimensional spectral analysis.

Vegetatio 1984; 56(2): 75–85.
37. Hallé F. Arquitectura de los árboles (Spanish) [Architecture of the trees]. Boletín de la Sociedad Argentina de Botánica 2010; 45(3–4): 405–418.
38. Smith FW, Long JN. Age-related decline in forest growth: an emergent property. Forest Ecology and Management 2001; 144(1–3): 175–181. doi: 10.1016/S0378-1127(00)00369-8.
39. Gillespie TJ, Duan RX. A comparison of cylindrical and flat plate sensors for surface wetness duration. Agricultural and Forest Meteorology 1987; 40(1): 61–70. doi: 10.1016/0168-1923(87)90055-4.
40. Amponsah IG, Comeau PG, Brockley RP, *et al*. Effects of repeated fertilization on needle longevity, foliar nutrition, effective leaf area index, and growth characteristics of lodgepole pine in interior British Columbia, Canada. Canadian Journal of Forest Research 2005; 35(2): 440–451. doi: 10.1139⁄x04-200.

Sustainable Forestry (2022) Volume 5 Issue 1
doi:10.24294/sf.v5i1.1616

ORIGINAL RESEARCH ARTICLE

Effects of forest fire disturbance on carbon density of eucalyptus forest ecosystem in Guangdong Province

Haiqing Hu[1], Sisheng Luo[1], Bizhen Luo[1*], Shujing Wei[2], Zhenshi Wang[2]

[1] Forestry Institute, Northeast Forestry University, Harbin 150040, China. E-mail: luobizhen8@163.com

[2] Guangdong Provincial Key Laboratory of forest cultivation, protection and utilization, Guangdong Academy of Forestry Sciences, Guangzhou 510520, China.

ABSTRACT

Forest fire, as a discontinuous ecological factor of forest, causes the changes of carbon storage and carbon distribution in forest ecosystem, and affects the process of forest succession and national carbon capacity. Taking the burned land with different forest fire interference intensity as the research object, using the comparison method of adjacent sample plots, and taking the combination of field investigation sampling and indoor test analysis as the main means, this paper studies the influence of different forest fire interference intensity on the carbon pool of forest ecosystem and the change and spatial distribution pattern of ecosystem carbon density, and discusses the influence mechanism of forest fire interference on ecosystem carbon density and distribution pattern. The results showed that forest fire disturbance reduced the carbon density of vegetation ($P < 0.05$). The carbon density of vegetation in the light, moderate and high forest fire disturbance sample plots were 67.88, 35.68 and 15.50 t·hm^{-2}, which decreased by 15.86%, 55.78% and 80.79% respectively compared with the control group. In the light, moderate and high forest fire disturbance sample plots, the carbon density of litter was 1.43, 0.94 and 0.81 t·hm^{-2}, which decreased by 28.14%, 52.76% and 59.30% respectively compared with the control group. The soil organic carbon density of the sample plots with different forest fire disturbance intensity is lower than that of the control group, and the reduction degree gradually decreases with the increase of soil profile depth. The soil organic carbon density of the sample plots with light, moderate and high forest fire disturbance is 103.30, 84.33 and 70.04 t·hm^{-2} respectively, which is 11.670%, 27.899% and 40.11% lower than that of the control group respectively; the carbon density of forest ecosystem was 172.61, 120.95 and 86.35 t·hm^{-2} after light, moderate and high forest fire disturbance, which decreased by 13.53%, 39.41% and 56.74% respectively compared with the control group; forest fire disturbance reduced the carbon density of eucalyptus forest, which showed a law of carbon density decreasing with the increase of forest fire disturbance intensity. Compared with the control group, the effect of light forest fire disturbance intensity on the carbon density of eucalyptus forest was not significant ($P > 0.05$), while the effect of moderate and high forest fire disturbance intensity on the carbon density of eucalyptus forest was significant ($P < 0.05$).

Keywords: Forest Fire Disturbance; Forest Ecosystem; Vegetation Carbon Pool; Regulated Litter Carbon Pool; Soil Organic Carbon Pool

ARTICLE INFO

Received: 22 January 2022
Accepted: 9 March 2022
Available online: 17 March 2022

1. Introduction

Forest carbon pools play an important role in the global carbon cycle[1], of which vegetation carbon pool is an indispensable part. Vegetation carbon pool is an important source of carbon elements for other carbon pools, and it is one of the symbols of carbon sequestration capacity, which plays an important role in carbon sink effect. As a hub connecting the vegetation carbon pool and soil organic carbon pool, the fallout carbon pool plays an important role in the ecosystem carbon

cycle. Soil organic carbon pool plays a role of source, sink and hub in the global carbon cycle, and has an important carbon sink effect. Forest fire disturbance significantly reduces the coverage of canopy by consuming forest biomass, changes the structure and function of terrestrial ecosystem, and then affects the redistribution of its nutrient cycle[2,3], promoting the composition of forest vegetation and national carbon capacity. Therefore, quantifying the ecological process of forest fire disturbance on forest ecosystem carbon sink is an important basis for balancing ecosystem carbon budget. Further understanding the carbon exchange mechanism between terrestrial ecosystem and atmosphere will help forest fire managers predict the ecosystem recovery response after fire and provide a scientific basis.

Forest fire disturbance can release nutrients into the soil through the immediate and high-concentration CO_2 emissions generated by biomass combustion[4], which can directly affect the soil carbon cycle, and indirectly affect the carbon balance and carbon cycle of the forest ecosystem in the process of forest restoration and forest succession after forest fire disturbance[5,6], thereby causing various ecological environmental problems. About 1% of the world's forests are burned every year (the burned area can reach $3.3 \times 10^7 \sim 4.3 \times 10^7$ hm^2) was disturbed by forest fires[7-10], and its carbon loss exceeded 2–4 Pg[5,11]. More and more attention has been paid to the research on carbon sink function and ecological civilization of forest ecosystem, which has become the hotspot of experts and scholars[8,9,10,12]. Increasing forest carbon density can improve the potential of forests in mitigating climate change[13]. The increase of energy released in the process of forest fire interference accelerates the loss of carbon through the decomposition of coarse wood residues, and further affects the carbon sequestration capacity and carbon balance of forests[14,15]. However, the impact of forest fire disturbance is usually not considered when measuring the carbon storage of each carbon pool in the forest ecosystem.

In recent years, the intensification of climate change has changed the cycle period and intensity of forest fire disturbance[16], and the distribution mode of vegetation composition and carbon storage may also be affected, changing the net carbon storage of forest ecosystem. The prediction model shows that the probability of forest fire will increase by 140% by the end of the 21st century[17,18]. Forest fire disturbance increases soil temperature and soil respiration, and affects the potential of forest ecosystem to accumulate carbon sinks. Quantitative research on the impact of forest fire disturbance on forest carbon pools is conducive to reducing the uncertainty in the estimation of global carbon balance. This study makes a quantitative analysis of the changes in carbon density of the eucalyptus forest ecosystem in Guangdong Province after forest fire disturbance, discusses the impact of forest fire disturbance on the carbon storage of each carbon pool in the ecosystem, and clarifies its impact mechanism on each carbon pool in the forest, which is helpful for people understanding the carbon cycle and carbon distribution process of each carbon pool in the forest ecosystem, and it is of great significance to formulate scientific and reasonable forest fire management measures aimed at mitigating global change.

2. Research area and research method

2.1 Overview of the study area

Located at the southernmost tip of Chinese Mainland, Guangdong Province is a province with large natural resources (20°09'N–25°31'N, 109°45'E–117°20'E). The land area is adjacent to Fujian in the East, Hunan and Jiangxi in the north, Guangxi in the west, the vast South China Sea in the south, Hainan Province in the southwest across the Qiongzhou Strait, and the Tropic of Cancer runs across the province from the line that links South Australia—Conghua—Fengkai. The climate of Guangdong Province belongs to the East Asian monsoon region, and the climate zone is divided into tropical monsoon, south subtropical monsoon and mid subtropical monsoon from south to north. The province has abundant precipitation, with an average annual precipitation of 1,777 mm. The an-

nual average temperature is 22.3 ℃, and July is the hottest month in all regions. The average temperature is about 28–29 ℃, and the average sunshine duration is 1,745.8 h. It is an area with sufficient heat, and has the basic characteristics of warm and humid climate at the same time. Guangdong is located in the low latitude. Under the interaction of biological factors and climatic factors, the whole territory has formed zonal soils mainly constitute of lateritic red soil, latosol, red soil, yellow soil and so on. These soil types not only occupy a relatively large distribution area, but also reflect the characteristics of soil conditions in some typical vegetation types distribution areas in the province.

Affected by subtropical and tropical monsoon climate, Guangdong Province has a high degree of visibility, with the distribution of forest vegetation similar to tropical rainforest. In general, the vegetation components of Leizhou Peninsula are mainly tropical components such as saparicaceae, Annonaceae, myrtle and dipterocarpaceae, and the vegetation types are diverse. In the subtropical part of the mainland of the province, the vegetation components are mainly tropical and subtropical components such as barrier family, Camellia family, Fagaceae, Magnoliaceae and Bambusoideae, forming subtropical evergreen seasonal rainforest, subtropical evergreen broad-leaved forest and other vegetation types, which respectively constitute the tropical vegetation zone and subtropical vegetation zone of the province with the characteristics of zonal forest vegetation. Due to the interference of human factors, the floristic components also changed. First, the plains and hilly areas are cultivated, and secondary vegetation (coniferous sparse shrubs, grass slopes) and various artificial vegetation are planted instead. The artificial forests are dominated by pure forests such as *Eucalyptus robusta*, *Pinus Massoni Ana*, *Cunninghamia lanceolata*, *Casuarina equisetifolia*, *Schima superba* and *Phyllostachys pubescens*. Secondly, artificial cultivation has introduced some other economic plants. According to the statistical results of forest fire data in Guangdong Province from 1990 to 2017, a total of 6,275 forest fires occurred in the province, with an annual average of 224.11. The total area of the fire was 86,684.45 hm^2, with an annual average of 3,095.87 hm^2.

2.2 Forest fire interference intensity division and sample plot setting

Table 1 shows the division of forest fire interference intensity[19-22]. In this paper, the burned land in Fogang County, Guangdong Province on April 4, 2017 is selected as the research object. Within one week after the fire, the forest fire interference intensity (light, moderate and high forest fire interference intensity) is basically the same (see **Table 2** for the basic situation of the forest fire interference sample land), and take the land of the specification of 20 m × 20 m that repeated 3 times in the burned land and the control sample land (adjacent non burned forest stand) respectively. A total of 12 fixed standard plots are selected, that is, 12 standard plots = (3 kinds of forest fire interference intensity + 1 control plot) × 3 repetitions. Field investigation and experimental sample collection were carried out one year after the fire, and vegetation biomass, falling biomass and soil samples were collected.

Table 1. Forest fire disturbance intensity classification

Forest fire disturbance intensity	Division standard of forest fire disturbance intensity
Light forest fire disturbance: Part of the shrub under the forest was burned (≤50%), and part of the litter was burned (≤50%)	Fire burned wood less than 30% Live standing timber (including burned wood) > 70% or more Tree blackening height ≤ 2 m
Moderate forest fire disturbance: The shrubs under the forest were almost burned (>50%), and the litter was almost burned (>50%)	Fire burned wood ≥ 30%-70% Live standing timber (including burned wood) ≥ 30%–70% Tree blackening height is 2–5 m
High forest fire disturbance: The shrubs under the forest were all burned, and the litter is burned out	Fire burned wood ≥ 70%–100% Standing timber (including burned wood) is below 30% Tree blackening height ≥ 5 m

Table 2. Basic situation of forest fire disturbance in *Eucalyptus robusta* forests (mean ± SD)

Sample plot	Ages (a)	Mean DBH (cm)	Mean height (m)	Stem density (plant·hm^{-2})	Canopy openness	Slope (°)	Slope position	Aspect	Altitude (m)	Soil type	Forest type
Control plot CK	8 ~ 9	14.36 ± 3.24	17.26 ± 3.24	1687 ± 318	0.80	10–20	Mid-slope	South slope	245–280	Latosolic red soil	Plantation
Light forest fire disturbance L	8 ~ 9	14.36 ± 3.24	17.26 ± 3.24	1687 ± 318	0.75	10–20	Mid-slope	South slope	245–280	Latosolic red soil	Plantation
Moderate forest fire disturbance M	8 ~ 9	14.36 ± 3.24	17.26 ± 3.24	1435 ± 176	0.65	10–20	Mid-slope	South slope	245–280	Latosolic red soil	Plantation
High forest fire disturbance H	8 ~ 9	14.36 ± 3.24	17.26 ± 3.24	1021 ± 102	0.50	10–20	Mid-slope	South slope	245–280	Latosolic red soil	Plantation

Note: CK, L, M and H represent control, light forest fire disturbance, moderate forest fire disturbance and high forest fire disturbance respectively. The same below

2.3 Biomass survey

Investigate the tree species, canopy density, stand growth status, etc. in the fixed standard sample plot, and measure the DBH and tree height; set five small quadrats, each 2 m × 2 m, on the diagonal of the fixed standard sample plot according to the vegetation distribution characteristics, especially the uniformity. Investigate shrubs, herbs and falling objects in the quadrat, and weigh the collected samples and take samples back to the laboratory. See **Table 2** for the basic information of the forest fire disturbance sample plot.

Table 3. Effect of forest fire disturbance on soil bulk density (mean ± SD, g·cm^{-3})

Soil layer (cm)	Contrast CK	Light forest fire disturbance L	Moderate forest fire disturbance M	High forest fire disturbance H
0–10	1.20 ± 0.025	1.23 ± 0.039	1.41 ± 0.041	1.43 ± 0.022
10–20	1.23 ± 0.026	1.27 ± 0.021	1.46 ± 0.042	1.49 ± 0.032
20–30	1.27 ± 0.038	1.32 ± 0.033	1.48 ± 0.040	1.49 ± 0.024
30–40	1.31 ± 0.024	1.36 ± 0.026	1.51 ± 0.029	1.52 ± 0.029
40–60	1.35 ± 0.024	1.39 ± 0.026	1.52 ± 0.025	1.53 ± 0.012
60–80	1.38 ± 0.024	1.41 ± 0.013	1.52 ± 0.023	1.54 ± 0.031
80–100	1.41 ± 0.023	1.42 ± 0.024	1.53 ± 0.013	1.54 ± 0.030

2.4 Collection and treatment of soil samples

In the standard sample plot, three soil profiles (lateritic red soil) are selected along the “S” shape, and each soil profile is divided into seven levels (0–10, 10–20, 20–30, 30–40, 40–60, 60–80 and 80–100 cm) for sampling. The soil bulk density was determined with the soil ring knife (100 cm^3) method (drying to constant weight at 105 °C) (**Table 3**). Take 500 g soil samples at different sampling points and take them back to the laboratory for experimental analysis, which is used to analyze and determine the content of soil organic carbon. Five soil samples were taken from each fixed standard sample plot in the burned area, with three kinds of forest fire interference intensity, and a total of 105 samples were taken from seven soil layers (5 sampling points for each standard sample plot × 3 kinds of forest fire interference intensity levels × 7 soil layers). A total of 35 soil samples were collected from the control sample plots (5 sampling points for each standard sample plot × 7 soil layers). Using a soil drill with an inner diameter of 10 cm, collect 5 soil cores with diameters of 0–10, 10–20, 20–30 and 30–40 cm respectively according to the root system with root diameters ≤2 mm, and bag them in layers. Through the processes of rinsing and sieving with running water, select the fine roots, weigh them after drying, dry them to constant weight, save the samples, and test the moisture content.

Table 4. Regression equation and regression coefficient of *Eucalyptus robusta* forests

Component	Regression equation	*a*	*b*	Coefficient of determination (R^2)	Number of samples (*N*)
Trunk	$Y = a(D^2H)^b$	0.0513	0.8902	0.9689	30
Branch	$Y = a(D^2H)^b$	0.0013	1.7895	0.8894	30
Leaf	$Y = a(D^2H)^b$	0.0201	0.2356	0.9569	30
Bark	$Y = a(D^2H)^b$	0.0098	0.7856	0.9235	30

2.5 Experimental methods

2.5.1 Determination of biomass

Generally, the relative growth method is used to estimate the biomass of trees. According to the "Allometric" equation proposed by Huxley[23], the formula is[22,24,25]:

$$Y = a(D^2H)^b \quad (1)$$

Where: Y is biomass, D is DBH, H is tree height, a, b are the coefficients. See **Table 4** for the regression equation and regression coefficient of the biomass of the arbor layer of the eucalyptus forest in Guangdong Province. The biomass of shrubs, herbs and fallout is measured mainly by measuring the moisture content. Vegetation biomass includes the sum of the biomass of trees, shrubs and herbs. See **Table 5** for the impact of different forest fire disturbances on vegetation biomass and regulated litter biomass.

2.5.2 Determination of carbon content

Determination of carbon content in vegetation, fallout and soil organic carbon: grind the vegetation and falling object samples dried and collected into 60 mesh (0.25 mm) and store them in glass bottles. The soil samples were sieved for 100 mesh (0.15 mm) and stored in glass bottles. MultiN/C3100 analyzer (MultiN/C3100, Analytik Jena AG, Jena, Germany) combined with solid module was used to determine the carbon content of vegetation, fallout and soil samples.

Table 5. Effect of forest fire disturbance on vegetation/litter biomass of *Eucalyptus robusta* forests (mean±SD, t ·hm^{-2})

Treatment	Vegetation	Litter
Control CK	163.73 ± 12.80	4.30 ± 0.30
Light forest fire disturbance L	137.78 ± 18.86	3.09 ± 0.21
Moderate forest fire disturbance M	72.56 ± 9.05	2.03 ± 0.28
High forest fire disturbance H	31.71 ± 5.53	1.75 ± 0.28

2.5.3 Calculation method of carbon density per unit area

(1) Biomass carbon density per unit area. Biomass carbon density (t·hm^{-2}) is represented by *M*, biomass carbon content (g·kg^{-1}) is represented by *F*, and 1,000 is the unit of carbon content converted into the coefficient of carbon content (%). The formula can be expressed as:

$$C_t = M \times F_c/100 \quad (2)$$

(2) Soil organic carbon density per unit area. The calculation formula of organic carbon density in a certain soil layer per unit area is:

$$SOC_d = \sum_{i=1}^{n} T_i \times \theta_i \times C_i \times (1 - \delta_i\%)/10 \quad (3)$$

Where, SOC_d is the density of soil organic carbon (t·hm^{-2}); i is the number of soil layers, n = 7; T_i is the thickness of soil layer i of soil profile (cm), that is, the interval in 1–4 layers is 10 cm, and the interval in 5–7 layers is 20 cm; θ_i is the soil bulk density of layer i of soil profile (g·cm^{-3}); C_i is the organic carbon content of layer i of soil profile (g·kg^{-1}); δ_i% is the gravel content coefficient of soil profile with diameter greater than 2 mm; 10 is the coefficient that converts the unit of SOC into t·hm^{-2}.

2.6 Data analysis

Data statistical analysis was processed with Microsoft Excel 2016 and SPSS 25.0 software. SPSS 25.0 software was used for one-way ANOVA to compare the difference of carbon density (LSD test) between sample plots with different forest fire interference intensity and control sample plots, and the significance level setting α = 0.05. Draw the chart with OriginPro 2019b.

3. Results and analysis

3.1 Impact of forest fire disturbance on vegetation carbon density

3.1.1 Carbon content of vegetation

As shown in **Table 6**, the order of carbon content of different components of vegetation from high to low is: arbor (493.24 g·kg^{-1}) > shrub (472.19 g·kg^{-1}) > herb (482.27 g·kg^{-1}), and the average carbon content of eucalyptus forest vegetation is 482.57 g·kg^{-1}. It reflects the difference of carbon sequestration capacity of vegetation components in the eucalyptus forest in photosynthesis.

3.1.2 Impact of forest fire disturbance on vegetation carbon density

After forest fire disturbance of different intensity, the vegetation carbon density of the eucalyptus forest is different from that of the control sample (**Figure 1(A)**). Only moderate and high forest fire disturbance significantly reduced the carbon density of vegetation ($P < 0.05$). Under the same intensity of forest fire disturbance, the change of carbon density of each component of vegetation is the largest in arbors, which presents as control > light forest fire disturbance > moderate forest fire disturbance > high forest fire disturbance, while forest fire disturbance significantly improves the carbon density of herbs ($P < 0.05$), which presents as high forest fire disturbance > moderate forest fire disturbance > light forest fire disturbance > control (**Figure 1(B)**). Compared with the control plots, the carbon density of vegetation in the light forest fire disturbance, moderate forest fire disturbance and high forest fire disturbance plots was 15.50–80.69 t·hm^{-2}, which decreased by 15.86%, 55.78% and 80.79% respectively, and the difference was significant only after the moderate and high forest fire disturbance ($P < 0.05$). The arbor carbon density of the eucalyptus forest showed a downward trend compared with the control sample after different forest fire interference, but the difference was significant only after moderate and high forest fire interference ($P < 0.05$); compared with the control plots, the shrub carbon density first decreased and then increased after different forest fire disturbances. After moderate and high forest fire disturbances, the shrub carbon density significantly increased ($P < 0.05$), and the herb carbon density increased after different forest fire disturbances compared with the control plots, and the difference was significant ($P < 0.05$), that is, the forest fire disturbances significantly increased the herb carbon density.

3.2 Effect of forest fire interference on carbon density of litter

3.2.1 Carbon content of litter

The carbon content of regulated litter in the eucalyptus forest is smaller than the average carbon content of vegetation, which is 462.53 g·kg^{-1}, indicating that the carbon content of each component of the forest is arbor > shrub > herb > litter, and the difference may be related to site conditions, climate, vegetation carbon content and the composition of regulated litter.

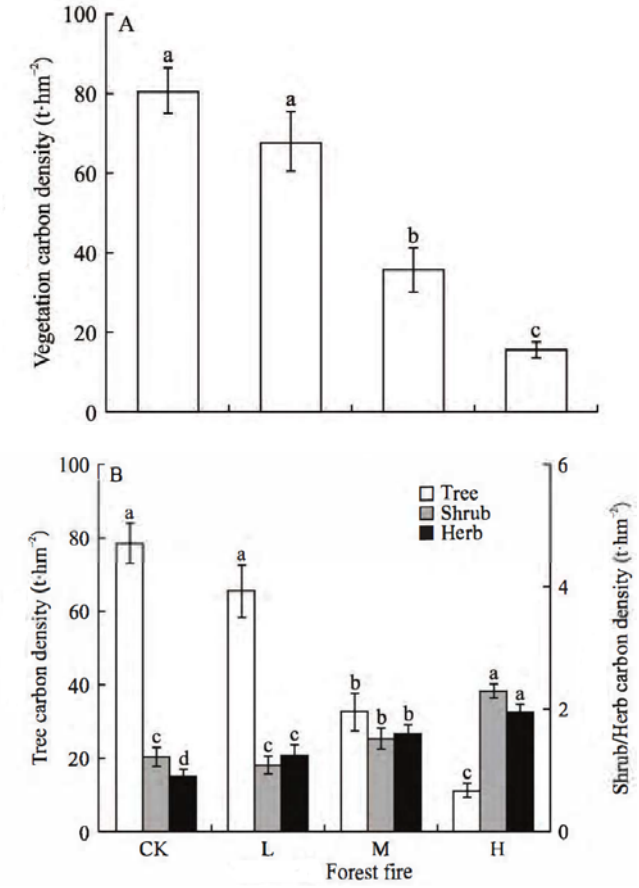

Figure 1. Effect of forest fire disturbance on vegetation carbon density of *Eucalyptus robusta* forest.
Note: Different small letters indicate significant difference between different forest fire disturbance intensity and control plot s in the same forest type at $P < 0.05$ Level. The same below.

Table 6. Vegetation carbon contents of *Eucalyptus robusta* forest (mean ± SD, g·kg^{-1})

Forest type	Carbon content
Tree	493.24 ± 78.20
Shrub	482.27 ± 67.20
Herb	472.19 ± 68.60
Mean	482.57 ± 71.34

3.2.2 Effect of forest fire interference on carbon density of fallout

It can be seen from **Figure 2** that different forest fire interference intensities have significantly reduced the carbon density of falling objects (P < 0.05), and the reduction degree increases with the increase of forest fire interference intensity. Compared with the control group, the carbon density of litter after light, moderate and high forest fire disturbance was 1.43, 0.94 and 0.81 t·hm^{-2}, which decreased by 28.14%, 52.76% and 59.30% respectively. The carbon density of litter after high forest fire disturbance reduced the most, which was consistent with the overall change of vegetation carbon density.

3.3 Effect of forest fire disturbance on soil organic carbon density

3.3.1 Soil organic carbon content

The content of soil organic carbon in each soil layer (0–100cm) with different forest fire interference intensities and in control plots varied in the range of 26.50–247.45 and 33.10–306.40 g·kg^{-1} respectively. The same soil layer showed a downward trend with the increase of forest fire interference intensity, and gradually decreased with the increase of soil profile depth (**Figure 3**). However, light forest fire disturbance had a significant effect on the density of soil organic carbon in the surface layer (0–20 cm) (P < 0.05), while moderate and high forest fire disturbance had a significant difference on the content of soil organic carbon in the surface layer and shallow layer (2,040 cm) of eucalyptus forest soil (P < 0.05).

3.3.2 Effect of forest fire disturbance on soil organic carbon density

After light forest fire disturbance, moderate forest fire disturbance and high forest fire disturbance in the eucalyptus forest, the soil organic carbon density of each soil layer (0–100 cm) was 103.30, 84.33 and 70.04 t·hm^{-2}, which decreased by 11.67%, 27.89% and 40.11% respectively compared with the control sample (**Figure 4(A)**). Light forest fire disturbance had no significant effect on soil organic carbon density (P > 0.05), while moderate and high forest fire disturbance significantly reduced soil organic carbon density (P < 0.05). The density of soil organic carbon in the surface layer (0–10 cm) decreased by 17.22%, 36.99% and 46.68% respectively, and the density of soil organic carbon in the sub surface layer (10–20 cm) decreased by 21.08%, 45.489% and 59.09% respectively. After the three kinds of forest fire interference intensity, the density of soil organic carbon in the surface layer decreased significantly (P < 0.05) (**Figure 4(B)**). The density of soil organic carbon in shallow soil (20–40 cm) decreased by 6.26%, 27.73% and 42.84% respectively. Only moderate and severe forest fire disturbance significantly reduced the density of soil organic carbon in shallow soil (P < 0.05). The density of soil organic carbon in deep layer (40–100 cm) decreased by 3.89%, 6.37% and 18.13% respectively. Only high forest fire disturbance had a significant effect on the density of soil organic carbon in deep layer (P < 0.05), while moderate forest fire disturbance had a significant effect on the density of soil organic carbon in deep layer (40–60 cm) (P < 0.05), while light and moderate forest fire disturbance had no significant effect on the density of soil organic carbon in deep layer (P > 0.05).

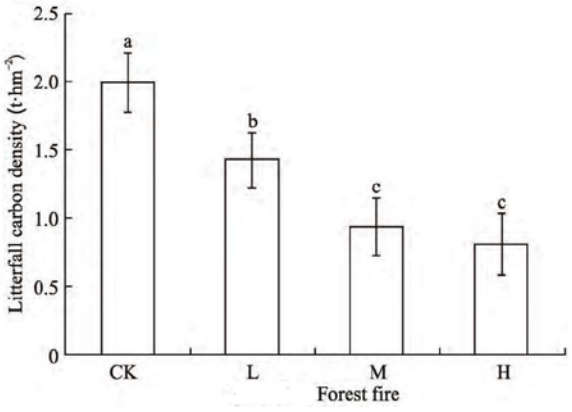

Figure 2. Effect of forest fire disturbance on litter carbon density of *Eucalyptus robusta* forest.

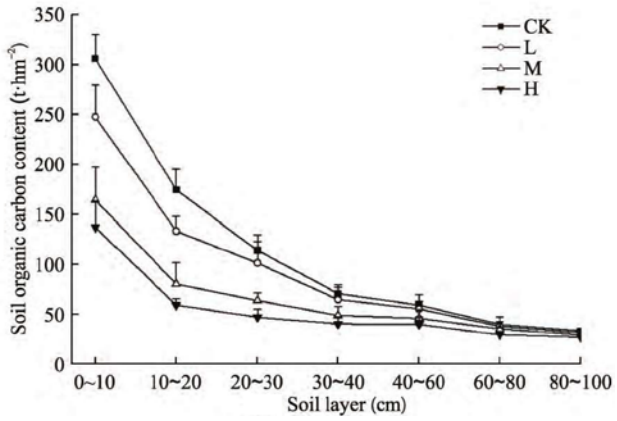

Figure 3. Effect of forest fire disturbance on soil organic carbon content of *Eucalyptus robusta* forest.
Note: For the sake of illustration, the results of the data of soil depth (40–60, 60–80 and 80–100 cm) is divided by 2. The same below.

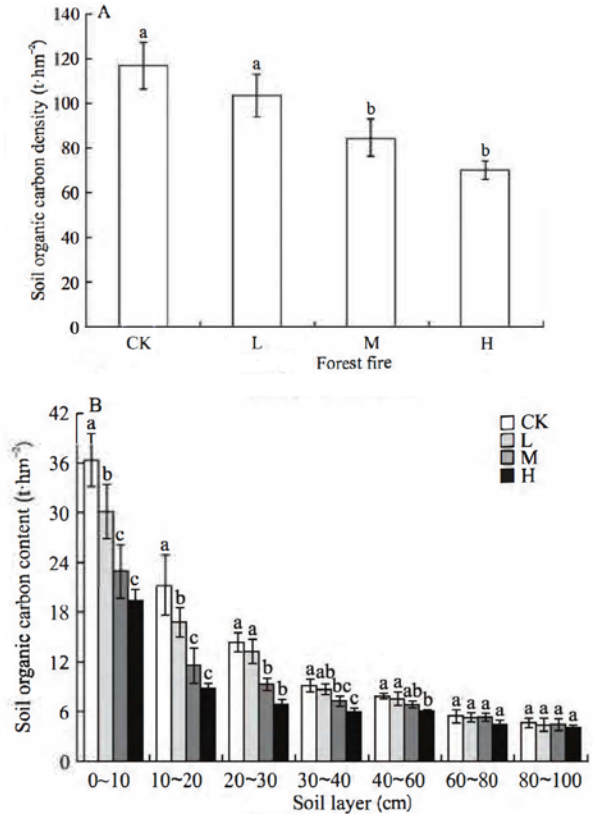

Figure 4. Effect of forest fire disturbance on soil organic carbon density of *Eucalyptus robusta* forest.

3.3.2 Effect of forest fire disturbance on soil organic carbon density

After light forest fire disturbance, moderate forest fire disturbance and high forest fire disturbance in the eucalyptus forest, the soil organic carbon density of each soil layer (0–100 cm) was 103.30, 84.33 and 70.04 t·hm^{-2}, which decreased by 11.67%, 27.89% and 40.11% respectively compared with the control sample (**Figure 4(A)**). Light forest fire disturbance had no significant effect on soil organic carbon density ($P > 0.05$), while moderate and high forest fire disturbance significantly reduced soil organic carbon density ($P < 0.05$). The density of soil organic carbon in the surface layer (0–10 cm) decreased by 17.22%, 36.99% and 46.68% respectively, and the density of soil organic carbon in the sub surface layer (10–20 cm) decreased by 21.08%, 45.489% and 59.09% respectively. After the three kinds of forest fire interference intensity, the density of soil organic carbon in the surface layer decreased significantly ($P < 0.05$) (**Figure 4(B)**). The density of soil organic carbon in shallow soil (20–40 cm) decreased by 6.26%, 27.73% and 42.84% respectively. Only moderate and severe forest fire disturbance significantly reduced the density of soil organic carbon in shallow soil ($P < 0.05$). The density of soil organic carbon in deep layer (40–100 cm) decreased by 3.89%, 6.37% and 18.13% respectively. Only high forest fire disturbance had a significant effect on the density of soil organic carbon in deep layer ($P < 0.05$), while moderate forest fire disturbance had a significant effect on the density of soil organic carbon in deep layer (40–60 cm) ($P < 0.05$), while light and moderate forest fire disturbance had no significant effect on the density of soil organic carbon in deep layer ($P > 0.05$).

Table 7. Effect of forest fire disturbance on fine root biomass of *Eucalyptus robusta* forests (t·hm^{-2})

Soil layer (cm)	Contrast CK	Light L	Moderate M	High H
0–10	4.04 ± 0.39 a	3.22 ± 0.32 b	2.56 ± 0.47 b	1.98 ± 0.22 b
10–20	3.12 ± 0.45 a	2.16 ± 0.35 b	1.59 ± 0·26 c	1.10 ± 0.11 c
20–30	2.18 ± 0.39 a	1.85 ± 0.47 a	1.04 ± 0.26 b	0.83 ± 0.18 b
30–40	0.94 ± 0.14 a	0.93 ± 0.19 a	0.67 ± 0.11 ab	0.57 ± 0.21 b

Note: Different small letters on the same line indicate significant differences between the same soil layer processing ($P < 0.05$)

3.3.3 Effect of forest fire disturbance on soil fine root biomass

It can be seen from **Table 7** that the fine root biomass of forest soil after forest fire interference is lower than that of the control sample, and the change trend is presented as high forest fire interference > moderate forest fire interference > light forest fire interference. After the disturbance of forest fires, the fine root biomass of the soil surface (0–10 cm) decreased significantly ($P < 0.05$), decreasing by 20.30%, 36.63% and 50.99% respectively; the soil fine root biomass in the sub surface layer (10–20 cm) decreased significantly ($P < 0.05$), decreasing by 30.77%, 49.04% and 64.74% respectively; the fine root biomass in shallow soil (20–40 cm) decreased by 8.10%, 40.51% and 47.98% respectively, and only the high and moderate forest fire disturbance decreased significantly ($P < 0.05$); the decrease of fine root biomass in shallow soil (20–40 cm) was smaller than that in surface soil (0–20 cm).

4. Discussion

In the global carbon cycle, the change of carbon pool in subtropical forest ecosystem is very important. Forest fire disturbance profoundly affects the ecological process of carbon balance in the ecosystem, changing the nutrient utilization rate[3], thereby reducing the carbon density of the forest ecosystem[26]. This is consistent with this study. The proportion of vegetation carbon density in the forest ecosystem in the control group of eucalyptus forest, forest with light, moderate and high forest fire interference is 40.42%, 39.33%, 29.50% and 17.95% respectively. The proportion of litter carbon density in the forest ecosystem is 1.00%, 0.83%, 0.78% and 0.94%, and the proportion of soil organic carbon density in the forest ecosystem is 58.58%, 59.85%, 69.72% and 81.11% respectively. The carbon density of vegetation and litter accounted for 41.42%, 40.15%, 30.28% and 18.89% of the forest ecosystem respectively. It can be seen that with the increase of forest fire interference intensity, the proportion of vegetation and litter carbon density in the ecosystem decreased. After forest fire interference, the carbon density of the ecosystem decreased, and the carbon density decreased with the increase of forest fire interference intensity. In addition, due to the relatively small proportion of litter carbon density, the change of vegetation and soil organic carbon density is the main influencing factor of ecosystem carbon density change[27,28]. Since the moderate and high forest fire disturbance intensity significantly affects the carbon density of eucalyptus forest vegetation ($P < 0.05$) and soil organic carbon density, the moderate and high forest fire disturbance intensity significantly affects the carbon density of eucalyptus forest ecosystem ($P < 0.05$), and the light forest fire disturbance has no significant impact on the carbon density of forest ecosystem ($P > 0.05$).

The overall impact of forest fire disturbance on forest ecosystems is complex and highly variable, ranging from the reduction of aboveground biomass (including vegetation biomass and litter biomass, etc.) to physical, chemical and microbial mediated processes in soil micro ecosystems, but the short-term and long-term impact of forest fire disturbance on underground micro organisms and the ultimate impact on ecosystem sustainability are uncertain, and it requires further study on how forest fire disturbance with different intensity can change the succession of vegetation, and then affect the structure of soil microbial community. The change of underground ecological process will affect the internal mechanism of soil carbon pool circulation, and then affect the carbon sequestration potential and key carbon processes of forest ecosystem. In addition, after the forest fire disturbance, due to the difference in the recovery speed of different vegetation types, in the early stage of vegetation recovery, the input of soil carbon source is reduced due to the reduction of the nutrient cycle process available to plants. It is necessary to systematically carry out a systematic study on “vegetation—litter—soil—microorganism—climate”, and explore the interaction mechanism of migration, transformation and storage of carbon pools in different stages after the fire disturbance. The distribution characteristics of each carbon pool and the relationship between energy conversion in a longer period of time should be analyzed, so as to realize the quantitative study of

different forest fire interference types on the dynamic changes of forest ecological carbon pool[29].

5. Conclusion

Forest fire disturbance reduced the carbon density of vegetation, the effect of light forest fire disturbance on the carbon density of vegetation was not significant ($P > 0.05$), while moderate and high forest fire disturbance significantly reduced the carbon density of vegetation ($P < 0.05$). Different forest fire disturbance intensities significantly reduced the carbon density of regulated litter ($P < 0.05$), and the reduction amplitude increased with the increase of forest fire disturbance intensity.

Forest fire disturbance reduced the density of soil organic carbon in the same soil layer. The soil organic carbon density of the sample plots with different forest fire interference intensity is lower than that of the control, and the reduction range gradually decreases with the increase of soil profile depth. Light forest fire disturbance only significantly reduced the density of soil organic carbon in the surface layer (0–20 cm) ($P < 0.05$); however, moderate and high forest fire disturbance significantly reduced the density of soil organic carbon in the surface layer and shallow layer (20–40 cm) ($P < 0.05$). After forest fire disturbance, the soil fine root biomass of each forest type was lower than that of the control sample. The effect of light forest fire disturbance on the soil surface fine root biomass was significantly different ($P < 0.05$), while moderate and high forest fire disturbance significantly reduced the soil surface and shallow fine root biomass ($P < 0.05$).

Forest fire disturbance reduced the carbon density of forest ecosystem. With the increase of forest fire disturbance intensity, the carbon density decreased gradually. After forest fire disturbance, it appears as control > light forest fire disturbance > moderate forest fire disturbance > high forest fire disturbance. Compared with the control, the impact of light forest fire disturbance intensity on ecosystem carbon density was not significant ($P > 0.05$), while the impact of moderate and high forest fire disturbance intensity on ecosystem carbon density was significantly different ($P < 0.05$).

Conflict of interest

The authors declared no conflict of interest.

References

1. Lal R. Forest soils and carbon sequestration. Forest Ecology and Management 2005; 220(1–3): 242–258.
2. Raval A, Ramanathan V. Observational determination of the greenhouse effect. Nature 1989; 342: 758–761.
3. Alcaniz M, Outeiro L, Francos M, *et al*. Effects of prescribed fires on soil properties: A review. Science of the Total Environment 2018; 613–614: 944–957.
4. Li F, Bond-Lamberty B, Levis S. Quantifying the role of fire in the Earth system—Part 2: Impact on the net carbon balance of global terrestrial ecosystems for the 20th century. Biogeosciences 2014; 11: 1345–1360.
5. van der Werf GR, Morton DC, DeFries RS, *et al*. CO_2 emissions from forest loss. Nature Geoscience 2009; 2: 737–738.
6. Marlier ME, DeFries RS, Voulgarakis A, *et al*. El Nino and health risks from landscape fire emissions in southeast Asia. Nature Climate Change 2013; 3: 131–136.
7. Giglio L, Randerson JT, van der Werf GR, *et al*. Assessing variability and long-term trends in burned area by merging multiple satellite fire products. Biogeoscience 2009; 7: 1171–1186.
8. Urbanski S. Wildland fire emissions, carbon, and climate: Emission factors. Forest Ecology and Managements 2014; 317: 51–60.
9. Andela N, Morton DC, Giglio L, *et al*. A human-driven decline in global burned area. Science 2017; 356: 1356.
10. Chen D, Pereira JMC, Masiero A, *et al*. Mapping fire regimes in China using MODIS active fire and burned area data. Applied Geography 2017; 85: 14–26.
11. Bowman DMJS. Balch JK, Artaxo P, *et al*. Fire in the earth system. Science 2009; 324: 481–484.
12. Pellegrini AF, Ahlstrom A, Hobbie SE, *et al*. Fire frequency drives decadal changes in soil carbon and nitrogen and ecosystem productivity. Nature 2018; 553: 194–198.
13. Canadell JG, Raupach MR. Managing forests for climate change mitigation. Science 2008; 320: 1456–1457.
14. Kashian DM, Romme WH, Tinker DB, *et al*. Carbon storage on landscapes with stand-replacing fires. Bioscience 2006; 56: 598–606.
15. Liu W, Wang X, Lu F, *et al*. Influence of afforestation, reforestation, forest logging climate change, CO_2 concentration rise, fire, and insects on the carbon sequestration capacity of the forest ecosystem. Acta Ecologica Sinica 2016; 36(8): 2113–2122.
16. Hurteau MD, Westerling AL, Wiedinmyer C, *et al*. Projected effects of climate and development on

California wildfire emissions through 2100. Environmental Science & Technology 2014; 48: 2298–2304.
17. Spracklen DV, Mickley LJ, Logan JA, *et al*. Impacts of climate change from 2000 to 2050 on wildfire activity and carbonaceous aerosol concentrations in the western United States. Journal of Geophysical Research: Atmospheres 2009; 114: D20301.
18. Wotton BM, Nock CA, Flannigan MD. Forest fire occurrence and climate change in Canada. International Journal of Wildland Fire 2010; 19: 253–271.
19. Alexander ME. Calculating and interpreting forest fire intensities. Canadian Journal of Botany 1982; 60: 349–357.
20. Luo J. Information on the calculation of forest fire intensity. Forest Fire Prevention 1988; (4): 13–15.
21. Hu H. Linhuo shengtai yu guanli (Chinese) [Forest fire ecology and management]. Beijing: China Forestry Publishing House; 2005.
22. Hu H, Wei S, Sun L. Estimation of carbon emissions from forest fires in 2010 in Huzhong of Daxing'anling Mountain. Scientia Silvae Sinicae 2012; 48(10): 109–119.
23. Huxley JS. Problems of Relative Growth. New York: Dial Press; 1932.
24. Jolicoeur P. The multivariate generalization of the allometry equation. Biometrics 1963; 19: 497–501.
25. Blackstone NW. Allometry and relative growth: Pattern and process in evolutionary studies. Systematic Zoology 1987; 36: 76–78.
26. Williams CA, Gu H, MacLean R, *et al*. 2016. Disturbance and the carbon balance of US forests: A quantitative review of impacts from harvests, fires, insects, and droughts. Global and Planetary Change 2016; 143: 66–80.
27. Hicke JA, Asner GP, Kasischke ES, *et al*. Postfire response of North American boreal forest net primary productivity analyzed with satellite observations. Global Change Biology 2003; 9: 1145–1157.
28. Carter MC, Foster CD. Prescribed burning and productivity in southern pine forests: A review. Forest Ecology and Management 2004; 191: 93–109.
29. Hu H, Luo S, Luo B, *et al*. Effects of forest fire disturbance on soil organic carbon in forest ecosystems: A review. Acta Ecologica Sinica 2020; 40(6): 1–12.

Sustainable Forestry (2022) Volume 5 Issue 1
doi:10.24294/sf.v5i1.1617

CASE REPORT

Analysis of biomass compatibility model of Chinese fir in Jiangle, Fujian Province

Mingjing Wu*

Jiangle National Forest Farm, Jiangle 353300, Fujian Province, China. E-mail: wmj0598@163.com

ABSTRACT

Aiming at the problem of incompatibility of biomass models of forest organs, taking Chinese fir in Fujian Jiangle State-owned Forest Farm as the research object, based on selecting the optimal independent model of each organ, the biomass compatibility model of Chinese fir was established with a three-level joint control scheme. The results show that the compatibility equation system based on the whole plant biomass can effectively solve the problem of incompatibility in the whole plant biomass, each sub-biomass and between sub-biomass. Besides, except for the leaf biomass model, all other biomass models have good fitting effect, which is of great significance to the guidance of the analysis of local Chinese fir biomass.

Keywords: Chinese Fir; Biomass; Compatibility Model

ARTICLE INFO

Received: 1 February 2022
Accepted: 18 March 2022
Available online: 27 March 2022

1. Introduction

Forest biomass is one of the most basic quantitative characteristics of forest ecosystem[1]. Measuring forest biomass is time-consuming and laborious, and establishing biomass model to reduce field work is currently recognized by people[2]. However, in terms of research methods, researchers at home and abroad generally select the model according to each organ (stem, branch, leaf and root) of forest tree respectively and fitting the parameters in their respective equations, that is, the estimation of each organ is carried out independently[3], which leads to the incompatibility between the fitted models. In order to solve the problem of incompatibility between models, Luo *et al.*[4] proposed to use linear simultaneous model and nonlinear joint estimation model to solve the problem of incompatibility between the total and the components. Tang *et al.*[3] used the nonlinear joint estimation scheme to fit the model, and compared the results with the proportional adjustment method, and considered that the two-level algebra and fitting distribution scheme was the best scheme; Dong *et al.*[5] established a compatibility model based on total biomass by using the ratio function hierarchical joint control equations to fit the biomass compatibility model of main tree species in Heilongjiang Province, and the model accuracy was high. In this paper, the Chinese fir in Jiangle State-owned Forest Farm in Fujian Province was taken as the research object, and the biomass compatibility model was established by using the three-level joint control scheme.

2. Overview of study area

The analysis data of this study were collected from Fujian Jiangle

State-owned Forest Farm, which is located in the southeast of Wuyi Mountain Range. It is a subtropical seasonal climate zone with marine and continental climate characteristics, with an average annual temperature of 18.7 ℃, an average annual precipitation of 1,676 mm, an average annual evaporation of 1,204 mm and an annual frost-free period of 298 d, and a warm and humid climate. The landform is mainly low hills, with an altitude of 140–1,403 m, and the forest coverage rate of the forest farm is 93.5%. The main conifer species for afforestation are *Cunninghamia lanceolata* (Lamb.) Hook., *Pinus massoniana* Lamb., *Pinus elliottii* Engelmann, etc.

3. Materials and methods

3.1 Standard wood selection and biomass determination

In this study, there are 14 standard Chinese fir trees in different age groups, including 3 young forests, 2 middle-aged forests, 3 near-mature forests, 3 mature forests and 3 over-mature forests. See **Table 1** for information of the standard land. On the basis of each wood gauge, two trees with no broken tip, no bifurcation, normal growth and typical crown width and length are selected as standard trees. The biomass is measured in the aboveground part and underground part respectively. The aboveground part is divided into the biomass of trunk and crown (branches and leaves), and the underground part refers to the biomass of roots. Dong *et al.*[6] provided the determination methods of biomass of each component (organ).

Table 1. Standard information table

Age group	Area/(m × m)	Average breast diameter/cm	Average tree height/m	Density/(a tree/hm^{-2})
Young and semi-mature forest	20 × 30	8.9	6.5	4,400
	20 × 30	10.3	7.3	4,000
	20 × 30	11.5	9.5	4,000
Middle-aged forest	20 × 30	11.4	9.8	3,667
	20 × 30	12.5	10.2	3,667
Near-mature forest	20 × 30	12.8	10.5	3,500
	20 × 30	13.2	10.8	3,500
	20 × 30	15.0	12.0	3,070
Mature forest	20 × 30	17.2	13.2	2,500
	20 × 30	18.2	13.7	2,500
	20 × 30	21.2	16.8	1,767
Overmature forest	30 × 30	22.0	18.3	1,250
	30 × 30	23.6	18.9	850
	30 × 30	26.0	18.8	800

3.2 biomass independent model fitting

The biomass of the whole plant and each component (organ) is fitted by using the unitary and binary models of biomass, which are: $W = aD^b$ (formula 1), $W = aD^bH^c$ (formula 2), where: W is biomass; D is the standard DBH of wood; H is the standard tree height; a, b and c are the parameters of the equation[7].

3.3 Biomass model test

The commonly used Bias, root mean square error (RMSE) and adjusted determination coefficient ($adj - R^2$) are used to test the accuracy of the above model.

$$\text{Bias} = \frac{\sum_{i=1}^{n}\left(\hat{y}_i - y_i\right)}{n},\ RMSE = \sqrt{\frac{\sum_{i=1}^{n}\left(\hat{y}_i - y_i\right)^2}{n-r}},$$

$$adj - R^2 = 1 - \frac{(n-1)\sum_{i=1}^{n}\left(\hat{y}_i - y_i\right)^2}{(n-r)\sum_{i=1}^{n}\left(\overline{y}_i - y_i\right)^2}$$

Where: y_i, $\hat{y}_i$ and $\overline{y}_i$ are the measured value, predicted value and average value of biomass respectively; n is the number of samples; r is the

number of parameters.

3.4 Biomass compatibility model fitting

A three-level joint control scheme is adopted to establish the biomass compatibility model: the first-level control variable is the whole plant biomass, and the independent optimal model of the whole plant biomass is regressed, and the sum of the aboveground biomass and the root biomass is equal to the whole plant biomass through proportional distribution of the first-level control; the second-level control variable is the aboveground biomass, and the aboveground biomass is equal to the sum of trunk biomass and crown biomass through the proportional distribution of the second-level control. Level 3 control variable is canopy biomass, which makes canopy biomass equal to the sum of branch biomass and leaf biomass.

Level 1 control: $\widetilde{w}_2 = \frac{f_2(x)}{f_2(x)+f_3(x)} \times \hat{w}_1$ (formula 3), $\widetilde{w}_3 = \frac{f_3(x)}{f_2(x)+f_3(x)} \times \hat{w}_1$ (formula 4); Level 2 control: $\widetilde{w}_4 = \frac{f_4(x)}{f_4(x)+f_7(x)} \times \widetilde{w}_2$ (formula 5), $\widetilde{w}_7 = \frac{f_7(x)}{f_4(x)+f_7(x)} \times \widetilde{w}_2$ (formula 6); Level 3 control: $\widetilde{w}_5 = \frac{f_5(x)}{f_5(x)+f_6(x)} \times \widetilde{w}_7$ (formula 7), $\widetilde{w}_6 = \frac{f_6(x)}{f_5(x)+f_6(x)} \times \widetilde{w}_7$ (formula 8); where, $f_2(x)$, $f_3(x)$, $f_4(x)$, $f_5(x)$, $f_6(x)$ and $f_7(x)$ are the optimal biomass models of above-ground part, root, trunk, branches, leaves and crown respectively; $\hat{w}_1$ is the fitting value of total biomass; $\widetilde{w}_i$ is the fitting value of compatibility model; *i* is 2–7, representing biomass of aboveground parts, roots, trunks, branches, leaves and crowns respectively[5].

4. Results and analysis

4.1 The optimal model of biomass of each organ

According to the measured biomass data of 28 Chinese fir standard trees, the biomass of each organ of Chinese fir was fitted with univariate and binary biomass models, and the optimal independent model of each organ was selected through the model inspection indexes, which are shown in **Table 2**.

Table 2. Evaluation indexes of unitary and binary models of various organs

Organ	Unitary model			Binary model		
	E	***RMSE***	***R²***	***E***	***RMSE***	***R²***
Whole plant	-1.0103	16.5508	0.9494	-0.0601	15.7621	0.9541
Aboveground	-0.7637	16.4009	0.9328	0.0155	15.9069	0.9368
Trunk	-1.3152	15.0502	0.9351	-0.2553	14.0613	0.9434
Root	-0.2336	6.5855	0.7192	-0.0650	6.4965	0.7267
Crown	0.0944	5.2154	0.3212	0.0217	5.0820	0.3555
Branch	0.0586	3.3507	0.4341	0.0271	3.3421	0.4370
Leaf	0.0105	2.2756	0.542	0.0015	2.1389	0.1645

As can be seen from **Table 2**, the error and root mean square error of binary model of each organ are smaller than that of unitary model, and the determination coefficient is higher than that of unitary model, so the binary model with DBH (*D*) and tree height (*H*) as independent variables is selected as the optimal model of biomass of each organ.

The biomass of each organ was fitted with the selected optimal independent model, and the differences (Δ_1) between the fitted values of the whole plant biomass and the sum of the fitted values of the biomass of trunk, branches, leaves and roots were calculated respectively: $\Delta_1 = total - (\text{trunk} + \text{branches} + \text{roots} + \text{leaves})$, $\Delta_1(\%) = \Delta_1/total \times 100$ (%); Difference (Δ_2) between aboveground biomass fitting value and sum of trunk biomass fitting value and canopy biomass fitting value: $\Delta_2 = \text{aboveground part} - (\text{trunk} + \text{crown})$, $\Delta_2(\%) = \Delta_2/\text{aboveground part} \times 100$; Difference ($\Delta_3$) between fitting value of canopy biomass and sum of fitting value of branch biomass and leaf biomass: $\Delta_3 = crown - (\text{branches} + \text{leaves})$, $\Delta_3(\%) = \Delta_3/\text{crown} \times 100(\%)$. The results are shown in **Table 3**.

Table 3. Incompatibility analysis of biomass of various organs

D	H	Δ_1/kg	$\Delta_1/\%$	Δ_2/kg	$\Delta_2/\%$	Δ_3/kg	$\Delta_3/\%$
8.0	6.6	-1.1618	-10.9457	-1.1690	-13.2817	-0.0780	-2.1812
10.1	6.9	-1.5735	-8.7681	-1.6018	-10.6507	-0.0320	-0.5559
10.3	7.6	-1.1565	-5.9031	-1.1816	-7.2098	0.0146	0.2655
10.7	7.8	-1.1109	-5.1585	-1.1393	-6.3166	0.0367	0.6294
11.1	9.4	-0.4441	-1.7455	-0.4626	-2.1778	0.0645	1.2145
11.3	10.2	-0.2298	-0.8364	-0.2421	-1.0570	0.0575	1.1242
11.4	9.4	-0.4476	-1.6605	-0.4702	-2.0867	0.0793	1.4066
11.4	11.2	-0.0571	-0.1951	-0.0585	-0.2402	0.0313	0.6549
11.7	8.2	-1.0176	-3.8046	-1.0553	-4.6959	0.0946	1.3918
12.8	10.4	-0.1003	-0.2761	-0.1319	-0.4331	0.1335	2.0129
12.9	12.8	0.2180	0.5356	0.2156	0.6351	0.0284	0.5113
13.1	8.0	-1.3592	-4.0255	-1.4145	-4.9545	0.1741	1.9452
13.4	10.2	-0.1177	-0.2961	-0.1598	-0.4782	0.1815	2.4251
13.6	10.5	-0.0063	-0.0152	-0.0482	-0.1377	0.1837	2.4413
14.7	13.6	0.5119	0.9214	0.4921	1.0572	0.0720	1.0278
15.8	15.0	0.5923	0.8712	0.5760	1.0101	0.0289	0.3856
16.9	15.8	0.6741	0.8364	0.6530	0.9642	0.0210	0.2525
18.0	19.4	-0.5098	-0.5013	-0.4830	-0.5667	-0.2482	-3.1545
18.5	17.0	0.6741	0.6646	0.6488	0.7592	-0.0061	-0.0648
19.1	16.5	1.0236	0.9551	0.9829	1.0860	0.0845	0.8069
20.7	19.9	-0.4553	-0.3269	-0.4582	-0.3901	-0.2163	-2.0618
21.8	21.3	-1.4207	-0.8835	-1.4087	-1.0378	-0.3397	-3.0767
22.0	20.1	-0.4015	-0.2515	-1.4135	-0.3062	-0.1862	-1.5642
22.4	19.3	0.3086	0.1895	0.2813	0.2038	-0.0581	-0.4515
23.2	20.5	-0.5477	-0.3031	-0.5597	-0.3653	-0.1823	-1.3859
24.1	20.0	0.0955	0.0492	0.0754	0.0458	-0.0554	-0.3779
26.5	19.8	0.9401	0.3965	0.9397	0.4640	0.1690	0.9248
27.7	20.3	0.6942	0.2630	0.7211	0.3193	0.1778	0.9025

From **Table 3**, it can be seen that there are different degrees of errors between the sum of the total amount of the whole plant, aboveground biomass, crown biomass and their corresponding components, which is consistent with the research results of Tang *et al.*[3] and Dong *et al.*[5], which is mainly because the model fitting of each organ is carried out independently, leading to the incompatibility between the biomass models of each organ.

4.2 Biomass compatibility model of various organs

Based on the obtained independent optimal model of biomass of each organ, the biomass compatibility model was established by using the three-level joint control scheme. The simultaneous equations based on the total biomass are used for joint estimation step by step, and the specific steps are as follows.

Level 1 control: Firstly, independent model regression is performed on formula 2 to obtain the total biomass model parameters and estimated values $\left(\hat{w}_1\right)$, and $\hat{w}_1$ is directly substituted into the formula 3 and formula 4, at the same time, substitute the optimal model of aboveground biomass and root biomass to simplify the equation, which can form the following equations: $\widetilde{w}_2 = \frac{1}{1+r_1 D^{r_2} H^{r_3}} \times \hat{w}_1$ (formula 9), $\widetilde{w}_3 = \frac{1}{1+\left(\frac{1}{r_1}\right) D^{-r_2} H^{-r_3}} \times \hat{w}_1$ (formula 10); level 2 control: taken $\widetilde{w}_2$ as the basis, the optimal model of biomass of the trunk and the crown is substituted into formula 5 and formula 6 respectively to simplify the equation, which can form the following equations: $\widetilde{w}_4 = \frac{1}{1+r_4 D^{r_5} H^{r_6}} \times \widetilde{w}_2$ (for-

mula 11), $\widetilde{w}_7 = \frac{1}{1+\left(\frac{1}{r_4}\right)D^{-r_5}H^{-r_6}} \times \widetilde{w}_2$ (formula 12); level 3 control: taken $\widetilde{w}_7$ as the basis, the optimal biomass models of branches and leaves were substituted into formula 7 and formula 8 to be simplified, and the following equations can be formed: $\widetilde{w}_5 = \frac{1}{1+r_7 D^{r_8} H^{r_9}} \times \widetilde{w}_7$ (formula 13), $\widetilde{w}_6 = \frac{1}{1+\left(\frac{1}{r_7}\right)D^{-r_8}H^{-r_9}} \times \widetilde{w}_7$ (formula 14). R software is used to fit the parameter values of the constructed biomass compatibility model, and the results are shown in **Table 4**.

Table 4. Parameter estimation of compatible simultaneous model

Total biomass			**Aboveground biomass, root biomass**			**Trunk biomass, crown biomass**			**Branch biomass, leave biomass**		
a	b	c	r_1	r_2	r_3	r_4	r_5	r_6	r_7	r_8	r_9
0.049	2.164	0.468	0.253	-0.532	0.442	6.101	-0.084	-1.285	8.521	0.393	-1.370

Through the test of the compatible biomass model (**Table 5**), we can see that the biomass compatibility model is based on solving the incompatibility between the whole plant biomass and sub-biomass and in the sub-biomass, and all the evaluation indexes of the model are ideal (except leaves), and the model fitting ability is good. On the one hand, it may be related to the fact that the biomass of branches and leaves is influenced by crown shape, size, saturation and tree growth, and these factors change with different climate and habitats. On the other hand, it may be the loss of biomass in the process of investigation and sampling of branches and leaves in the field; so the evaluation index of crown biomass is low.

Table 5. Evaluation index of compatibility simultaneous model

Organ	***E***	***RMSE***	$\mathbf{R^2}$
Whole plant	-0.060	15.762	0.954
trunk	-0.500	14.328	0.941
root	0.075	6.631	0.714
branch	0.215	3.438	0.403
leave	0.128	2.194	0.118

5. Conclusion

In this study, the unilateral model including DBH and binary model including DBH and tree height were used to fit the biomass of Chinese fir. The results showed that the binary model including DBH and tree height had better fitting effect. On the basis of selecting the optimal independent model of each organ, a three-level joint control scheme was adopted to establish the compatibility model among the biomass of each organ. The results show that the compatibility equation system based on the whole plant biomass can effectively solve the problem of incompatibility between the whole plant biomass and sub-biomass and in the sub-biomass, and the fitting effect of other biomass models is good except the tree leaf biomass model.

The evaluation index of the biomass model of branches and leaves in this study is low. On the one hand, it may be related to the influence of the biomass of branches and leaves on the shape, size and fullness of crown and the growth of trees, and these factors are related to the change of climate and habitat; on the other hand, it may be related to the loss of some biomass of branches and leaves in the field investigation and sampling process, which should be paid attention to in the later related work.

Conflict of interest

The author declares no conflict of interest.

References

1. Feng Z, Wang X, Wu G. Zhongguo senlin shengtai xitong de shengwuliang he shengchanli (Chinese) [Biomass and productivity of forest ecosystems in China]. Beijing: Science Press; 1999.
2. Peng X. Study on the biomass model of Cunninghamia lanceolata plantations in Northern Fujian [MSc thesis]. Fuzhou: Fujian Agriculture and Forestry University; 2007.
3. Tang S, Zhang H, Xu H. Study on establish and estimate method of compatible biomass model. Scientia Silvae Sinicae 2000; 36(S1): 19–27.
4. Luo Q, Zeng W. Establishment and application of compatible tree above ground biomass models. Journal of Natural Resources 1999; 14(3): 271–277.

5. Dong L, Li F, Jia W, *et al*. Compatible biomass models for main tree species with measurement error in Heilongjiang Province of Northeast China. Chinese Journal of Applied Ecology 2011; 22(10): 2653–2661.
6. Wang T. A study on individual tree biomass models of pinus massoniana plantation of Jiangle Fujian [MSc thesis]. Beijing: Beijing Forestry University; 2012.
7. Xia Z, Zeng W, Zhu S, *et al*. Construction of tree volume equations for Chinese fir plantation in Guizhou Province, Southwestern China. Journal of Beijing Forestry University 2012; 34(1): 1–5.

Sustainable Forestry (2022) Volume 5 Issue 1
doi:10.24294/sf.v5i1.1618

ORIGINAL RESEARCH ARTICLE

A model of cross-sectional growth of *Cunninghamia lanceolata* plantation in Hunan province with climate effects

Zhantao Qi, Guangyu Zhu, Bingbing Yu, Hongna Liu, Yong Lv*

Forestry Institute, Central South University of Forestry and Technology, Changsha 410004, China.
E-mail: 727065572@qq.com

ABSTRACT

Objective: The influence of climate on forest stands cannot be ignored, but most of the previous forest stand growth models were constructed under the presumption of invariant climate and could not estimate the stand growth under climate change. The model was constructed to provide a theoretical basis for forest operators to take reasonable management measures for fir under the influence of climate. **Methods:** Based on the survey data of 638 cedar plantation plots in Hunan Province, the optimal base model was selected from four biologically significant alternative stand basal area models, and the significant climate factors without serious covariance were selected by multiple stepwise regression analysis. The optimal form of random effects was determined, and then a model with climatic effects was constructed for the cross-sectional growth of fir plantations. **Results:** Richards formula is the optimal form of the basic model of stand basal area growth. The coefficient of adjustment (R_a^2) was 0.8355; the average summer maximum temperature (T_{max}) and the water vapor loss (C_{MD}) in Hargreaves climate affected the maximum and rate of fir stand stand growth respectively, and were negatively correlated with the stand growth. The adjusted coefficient of determination (R_a^2) of the fir stand area break model with climate effects was 0.8921, the root mean square error (RMSE) was 3.0792, and the mean relative error absolute value (MARE) was 9.9011; compared with the optimal base model, R_a^2 improved by 6.77%, RMSE decreased by 19.04%, and MARE decreased by 15.95%. **Conclusion:** The construction of the stand cross-sectional area model with climate effects indicates that climate has a significant influence on stand growth, which supports the rationality of considering climate factors in the growth model, and it is important for the regional stand growth harvest and management of cedar while improving the accuracy and applicability of the model.

Keywords: Fir Plantation Forest; Climate Factor; Stand Area Cut-Off Growth Model; Mixed-Effects Model

ARTICLE INFO

Received: 22 February 2022
Accepted: 1 April 2022
Available online: 11 April 2022

1. Introduction

Broken area is one of the important indexes for evaluating forest quality and calculating yield[1,2], which has the advantages of easy measurement and accurate data, and is the basis for developing forest management measures and harvesting plans. As an indicator reflecting the growth process of forest stands also affects the stand stock[3], and its model accuracy is more directly related to the prediction accuracy of the overall model of the whole forest, so it has become one of the hot spots of domestic and international research[3].

Cunninghamia lanceolata is one of the main silvicultural and timber species in Southern China[5], and is also an excellent timber species unique to the subtropical region of China[6]. The eighth national forest resources inventory showed that the existing plantation area of fir plantations is about 1.24×10^3 million hm^2, accounting for about 26.6% of

the national plantation area, and its share in commercial timber is about 1/4. It has an important position and role in meeting the national economic development and people's demand for multiple benefits of forests[7].

Stand age, stand quality and stand density are the variables used to construct the stand area model, and most of the current simulations of stand area models are limited to factors such as topography and geomorphology[8,9]. Gao *et al.*[10] used a dummy variable approach to construct a stand break area growth model for Pinus sylvestris based on the average height of the dominant wood as the stand index; Hu[3] used a mixed-effects model approach to construct a stand break area growth model for oak natural forests in Hunan, using the dominant height of the stand at a standard age of 20 a as the stand index. Yan *et al.*[11] chose the base model without stand index taking into account the errors arising from the complexity of the stand, and constructed a stand area model for poplar and oak. Although the above models solve the corresponding problems, most of them assume a constant climate and cannot estimate the stand growth under the influence of climate factors. In contrast, the *Second National Assessment Report on Climate Change* shows that the average annual temperature and annual precipitation in China will increase by 3.5 ℃ and 4.2% respectively[12]. The IPCC also suggested in the *Fifth Assessment Report* that the warming rate in the past 50 a is almost twice as high as that in the past 100 a[13,14], and the rate of climate change has increased significantly. Considering the sensitivity of fir to climate, this study added climatic factors such as temperature and precipitation in the subsequent modeling process based on using the average height of dominant trees in the stand as an index of stand quality, and analyzed their effects on the growth of fir stands in the cross-sectional area, which provided a theoretical basis for the fir management measures adopted by forest operators under the influence of climate.

2. Overview of the study area

Hunan is located in the transition zone from the Yunnan-Guizhou plateau to the hills of Jiangnan and from the Nanling Mountains to the Jianghan Plain. It is surrounded by mountains on three sides, with a horseshoe-shaped landscape opening toward the north, located at 24°38′–30°08N′, 108°47′–114°15′E. It seats east of Jiangxi, west of Chongqing and Guizhou, south of Guangdong and Guangxi, and north of Hubei, with a total area of 211,800 km^2. The climate type is subtropical monsoon humid climate, with variable temperature in spring and autumn, cold winter and hot summer, rainy spring and summer, and dry autumn and winter. The average daily temperature is stable in most areas, the average annual temperature is 16–19°C, the frost-free period is 253–311 d, and the average annual precipitation in the province is 1,200–1,700 mm, with abundant rainfall and sufficient water and heat.

3. Materials and methods

3.1 Data sources

The data used for constructing the model in this study were obtained from the 1980 cedar plantation sample plot survey data from various cities and counties in Hunan Province, with a sample plot size of about 667 m^2, which mainly distributed in the east (Changsha, Zhuzhou, Xiangtan), north (Changde, Yiyang), and south (Yongzhou, Chenzhou, Hengyang) of Hunan Province. Latitude and longitude coordinates, elevation, soil texture, slope position, average diameter at breast height of stand, slope shape, gradient, soil thickness, stand age, number of plants per hectare, average height of dominant trees, etc. were the main sample plot survey factors, of which 638 sample plots have complete data that required. Based on the latitude and longitude coordinates and elevation of each site, climate data were obtained from ClimateAP (2019) wrote by Wang *et al.*[12], which can extract climate data for the Asia-Pacific region, with 12 types of climate factors (**Table 1**).

Table 1. Definition of climate variables

Variable	Description
T_{MA}(℃)	Average annual temperature
T_{MWM}(℃)	Average temperature in the hottest month
T_{MCM}(℃)	Average temperature in the coldest month
$T_D(°C)$	Average temperature difference
$P_{MA}(mm)$	Annual precipitation
A_{HM}	Dryness index= $(T_{MA}+10)/(P_{MA}/1000)$
$D_{D5}(°C)$	Growth accumulated temperature
C_{MD}	Hargreaves climate water vapor deficit
$T_{ave}(°C)$	Average summer temperature
$T_{max}(°C)$	Average summer maximum temperature
$T_{min}(°C)$	Average summer minimum temperature
$P_{PT}(mm)$	Summer precipitation

In order to improve the accuracy of modeling and the rationality of model evaluation, this study divided the sample plot data into 478 groups of modeling data and 160 groups of testing data according to the ratio of 3:1, which were used to simulate and test the fir plantation stand cross-area growth model, and the relevant statistics are shown in **Table 2**.

3.2 Research methods

3.2.1 Screening of independent variables

In this study, multivariate stepwise regression analysis was used to screen the independent variables for climate factors, and factors with severe covariance were excluded according to the variance inflation factor (VIF), thus retaining factors with weak covariance and significant effects as follows[3].

Table 2. Modeling and verifying data statistics*

Variable	Modeling data				Validation data			
	Min	Max	Max	Stand error	Min	Max	Mean	Stand error
T/a	11	26	19.6	3.3	11	26	19.8	3.2
H_D/m	7.6	18.7	12.6	2.3	7.7	19.1	12.8	2.1
N/(plant/hm^{-2})	750	5,175	2,150.6	704.1	1,035	4,275	2,118.1	685.2
SDI	695.9	2,844.5	1,369.1	365.1	722.8	2,454.1	1,351.5	355.4
B_A/(m^2/hm^{-2})	10.6	52.9	27.6	9.4	9.8	54.9	27.3	9.6
T_{MCM}/℃	1.6	8.0	5.9	0.9	3.3	8.0	6.0	1.0
P_{PT}/mm	349	811	496.6	71.6	388	656	495.7	60.8
T_{max}	22.6	33.1	30.3	2.6	24.1	32.9	30.6	2.0
C_{MD}	0	185	97.9	56.3	0	184	93.7	54.6

*T, H_D, B_A and N represent stand age, average height of dominant trees, per hectare basal area and number of trees per hectare respectively.

1) Given the significance α, the corresponding critical values are noted as $F^{(1)}$. The i independent variables X_i in the regression model were subjected to one-way linear regression analysis with the dependent variable respectively. The test F statistic $F_i^{(1)}$ of the regression coefficients of the respective variables is calculated and the maximum value $F_{il}^{(1)}$ is selected, and is introduced into the regression model X_{il} when $F_{il}^{(1)} \geq F^{(1)}$.

2) Given the significance α, the corresponding critical value is noted as $F^{(2)}$, a binary regression model of the dependent variable and the subset of independent variables is established, and the value of F test statistic $F_j^{(2)}$ of the regression coefficient of the independent variable is calculated, and the maximum $F_{j2}^{(2)}$ of which is selected, and when $F_{j2}^{(2)} \geq F^{(2)}$, introduce X_{j2} into the regression model, otherwise terminate it[3].

3) Repeat step 2 and substitute the respective variables into the model one by one for F test, and when the original independent variables become no longer significant due to the later introduced independent variables, they are removed to ensure that the model contains only significant variables[3].

3.2.2 Construction of the model for stand area break

The growth and development of a stand is strongly influenced by its stand age, stand quality, and the degree of utilization of the stand resources[15,16], so three variables, stand quality index,

density index, and stand age, need to be included in the construction of a stand area break growth model[17]. In this study, four commonly used models were selected as candidate base models, and in the construction of the base model, the stand quality index was selected as the average height of the dominant tree HD in the stand. The density index was selected from the stand density index SDI and the number of plants per hectare *N* after comparing the differences in the accuracy of the base models[7], and the specific model form was as follows.

$$B_A = aH_D^b\left(1 - e^{(-cT(SDI/1000))^d}\right)^f \tag{1}$$

$$B_A = aH_D^b\left(1 - e^{(-cT(N/1000))^d}\right)^f \tag{2}$$

$$B_A = H_D^{(a+b/T)}(SDI/1000)^{(c+d/T)}e^{(f+g/T)} \tag{3}$$

$$B_A = H_D^{(a+b/T)}(N/1000)^{(c+d/T)}e^{(f+g/T)} \tag{4}$$

Where: *T*, B_A, SDI, H_D are stand age, stand cross-sectional area, stand density index, and mean height of dominant trees in the stand respectively; *a*, *b*, *c*, *d*, *f*, and *g* are all model fixed parameters.

3.2.3 Construction of the mixed-effects model

The model built based on the regression relationship of the regression function depending on both fixed effect parameters and random effect parameters is called mixed effects model, and its general form[3,18] is as follows.

$$y_i = f(\beta, \mu_i, x_i) + \varepsilon_i \tag{5}$$

Where: y_i and x_i are the vector of dependent and independent variables for the *i* sample respectively; ε_i is the error term; β and μ_i are the vector of fixed effect parameters and the vector of random parameters respectively.

In the process of constructing the mixed-effects model, the key step is the parameter construction of the two major effects of the model—random effects and fixed effects, that is, all the independent variables related to the research object are added to each parameter of the model in the form of permutation and combination as random effects fit, and the model is evaluated according to AIC, BIC, and the smaller the value of AIC and BIC, the better the model fits. However, surplus independent variables as well as parameters can cause non-convergence of the model[19,20]. In order to avoid this problem and select a parametric construction with fewer parameters and convergent form, this study first conducts the significance factor screening of the study object and then conducts a multi-parameter effect simulation test using the optimal base model[3].

3.3 Evaluation of model accuracy

In this study, model evaluation was performed using adjusted coefficients of determination R_a^2, root mean square error RMSE, mean relative error absolute value MARE, Akaike info criterion AIC, and Bayesian information quantity BIC, with the following formula.

$$\mathrm{AIC} = -2\ln l + 2 \tag{6}$$

$$\mathrm{BIC} = -2\ln l + \ln np \tag{7}$$

$$R_a^2 = 1 - \frac{\sum_{i=1}^n (y_i - \hat{y}_i)^2}{\sum_{i=1}^n (y_i - \bar{y}_i)^2}\left(\frac{n-1}{n-p}\right) \tag{8}$$

$$\mathrm{RMSE} = \sqrt{\frac{\sum_{i=1}^n (y_i - \hat{y}_i)^2}{n - P}} \tag{9}$$

$$\mathrm{MARE} = \frac{1}{n}\sum_{i=1}^{n}\left|\frac{y_i - \hat{y}_i}{y_i}\right| \times 100 \tag{10}$$

Where: y_i is the *i*-th sample measured value; $\hat{y}_i$ is the *i*-th sample predicted value; $\bar{y}$ is the average measured value; *p* is the number of parameters in the model; *n* is the number of samples; and *l* is the maximum likelihood function value of the model.

4. Results and analysis

4.1 Climate factor screening and classification

The annual mean temperature (T_{MA}), annual cumulative temperature (D_{D5}), hottest monthly mean temperature (T_{MWM}), coldest monthly mean temperature (T_{MCM}), mean temperature difference (T_D), annual precipitation (P_{MA}), dryness index (A_{HM}), Hargreaves climate water vapor deficit

(C_{MD}), summer mean air temperature (T_{ave}), summer mean maximum temperature (T_{max}), summer mean minimum temperature (T_{min}), summer mean precipitation (P_{PT}), and other 12 climatic factors affecting cedar growth were selected. The independent variables with severe covariance VIF > 5 were excluded by using variance expansion factor[21]. As shown in **Table 3**, the climate factors with weak covariance and high contribution were T_{MCM}, P_{PT}, T_{max} and C_{MD}, whose corresponding standardized coefficients were 0.268, 0.135, -0.597 and -0.322 respectively. It can be concluded that T_{MCM} and P_{PT} is positively correlated with the growth of section area, while T_{max} and C_{MD} is negatively correlated with the growth of section area.

Table 3. Results of multiple stepwise regression analysis of climate factors

Variables	Unstandardized coefficients	Stand error	Standardized coefficients	*t* test	*P* value	Tolerance	VIF
VIF	0.319	0.084	0.109	3.808	<0.001	0.764	1.309
T_{MCM}	2.667	0.298	0.268	8.951	<0.001	0.705	1.417
P_{PT}	0.018	0.005	0.135	3.696	<0.001	0.470	2.129
T_{max}	-2.561	0.138	-0.597	-18.608	<0.001	0.613	1.631
C_{MD}	-0.054	0.006	-0.322	-9.564	<0.001	0.555	1.802
T_{ave}	-2.638	0.845	-0.382	-3.121	0.002	0.042	23.807
T_{min}	4.911	0.905	0.668	5.428	<0.003	0.042	24.024

The significant climate factors obtained from the screening were selected and scaled into classes according to their respective ranges of values (**Table 4**). The final coldest monthly mean temperature (T_{MCM}) was classified as level 8, the Hargreaves climate moisture deficit (C_{MD}) was classified as level 10, the average summer precipitation (P_{PT}) was classified as level 9, and the average summer maximum temperature (T_{max}) was classified as level 12.

Table 4. The division of climatic factors grades

Climate factors	Symbol	Grade division
Mean coldest month temperature	T_{MCM}	One level per degree Celsius
Hargreaves climatic moisture deficit	C_{MD}	The division of climatic factors grades per 20 units
Summer mean precipitation/mm	P_{PT}	Every 50 mm
Summer mean maximum temperature	T_{max}	One level per degree Celsius

4.2 Base model

4.2.1 Calculation of stand density index

The stand density index (SDI) is one of the common density indices used in the construction of the stand sectional area or accumulative growth model[22], and its expression is as follows.

$$\mathrm{SDI} = N(D_0/D)^{\beta} \tag{11}$$

Where: SDI is the stand density index; N is the number of plants per hectare in the stand; D_0 is the standard average diameter at breast height; D is the average diameter at breast height in the stand; and β is the natural thinning rate.

In order to determine the SDI value, β must be estimated first. In this study, β was estimated using the method of quadratic exclusion of sample plots with insufficient stand size[23]. First took all samples to build the regression equation $\ln N = a_1 - b_1 \ln D_g$, and excluded sample plots of $\ln N < a_1 - b_1 \ln D_g$. Then the remaining sample plots are used to establish the regression equation $\ln N = a_2 - b_2 \ln D_g$, and the sample plots of $\ln N < a_2 - b_2 \ln D_g$ are excluded. Finally, the regression equation was established with the remaining sample plots[23].

$$\ln N = \alpha - \beta \ln D \tag{12}$$

The regression equation was finally obtained by taking all the sample data and fitting each regression model nonlinearly in Forstat 2.2 software according to the abovesteps, with the following expressions for the above regression equation and its adjusted coefficient of determination $R_a^2 = 0.71$.

$$\ln N = 4.5273 - 0.9605 \ln D \tag{13}$$

Combine the natural thinning rate $\beta =$

-0.96053 with the relevant variables, and substituted into the SDI expression to calculate the stand density index for each site.

4.2.2 Selection of the model

The above basic models (1) to (4) were fitted nonlinearly with R software, and the final results of fitting and accuracy evaluation are shown in **Table 5**. Models (1) and (3) outperformed models (2) and (4) in all indices, indicating that the stand density index would be more appropriate than using the number of plants per hectare to express the density index. Among them, model (1) has the best simulation effect, the highest modeling data, and the lowest error index, so model (1) is chosen as the base model for simulating the growth of stand cross-sectional area.

Table 5. Parameter fitting and precision evaluation of candidate models

Data	Index	Model (1)		Model (2)		Model (3)		Model (4)	
		Estimated value	Stand error	Estimated value	Stand error	Estimated value	Stand error	Estimated value	Stand error
Parameter	*a*	6.1818	0.7593	1.7035	3.5770	0.8707	0.2158	1.0022	0.3929
	b	0.8016	0.0409	1.3405	0.0726	-1.2246	4.0778	7.0178	7.2819
	c	0.0012	0.0004	<0.0001	<0.0001	1.0061	0.1395	0.2327	0.2031
	d	9.8364	3.8411	9.5872	12.1026	-0.9635	2.5781	6.0671	3.7699
	e	0.1016	0.0414	0.0591	0.0753	0.8885	0.5540	0.6033	1.0797
	g					1.6024	10.2745	-22.1470	19.7498
Modeling data	R_a^2	0.8355		0.5145		0.8331		0.5199	
	RMSE	38.035		65.392		38.296		65.026	
	MARE	117.796		214.470		119.299		212.944	
Validation	RMSE	41.842		72.176		42.006		71.856	
	MARE	130.976		237.118		132.269		235.809	

Table 6. Evaluation results of the random effects of climatic factors*

Random effects position					Index	
a	***b***	***c***	***d***	***f***	**AIC**	**BIC**
X	C				2,583.301	2,616.658
X	P+C				2,586.629	2,624.156
	X+P+C				2,587.294	2,624.820
	M+X+P+C				2,583.632	2,625.329
	X+P+C		M		2,583.672	2,625.368
M+P	X+C				2,584.186	2,625.882
X	P+C		M		2,584.203	2,625.899
M+X	P+C				2,584.216	2,625.912
	M+X+C				2,599.808	2,637.335
X	M+C				2,599.846	2,637.373
	C	P			2,617.770	2,651.127
	X+P		M		2,615.220	2,652.746
	P+C	M			2,619.189	2,656.716
	X+P				2,628.985	2,662.341
	X		M		2,635.018	2,668.375

**M*, *X*, *P* and *C* respectively represent the random effects of climate factors T_{MCM}, T_{max}, P_{PT} and C_{MD}; *a*, *b*, *c*, *d* and *f* are the five parameters of the optimal foundation model.

4.3 Construction of mixed-effects model

In order to compare and analyze the effects of each of the four significant climate factors and their comprehensive differences on the stand area growth, a stand area growth model with random effects was constructed for model (1).

Using the hybrid model module of R software, the four climate factors T_{MCM}, P_{PT}, T_{max}, C_{MD} and their combinations, which had no serious covariance and had significant effects on area break, were screened as random effects, and the effects were added to the parameters *a*, *b*, *c*, *d*, *f* and their

combinations (1,150 types) for random effects simulation, and the non-converging types were excluded, and each model was evaluated according to AIC and BIC. The results are shown in **Table 6**.

As shown in **Table 6**, the best mixed-effects model was constructed by adding T_{max} to parameter a, C_{MD} to parameter b in the random effects construction. Therefore, the final expression of the stand cross-sectional area growth model with climate random effects was constructed as follows:

$$B_{Aij} = (a_0 + a_{i0}) H_{Dij}^{(b_0+b_{0j})} \left(1 - e^{\left(-cT_{ij}(\mathrm{SDI}_{ij}/1000)^d\right)}\right)^f + \varepsilon_{ij} \quad (14)$$

Where: B_{Aij}, H_{Dij}, T_{ij}, and SDI_{ij} denotes the stand area, mean height of dominant wood, stand age and stand density index for the mean summer maximum temperature (T_{max}) at level i, the water vapor deficit (C_{MD}) at level j in Hargreaves climate, a_{i0} and b_{i0} are the random effect parameters for T_{max} and C_{MD} respectively, and a, b, c, d, and f are model fixed parameters.

4.4 Model simulation analysis

The non-linear mixed-effects simulation of model (14) was performed using R software, and the obtained parameter fitting results and model testing results are shown in **Table 7**.

Table 7. Fitting results of model parameters

Data	Index	Model (1)		Model (14)	
		Estimated value	**Stand error**	**Estimated value**	**Stand error**
Parameter	*a*	6.1818	0.7593	6.2813	0.6408
	b	0.8016	0.0409	0.7451	0.0365
	c	1.24E-05	3.97E-05	0.0002	0.0004
	d	9.8364	3.8421	7.9746	2.7091
	f	0.1016	0.0415	0.1218	0.0456
Estimate	AIC	2,640.35		2,583.30	
	BIC	2,665.36		2,616.66	
Modeling data	R_a^2	0.8355		0.8921	
	RMSE	3.8035		3.0792	
	MARE	11.7796		9.9011	
Validation data	RMSE	4.1842		3.4665	
	MARE	13.0978		11.4833	

From **Table 7**, the results of fitting the parameters of each model are significant. Comparing AIC and BIC, it can be seen that the fitting effect of the model (14) after adding the random effect is better than the base model (1), and the effect of random effect is obvious. From R_a^2, RMSE, and MARE, the model (14) after adding random effects outperforms the base model (1) in terms of modeling and testing accuracy. The adjusted coefficient of determination R_a^2 of the modeled sample increased from 0.8355 to 0.8921, an increase of 6.77%; the root mean square error RMSE decreased by 19.04%, and the mean relative error MARE decreased by 15.95% in absolute value; the root mean square error RMSE of the test sample decreased by 17.15%, and the mean relative error MARE decreased by 12.33%.

5. Conclusion and discussion

5.1 Discussion

The study of stand area growth prediction model is important for predicting forest growth and harvest, and coordinating the overall forest management, while the expression of stand age, stand quality index and density index are necessary parts for constructing stand area growth model. In this study, a hybrid model was used to add each climate factor to the base model in the form of random effects to analyze the stochastic effects of each level of climate factor on the growth of stand area. Hu[3] used the same method to analyze the effects of different stand types and stand type differences on the stand area growth of oak, and although the study objects were not consistent, the model accuracy was

significantly improved; Li *et al.*[24], after comparing the traditional regression model method with the mixed model method to construct a stand area model of larch spruce fir, concluded that the mixed model method had higher accuracy. The results showed that the mixed model approach was more accurate, indicating that it was reasonable and effective to use the mixed model approach to construct the stand area model.

The final climatic factors added to the model random effects were mean maximum summer temperature T_{max} and Hargreaves climate moisture deficit C_{MD}, where T_{max} affects the maximum growth rate of the basal area and C_{MD} affects the growth rate of the basal area. The normalized coefficients of C_{MD} and T_{max} were negative, which were -0.597 and -0.322 respectively, indicating that the maximum value of the broken area and growth rate were negatively correlated with T_{max} and C_{MD} respectively, which was consistent with the research results made by Zhu[25] in the study of climatic factors on cedar tree whorls of different seed sources. It may be that because of the subtropical monsoon climate in Hunan, the temperature is generally higher during the growing season, and temperature is no longer the main requirement for tree growth. Excessive heat intensifies transpiration, and water vapor loss also intensifies water deficit in the forest, resulting in water deficit growth of fir trees being hindered. At the same time, the climatic factors with weak covariance and high contribution from multiple stepwise regression analysis in this study were T_{MCM}, P_{PT}, T_{max}, C_{MD}, which were similar to the significant climatic factors obtained by the same method in screening on the larch standing index model by Zang[12]; in the study of the distribution of suitable areas for Mongolian oak dominant species by Lv *et al.*[26], by using the knife cut method, it is concluded that the hottest monthly mean temperature, wet season precipitation, annual accumulated temperature all had significant effects on Mongolian oak, which all indicated that the climatic factors had significant effects on the growth of forest trees.

For the convenience of modeling, only the mean height of dominant trees was used to represent the stand quality index in the constructed cross-sectional area model, without directly considering the influence of topography, landform and other stand factors. In the subsequent study, we can consider using topographic and geomorphological data to construct a stand index model for cedar plantation first and obtain various status indices, and then consider climatic factors to construct a sectional area model, which may further improve the accuracy of the model.

5.2 Conclusion

In this study, the stand density index SDI (β = -0.96053) was estimated using 638 fir plantation sample plots in Hunan Province. Comparing the fitting results of different base basal area growth equations, the Richards model was determined to have the best effect ($R_a^2 = 0.8355$, RMSE = 3.8035, MARE = 11.7796). To consider the effects of different climatic factors, the climatic factors with weak covariance and high contribution were screened as T_{MCM}, P_{PT}, T_{max} and C_{MD} using multiple stepwise regression analysis, of which the first two were positively correlated with basal area growth and the last two were negatively correlated with it. The growth model of basal area distribution of Chinese fir plantation with climate random effects was constructed by using the method of mixed-effects model, thus the optimal random-effects parameter construction form was determined. Compared with the base model, the model accuracy of the model with climate random effects was significantly improved with the modeling accuracy $R_a^2 = 0.8921$, improved by 6.77%; RMSE = 3.0792, reduced by 19.04%; MARE = 9.9011, reduced by 15.95%. The results illustrate the significant influence of climate on stand growth and provide support for the rationality of adding a climate factor to the growth model, which is beneficial to the regional forest management of fir plantations while improving accuracy.

Conflict of interest

The authors declared no conflict of interest.

References

1. Rodríguez F, Pemán J, Aunós A. A reduced growth model based on stand basal area: A case for hybrid poplar plantations in northeast Spain. Forest Ecology and Management 2010; 259(10): 2093–2102.
2. Gao D. The research of stand growth forecast models for Quercus mongolica and Pinus tabulaeformis in Beijing [MSc thesis]. Beijing: Beijing Forestry University; 2014.
3. Hu S. Research on basal area growth model for oak natural forest in Hunan province [MSc thesis]. Changsha: Central South University of Forestry and Technology; 2019.
4. Duan A, Zhang J, Sun H, *et al*. Research progress of growth simulation theories and technologies for stand basal area. World Forestry Research 2013; 26(2): 43–47.
5. Zhao Y, Wang X, Jiang T, *et al*. Growth model for thinned and un-thinned stand of Chinese fir reserve forest based on error measurement method. Journal of Northwest Forestry University 2019; 34(4): 185–191.
6. Che S. Growth modeling for Chinese fir plantation based on artificial neural network [PhD thesis]. Beijing: Chinese Academy of Forestry; 2012.
7. Li C. Application of mixed effect models in forest growth models [PhD thesis]. Beijing: Chinese Academy of Forestry Sciences; 2010.
8. Colbert JJ, Schuckers M, Fekedulegn D, *et al*. Individual tree basal-area growth parameter estimates for four models. Ecological Modelling 2004; 174(1–2): 115–126.
9. Hostin PJ, Titus SJ. Indirect site productivity models for white spruce in Alberta's boreal mixedwood forest. The Forestry Chronicle 1996; 72(1): 73–79.
10. Gao D, Deng H, Jiang Y, *et al*. Forecast models research of stands basal area growth for *Pinus tabulaeformis*. Journal of Southwest Forestry University 2015; 35(1): 42–46.
11. Yan W, Duan G, Wang Y, *et al*. Construction of stand basal area and volume growth model for Quercus and Populus in Henan Province of Central China. Journal of Beijing Forestry University 2019; 41(6): 55–61.
12. Zang H. Regional-scale climate-sensitive stand growth models for larch plantations [PhD thesis]. Beijing: Chinese Academy of Forestry; 2016.
13. Liao Y, Peng J, Guo Q. Response of Hunan climate to global climate change. Transactions of Atmospheric Sciences 2014; 37(1): 75–81.
14. Mei G. Study on growth model and multi-functional simulation of Chinese fir plantation [PhD thesis]. Beijing: Beijing Forestry University; 2017.
15. Gao D, Deng H, Cheng Z, *et al*. Study on growth models for thinned and un-thinned stands of *Quercus mongolica*. Journal of Central South University of Forestry & Technology 2014; 34(2): 50–54.
16. Zhu G, Hu S, Fu L. Basal area growth model for oak natural forest in Hunan Province based on dummy variable. Journal of Nanjing Forestry University (Natural Sciences Edition) 2018; 42(2): 155–162.
17. Guo X. Crown structure and growth model for *Larix olgensis* plantation [PhD thesis]. Beijing: Beijing Forestry University; 2013.
18. Chen Z, He D, He P. Using mixed-effects modeling method to establish standing volume equations for rubber tree in Hainan Province. Journal of Central South University of Forestry & Technology 2016; 36(12): 31–36.
19. Pandhard X, Samson A. Extension of the SAEM algorithm for nonlinear mixed models with 2 levels of random effects. Biostatistics 2009; 10(1): 121–135.
20. Sharma M, Parton J. Height-diameter equations for boreal tree species in Ontario using a mixed-effects modeling approach. Forest Ecology and Management 2007; 249(3): 187–198.
21. Liu F, Huang R, Jiang S, *et al*. Study on the growth rhythm of *Keteleeria fortunei* var. *cyclolepis* plantation. Journal of Central South University of Forestry & Technology 2020; 40(3): 39–52.
22. Li Y, Kang X. Mixed model of forest space utilization in spruce-fir coniferous and broadleaved mixed forest of Changbai Mountains, Northeastern China. Journal of Beijing Forestry University 2020; 42(5): 71–79.
23. Li X, Tang S, Wang S. The establishment of variable density yield table for Chinese fir plantation in Dagangshan experiment bureau. Forest Research 1988; 1(4): 382–389.
24. Li C, Tang S. The basal area model of mixed stands of *Larix olgensis*, *Abies nephrolepis* and *Picea jezoensis* based on nonlinear mixed model. Scientia Silvae Sinicae 2010; 46(7): 106–113.
25. Zhu A. Response of tree ring to climate change of different provenances of *Cunninghamia lanceolata* [MSc thesis]. Beijing: Chinese Academy of Forestry Sciences; 2016.
26. Lv Z, Li W, Huang X, *et al*. Predicting suitable distribution area of three dominant tree species under climate change scenarios in Hebei Province. Scientia Silvae Sinicae 2019; 55(3): 13–21.

Sustainable Forestry (2022) Volume 5 Issue 1
doi:10.24294/sf.v5i1.1619

ORIGINAL RESEARCH ARTICLE

The response system of the growth, physiological and uptake characteristics of *Pinus bungeana* under ozone stress

Jingjing Xu[1,2], Peng Liu[3], Shuqi Zheng[2], Bo Chen[2*], Xinbing Yang[1*]

[1] College of Forestry, Hebei Agriculture University, Baoding 071001, Hebei, China. E-mail: hbyxb2008@126.com
2 Beijing Academy of Forestry and Pomology Sciences, Beijing 100093, China. E-mail: zhyechb2010@163.com
[3] Beijing World Hazard Preventing Tech. Co. Ltd, Beijing 100048, China.

ABSTRACT

Objective: To study the changes of growth, physiological and absorption characteristics of *Pinus bungeana* under ozone (O_3) stress, to elucidate the correlations among the indicators, and to determine its degree of response to O_3. **Methods:** The growth, physiological characteristics and O_3 uptake capacity of *Pinus bungeana* seedlings were measured in an open-top O_3 fumigation manual control experiment with three concentration gradients (NF: normal atmospheric O_3 concentration, NF40: normal atmospheric O_3 concentration plus 40 nmlol/mol; NF80: normal atmospheric O_3 concentration plus 80 nmol/mol), and the relationships between the characteristics of *Pinus bungeana* under different O_3 concentrations were investigated with correlation analysis, redundancy analysis and analysis of variance. **Results:** (1) Plant height growth (ΔH), diameter growth at 50 cm (ΔDBH), stomatal size (S), stomatal density (M), stomatal opening (K), stomatal conductance (G_s), net photosynthetic rate (P_n), transpiration rate (E_t), water use efficiency (WUE), maximum photochemical efficiency (F_v/F_m), chlorophyll content (CHL), whole tree water consumption (W), and O_3 uptake rate (F_{O_3}) all decreased with the increase of O_3 concentration; while intercellular CO_2 concentration (C_i) and relative conductivity (L) increased with the increase of O_3 concentration; (2) growth indicators of *Pinus bungeana* under O_3 stress (ΔH, ΔDBH) were the most correlated with O_3 uptake status (F_{O_3}, W), followed by photosynthetic indicators (P_n, WUE, E_t, G_s, C_i) and growth indicators (ΔH, ΔDBH) and stomatal characteristics (K, M, S) under O_3 stress, some physiological indicators (L, F_v/F_m) were relatively weakly correlated with photosynthesis (P_n, WUE, E_t, G_s, C_i) and stomatal (K, M, S); (3) all the indicators of *Pinus bungeana* were significantly different under O_3 treatments of NF and NF80 ($P < 0.05$), ΔH, ΔDBH, M, CHL, P_n, G_s, W and F_{O_3} were most significantly different under NF and NF40 treatments, and K, S, WUE, F_v/F_m, E_t, C_i, L were more significantly different under NF40 and NF80 treatments. **Conclusion:** The experiment proved that the growth of *Pinus bungeana* was slowed, photosynthetic capacity was reduced, and the absorption capacity of O_3 was further reduced by long-term exposure to high concentration of O_3. The growth of *Pinus bungeana* was most correlated with the changes of O_3 absorption characteristics, and the stomatal characteristics were most correlated with photosynthetic physiological characteristics, and the reduction of photosynthetic capacity etc. further led to the curtailment of its growth.

Keywords: Pinus Bungeana; O_3 Stress; Growth; Physiological Characteristics; Ozone Uptake; Correlation

1. Introduction

ARTICLE INFO

Received: 3 March 2022
Accepted: 15 April 2022
Available online: 1 May 2022

Human activities have long influenced atmospheric ozone (O_3) concentrations, and from the last 100 years or so to the present, human activities have led to the increasing emissions of O_3 into the atmosphere[1]; tropospheric O_3 is one of the major air pollutants today, and its

precursors are generally nitrogen oxides (NO_x) and volatile organic compounds (VOCs), among others[2]. Due to accelerated urbanization, human activities have led to a large increase of O_3 precursors emitted into the atmosphere, creating conditions for an increase in near-surface O_3 concentrations. O_3-induced pollution is more serious in urban areas, especially in the urban agglomerations of Beijing-Tianjin-Hebei, Yangtze River Delta and Pearl River Delta in China[3,4]. In 2019, $PM_{2.5}$, PM_{10}, SO_2, NO_2, and CO decreased to varying degrees in 338 prefecture-level and above cities across China, only the O_3 concentration was 148 μg/m^3, a year-on-year increase of 6.5%[5], which has attracted academic attention. In recent years, O_3 concentrations have also been increasing year by year in Beijing[6], and monitoring results from the Beijing Municipal Environmental Protection Bureau show that from 2013–2015, the maximum daily (8 h) average O_3 concentration in Beijing increased from 183.4 μg/m^3 to 202.6 μg/m^3[7,8], and O_3 has become the primary pollutant in the region in summer; in 2017 May, the Ministry of Environmental Protection informed the media that according to the latest air quality forecast results, the primary pollutant in Beijing, Tianjin, Hebei and surrounding areas is O_3; the maximum daily 8-h sliding average 90th percentile concentration value of O_3 in Beijing in 2019 was 191 μg/m^3, exceeding the national secondary standard (160 μg/m^3) of 19.4%[9].

In recent years some scholars have applied other methods such as artificially controlled air chamber simulation experiments (closed O_3 fumigation experiment method, large artificial climate chamber method, open-top chambers (OTC), and also free-air gas concentration enrichment (FACE)) to study the damage of O_3 on crops and trees[10]. Several researchers have found from various indicators of individual plants that long-term exposure to O_3 results in a series of physiological changes, such as premature leaf decay and abscission, reduced number of stomata[11], reduced photosynthetic carbon fixation capacity, and reduced carbon assimilates in the return roots[12,13]. Schaub *et al.*[14] demonstrated that O_3 uptake affects photosynthesis and conductance of wild Prunus serotina, especially later in the growing season.

In Beijing, with the increasing O_3 pollution, the effect of O_3 on plants is also increasing. Through field observations, Wan *et al.*[15] found that a large number of trees, shrubs and herbaceous plant leaves in the suburbs of Beijing were damaged by O_3. With the premise that O_3 concentrations will continue to increase in the future, the degree of plant damage will also continue to increase[16]. The relationship between different O_3 concentrations on the indicators of *Pinus bungeana* is less studied and the extent of this effect is less explored. Which indicators of *Pinus bungeana* respond most rapidly at elevated O_3 concentrations, which indicators are most affected, and how these indicators affect the growth and development of *Pinus bungeana* are not clearly defineded and require in-depth analysis. To this end, this study investigates the

changes in growth, physiology, photosynthesis, and O_3 uptake indicators of *Pinus bungeana* under elevated O_3 concentrations using an open-top chambers, thus providing data and theoretical support for studying the response of trees to O_3 stress from a physiological perspective.

2. Materials and methods

2.1 Overview of the study site and experimental materials

The study site, Beijing Botanical Garden (39°48′N, 116°28′E), is located at the foot of the Fragrant Hill, with an altitude of 76 m, and belongs to temperate continental climate. The average annual temperature is 11.6 ℃, with an average temperature of -3.7 ℃ in January and 26.7 ℃ in July. The extreme high temperature is 41.3 ℃, the extreme low temperature is -17.5 ℃, the annual precipitation is 634.20 mm, and the relative humidity ranges from 43% to 79%. *Pinus bungeana* is a common landscaping species in North China and is widely planted in the study area. It is well adapted and resistant to adversity, and is an excellent tree species for afforestation in mountainous and semi-arid areas, as well as one of the preferred species for urban greening. In this study, *Pinus bungeana* seedlings were selected as the material for artificially controlled pot planting trials. The *Pinus bungeana* seedlings were all 3 years old, and some studies have shown that 3-year-old trees are in the early stages of growth and development, making the results more significant[17]. The seedlings pot has a diameter of 40 cm and a height of 50 cm. The size, crown width, basal diameter and height of *Pinus bungeana* seedlings in different air chambers were basically the same.

2.2 Experimental methods

Nine 3-year-old *Pinus bungeana* seedlings were placed in each open-top chamber (OTC). A total of 15 OTCs were set up, and the O_3 generator was used to control the O_3 concentration entering the chamber, and the O_3 generator outlet was equipped with an O_3 concentration detector BMT 964. One of the OTCs was fumigated without any O_3-related treatment at NF concentration (normal atmospheric O_3 concentration); the other two were fumigated at NF 40 (normal atmospheric O_3 concentration plus 40 nmol/mol) and NF 80 (normal atmospheric O_3 concentration plus 80 nmol/mol), respectively, and every three OTCs were grouped into five groups.

Table 1. Different processing methods in experiment

Types	Treatment steps
NF	Normal atmospheric O_3 concentration, no treatment
NF 40	Normal atmospheric O_3 concentration plus 40 nmlol/mol, growing season (May to October) Daily O_3 fumigation treatment from 8:00 to 16:00
NF 80	Normal atmospheric O_3 concentration plus 80 nmol/mol, growing season (May to October) daily O_3 fumigation treatment from 8:00 to 16:00

2.3 Determination of functional trait indexes

At the beginning and end of the experiment, the height and diameter at 50 cm of *Pinus bungeana* plants were measured with a ruler, and the difference was calculated to obtain the change in plant height (ΔH) and the change in diameter at 50 cm (ΔDBH), respectively. The number of stomata in the field of view was observed using an optical microscope, and the field of view area was calculated; the field density (M) = the average number of stomata in the field of view/field area in "per/mm^2". The actual size of stomata (S/μm^2) and stomatal opening (K/μm^2) can be obtained by the proportional method. The net photosynthetic rate (P_n/μmol·m^{-2}S^{-1}), transpiration rate (E_t/mnol·m^{-2}S^{-1}), intercellular CO_2 concentration (C_i/μmol·mmol^{-1}), and stomatal conductance (G_s/mnol·m^{-2}S^{-1}) of *Pinus bungeana* under different treatments were measured by CI340 photosynthesizer, and water utilization (WUE/μmol·mmol^{-1}), $WUE = P_n/E_t$ were calculated by equation. The chlorophyll content CHL/mg·g^{-1} was measured by spectrophotometer. The maximum photochemical efficiency F_v/F_m was determined using a Yaxin-1161G chlorophyll fluorometer; the relative conductivity (L) was obtained by measuring the initial and final conductivity values by a conductivity meter (DDS-307) to calculate the ratio. Whole-tree water consumption (W) and O_3 uptake rate (F_{O_3}) were determined and calculated by the trunk sap flow technique[18].

2.4 Data processing

The test data were organized using SPSS 24.0 software and Canoco 5.0 software, and cluster analysis, correlation analysis, redundancy analysis and one-way ANOVA were performed to investigate the correlation between the indicators and whether there were significant differences in the indicators under different O_3 concentration treatments to systematically evaluate the damage of different concentration gradients of O_3 on *Pinus bungeana*.

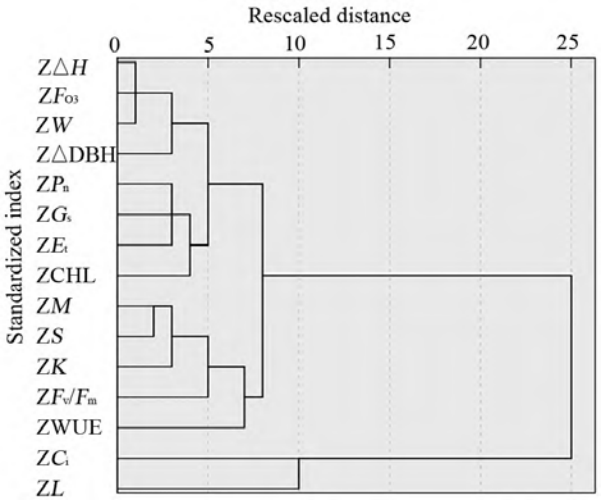

Figure1. Cluster analysis.

3. Results and analysis

3.1 Cluster analysis of each characteristic index of *Pinus bungeana* under O_3 stress

Using SPSS software, all the measured indicators were standardized and subjected to systematic cluster analysis (**Figure 1**). It was possible to classify the 15 indicators into categories 15, 13, 8, 7, 5, 4, 3, 2, and 1. To facilitate the integrated analysis and to combine the knowledge of plant physiology, we divided all the indicators tested into 5 major categories and 7 subcategories. The first category includes ΔH, F_{O_3}, W, ΔDBH, P_n, G_s, E_t and CHL, which are subdivided into ΔH, F_{O_3}, W, ΔDBH and P_n, G_s, E_t, and CHL; the second category is *M*, *K*, *S* and *F*v/*F*m; the third category is WUE; the fourth category is C_i; and the fifth category is *L*.

The first category of indicators mainly reflects the growth, O_3 absorption and photosynthesis capacity of *Pinus bungeana*, where plant height and diameter at 50 cm respond to the growth of *Pinus bungeana*, and water consumption and O_3 absorption rate respond to the O_3 absorption of *Pinus bungeana*. Typical correlation analysis showed a high positive correlation between the two data sets ($P < 0.001$) with a correlation of 0.998. This indicates that the variation in plant height (ΔH), O_3 uptake rate (F_{O_3}), water consumption (W) and diameter change at 50 cm (ΔDBH) show very similar changes with the increase of O_3 concentration. P_n, G_s, E_t and CHL responded to the photosynthetic physiological properties of *Pinus bungeana*, which were close to the growth status and O_3 uptake status from the intra-group mean linkage distance, indicating that some of the changes in photosynthetic physiological properties of *Pinus bungeana* may be closely related to its growth changes and O_3 uptake status.

The second group of indicators, *M*, *K*, *S* and F_v/F_m, mainly reflected the stomatal characteristics and maximum photochemical efficiency, which decreased with the increase of O_3 concentration. The correlation between stomatal indicators and F_v/F_m was positive, with a correlation coefficient of 0.946 ($P < 0.001$).

The third category of indicators was water use efficiency (WUE), which showed a gradual decrease with the increase of O_3 concentration.

The fourth category of indicators was intercellular CO_2 concentration (C_i), which gradually increased with the increase of O_3 concentration in *Pinus bungeana*. The fifth category of indicators is relative conductivity (*L*), and the closest indicator to its change is intercellular CO_2 concentration (C_i).

3.2 Correlations among the characteristic indicators of *Pinus bungeana* under O_3 stress

C_i and L were positive correlated with a correlation coefficients of 0.775, and negative with the other physiological factors (**Table 2**), indicating that the trend of the changes was the same with the increase of O_3 concentration, while the increase of intercellular CO_2 concentration (C_i) and relative conductivity (*L*) indicated that the leaf cell structure of *Pinus bungeana* might be damaged to some ex-

tent. Both ΔH and ΔDBH had the highest correlations with W, F_{O_3}, with correlation coefficients above 0.92, indicating that the uptake of O_3 and water depletion of *Pinus bungeana* significantly affected its own growth. M and K had the highest correlation with S, with correlation coefficients above 0.92, indicating that changes in stomatal density and openness were strongly correlated with stomatal size. WUE was highly correlated with G_s with a correlation coefficient of 0.79. The correlations between P_n, E_t and G_s were high with correlation coefficients greater than 0.91. These three indicators were closely related to the photosynthetic characteristics of *Pinus bungeana*, and the changes of the three were consistent with the increase of O_3 concentration. The results of redundancy analysis showed that C_i and L were highly positively correlated with O_3 concentration, while the rest of the indices were negatively correlated with the first three, and the photosynthetic physiological characteristics such as WUE, CHL, P_n, E_t were the most correlated with O_3 concentration, and the photosynthetic performance of *Pinus bungeana* became lower and lower with the increase of O_3 concentration.

Table 2. Correlation analysis of indices of *Pinus bungeana*

Index	ΔH	ADBH	M	K	S	WUE	P_n	E_t	G_s	C_i	F_v/F_m	CHL	L	W	F_{O_3}
ΔH	1														
ADBH	0.889	1													
M	0.727	0.836	1												
K	0.728	0.758	0.883	1											
S	0.823	0.891	0.963	0.924	1										
WUE	0.649	0.798	0.819	0.735	0.846	1									
P_n	0.83	0.817	0.784	0.802	0.86	0.652	1								
E_t	0.821	0.815	0.743	0.744	0.817	0.71	0.928	1							
G_s	0.888	0.842	0.827	0.857	0.915	0.789	0.932	0.91	1						
C_i	-0.787	-0.882	-0.821	-0.8	-0.876	-0.81	-0.929	-0.953	-0.908	1					
F_v/F_m	0.728	0.76	0.826	0.875	0.919	0.695	0.851	0.769	0.879	-0.797	1				
CHL	0.819	0.78	0.826	0.781	0.859	0.675	0.879	0.844	0.914	-0.814	0.833	1			
L	-0.708	-0.763	-0.859	-0.878	-0.851	-0.733	-0.74	-0.715	-0.791	0.775	-0.787	-0.733	1		
W	0.98	0.921	0.808	0.772	0.872	0.699	0.867	0.863	0.909	-0.842	0.761	0.87	-0.755	1	
F_{O_3}	0.991	0.92	0.744	0.75	0.849	0.697	0.827	0.832	0.894	-0.815	0.755	0.821	-0.707	0.972	1

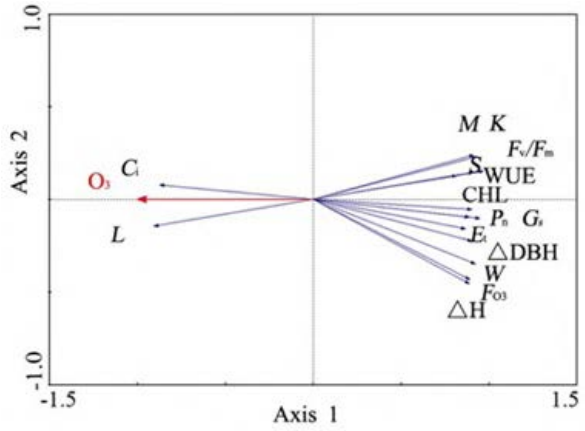

Figure 2. RDA sequence of O_3 and the growth, physiology and uptake characteristics of *Pinus bungeana*.

3.3 The effects of different varied O_3 concentrations on *Pinus bungeana*

The results of chi-square test showed that the variation of plant height (ΔH), transpiration rate (E_t) and intercellular CO_2 concentration (C_i) did not meet the chi-square test ($P < 0.05$), while the rest of the indicators passed the chi-square test. These indicators were subjected to ANOVA to obtain the differences in indicator values of *Pinus bungeana* under different treatments.

In the control test, the differences in all indicators of *Pinus bungeana* varied significantly ($P < 0.001$), indicating that the high O_3 concentration had a large effect on all indicators tested in the test (**Table 3**). The F values were ranked in order of magnitude:$F_{O_3} > W > S > M > G_s >$ K > ΔDBH > F_v/F_m > L > CHL > P_n> WUE, indicating that O_3 uptake characteristics and stomatal changes were the most sensitive and responsive under NF, NF40

and NF80 treatments, followed by the growth condition of *Pinus bungeana* and finally the physiological and photosynthetic characteristics.

Table 3. Single factor variance analysis

Index	Group	Square sum	Freedom	Mean square	Mean square	Significance
ΔDBH	Between groups	0.624	2	0.312	40.133	0.000
	Within group	0.093	12	0.008		
	Total	0.717	14			
M	Intergroup	58,677.271	2	29,338.636	63.085	0.000
	Within group	5,580.785	12	465.065		
	Total	64,258.056	14			
K	Intergroup	14,533.211	2	7,266.606	46.204	0.000
	Within group	1,887.246	12	157.271		
	Total	16,420.457	14			
S	Intergroup	60,601.615	2	30,300.807	204.818	0.000
	Within group	1,775.282	12	147.940		
	Total	62,376.897	14			
WUE	Between groups	0.050	2	0.025	13.455	0.001
	Within group	0.022	12	0.002		
	Total	0.073	14			
P_n	Between groups	3.237	2	1.619	22.819	0.000
	Within group	0.851	12	0.071		
	Total	4.088	14			
G_s	Between groups	388.872	2	194.436	60.243	0.000
	Within group	38.731	12	3.228		
	Total	427.603	14			
F_v/F_m	Between groups	0.017	2	0.009	39.141	0.000
	Within group	0.003	12	0.000		
	Total	0.020	14			
CHL	Between groups	2.231	2	1.115	24.805	0.000
	Within group	0.540	12	0.045		
	Total	2.771	14			
L	Between groups	49.890	2	24.945	30.213	0.000
	Within group	9.908	12	0.826		
	Total	59.798	14			
W	Intergroup	0.209	2	0.105	307.373	0.000
	Within group	0.004	12	0.000		
	Total	0.213	14			
F_{O_3}	Between groups	3,172.262	2	1,586.131	450.051	0.000
	Within group	42.292	12	3.524		
	Total	3,214.554	14			

Since plant height change (Δ*H*), transpiration rate (E_t) and intercellular CO_2 concentration (C_i) did not satisfy chi-square ($P < 0.05$), non-chi-square multiple comparisons were used (**Table 4**). The height changes (Δ*H*) of *Pinus bungeana* seedlings under different O_3 concentration treatments showed significant differences ($P < 0.05$), with highly significant differences ($P < 0.001$) between the height changes (Δ*H*) of *Pinus bungeana* seedlings in the NF gas chamber compared with the NF40 and NF80 gas chambers, and relatively small differences in ΔH between the NF40 and NF80 treatments. In contrast, the differences in transpiration rate (E_t) and intercellular CO_2 (C_i) concentrations were the opposite, with the most significant differences under NF40 and NF80 treatments ($P < 0.001$), followed by NF and NF80 treatments, and non-significant differences under NF and NF40 treatments ($P > 0.05$).

Table 4. Non-homogeneous multiple comparison

Dependent variable				(I-J) Mean value difference	Standard error	Significance	95% confidence interval	
							Lower limit	Upper limit
ΔH	Tamheni	NF	NF40	4.85393*	0.17787	0.000	4.1706	5.5373
			NF80	5.01060*	0.17990	0.000	4.3355	5.6857
		NF40	NF80	0.15667*	0.04629	0.033	0.0135	0.2998
E_t tamheni	Tamheni	NF	NF40	0.28700	0.08376	0.059	-0.0131	0.5871
			NF80	0.42500*	0.08224	0.014	0.1207	0.7293
		NF40	NF80	0.13800*	0.03225	0.009	0.0397	0.2363
C_i tamheni	Tamheni	NF	NF40	-28.91200	9.02670	0.087	-63.1628	5.3388
			NF80	-52.02600*	9.42784	0.008	-85.1489	-18.9031
		NF40	NF80	-23.11400*	3.59442	0.002	-34.8660	-11.3620

Table 5. Multiple comparisons

Dependent variable				Mean value significance	Standard error	Significance	95% confidence interval	
							Lower limit	Upper limit
ΔDBH	LSD	NF	NF40	0.35667*	0.05577	0.000	0.2352	0.4782
			NF80	0.48133*	0.05577	0.000	0.3598	0.6028
		NF40	NF80	0.12467*	0.05577	0.045	0.0032	0.2462
M	LSD	NF	NF40	48.19933*	13.63914	0.004	18.4822	77.9165
			NF80	150.03933*	13.63914	0.000	120.3222	179.7565
		NF40	NF80	101.84000*	13.63914	0.000	72.1229	131.5571
K	LSD	NF	NF40	25.09933*	7.93147	0.008	7.8181	42.3805
			NF80	74.89933*	7.93147	0.000	57.6181	92.1805
		NF40	NF80	49.80000*	7.93147	0.000	32.5188	67.0812
S	LSD	NF	NF40	66.13333*	7.69260	0.000	49.3726	82.8941
			NF80	155.13333*	7.69260	0.000	138.3726	171.8941
		NF40	NF80	89.00000*	7.69260	0.000	72.2393	105.7607
WUE	LSD	NF	NF40	0.05098	0.02735	0.087	-0.0086	0.1106
			NF80	0.14016*	0.02735	0.000	0.0806	0.1997
		NF40	NF80	0.08918*	0.02735	0.007	0.0296	0.1488
P_n	LSD	NF	NF40	0.69400*	0.16844	0.001	0.3270	1.0610
			NF80	1.12800*	0.16844	0.000	0.7610	1.4950
		NF40	NF80	0.43400*	0.16844	0.024	0.0670	0.8010
G_s	LSD	NF	NF40	7.47900*	1.13623	0.000	5.0034	9.9546
			NF80	12.38300*	1.13623	0.000	9.9074	14.8586
		NF40	NF80	4.90400*	1.13623	0.001	2.4284	7.3796
F_v/F_m	LSD	NF	NF40	0.02813*	0.00935	0.011	0.0078	0.0485
			NF80	0.08147*	0.00935	0.000	0.0611	0.1018
		NF40	NF80	0.05333*	0.00935	0.000	0.0330	0.0737
CHL	LSD	NF	NF40	0.56133*	0.13412	0.001	0.2691	0.8536
			NF80	0.93867*	0.13412	0.000	0.6464	1.2309
		NF40	NF80	0.37733*	0.13412	0.016	0.0851	0.6696
L	LSD	NF	NF40	-1.53133*	0.57468	0.021	-2.7835	-0.2792
			NF80	-4.40000*	0.57468	0.000	-5.6521	-3.1479
		NF40	NF80	-2.86867*	0.57468	0.000	-4.1208	-1.6165
W	LSD	NF	NF40	0.22800*	0.01166	0.000	0.2026	0.2534
			NF80	0.26800*	0.01166	0.000	0.2426	0.2934
		NF40	NF80	0.04000*	0.01166	0.005	0.0146	0.0654
F_{O_3}	LSD	NF	NF40	29.72600*	1.18732	0.000	27.1390	32.3130
			NF80	31.86160*	1.18732	0.000	29.2746	34.4486
		NF40	NF80	2.13560	1.18732	0.097	-0.4514	4.7226

The differences of the remaining indicators under different treatments were compared by

chi-square analysis of variance (**Table 5**), and the differences of ΔDBH under NF and NF40, NF and NF80 treatments were highly significant (P < 0.001), and the differences of ΔDBH under NF40 and NF80 treatments were smaller, indicating that the growth of *Pinus bungeana* had been more significantly inhibited under NF40 treatment; K and S were significantly different in NF, NF40 and K and S were significantly different (P < 0.001) under NF, NF40 and NF80 treatments, indicating that stomatal characteristics were most actively changed under different ozone concentrations, with the most significant differences in K and S under the O_3 concentration treatments of NF and NF80, followed by NF40 and NF80; M was more significantly different (P < 0.05) under NF and NF40 treatments; WUE was the most different under NF and NF80 treatments, followed by NF40 and NF80. The difference between NF and NF40 was not significant (P > 0.05), indicating that water utilization of *Pinus bungeana* was significantly reduced only under higher concentrations of O_3 stress; P_n and G_s were the most different under NF and NF80 treatments (P < 0.001), more significant under NF and NF40 treatments (P < 0.05), and relatively small differences under NF40 and NF80 treatments; F_v/F_m had the least significant differences under NF and NF40 treatments, significant differences under NF40 compared to NF80 F_v/F_m, and the most significant differences between NF and NF80 (P < 0.001); CHL had the most significant differences under NF and NF80 treatments, followed by NF and NF40, and the smallest difference between NF40 and NF80; L was the least significant difference under NF and NF40 treatment, while the other two groups were significantly different in comparison (P < 0.001); W and F_{O_3} were less different under NF40 and NF80 treatment, where W was more significant (P < 0.05) in both groups, F_{O_3} was not significant (P > 0.05), and W and F_{O_3} showed larger difference under the treatment of NF and the other two groups.

4. Discussion

Throughout the experimental period, it could be measured that the growth indicators of *Pinus bungeana* showed differences with different concentrations of O_3 fumigation treatments, with the height and diameter of *Pinus bungeana* plants under NF80 treatment being lower than NF40, and those under NF40 treatment being lower than NF, indicating that O_3 inhibited the growth of *Pinus bungeana* seedlings. This is consistant with the results of hybrid poplar *Populus tremula* × *P. Tremuloides* conducted by Niu *et al*.[19], in which the plant height, diameter, and biomass of hybrid poplar under the influence of O_3 were lower than the values in normal environment. Cluster analysis, correlation analysis, and redundancy analysis revealed that *Pinus bungeana* growth indicators (Δ*H*, ΔDBH) had the highest correlation with O_3 uptake status (F_{O_3}, W), which is due to the fact that O_3 entering the plant affects the function of various parts, thus leading to a reduction in water uptake by the plant and a certain effect on the supply of plant organs, which can further lead to the slow growth of plant.

Stomata are the main channels through which gases enter the plant. Generally speaking, the larger the stomatal opening and size, the more O_3 will enter the plant; when the tolerance limit of the plant body is exceeded, the plant will narrow the stomata. This was confirmed by the experimental results, where the stomatal density, opening and size of *Pinus bungeana* were reduced under the treatment of NF, NF40 and NF80 concentrations of O_3. It has been pointed out that stomatal density tends to increase with the increase of pollution in urban environments, while stomatal area and stomatal opening decrease[20], probably because the nature of O_3 involved in this study is quite different from that of $PM_{2.5}$ and PM_{10} in the environment, and in urban polluted atmospheres, some stomata are blocked by suspended particulates affecting the water vapor exchange process of plants, and the adoption of increasing the number of stomata to compensate is also possible . It has also been shown that elevated O_3 concentrations reduce stomatal flexibility, making stomata less responsive to the external environment[21-23]. The response rate of stomatal closure and the amount of O_3 entry are related to the sensitivity of different tree species to

O_3, and the more sensitive species have smaller tolerance values at the same O_3 concentration, which may cause a failure of cellular defense of the plant, not only increasing stomatal opening and size, but also making the plant unable to close stomata quickly. This does not occur for *Pinus bungeana* in the test which may be due to the fact that the stomatal size and opening of *Pinus bungeana* are lower than those of trees with wider leaves, and they inhale less in the same concentration of O_3 and have higher tolerance values. Stomatal characteristics (*K*, *M*, *S*) and photosynthetic physiological indicators (P_n, WUE, E_t, G_s, C_i, CHL, F_v/F_m, *L*) correlated the most, because plant leaves are the main site of photosynthesis, and stomata are the main channel for O_3 to enter the leaves, and as O_3 concentration increases, the stomatal size, density and opening of plants gradually decrease, which will lead to a large reduction of CO_2 entering the leaves, thus reducing the photosynthetic rate, transpiration rate, stomatal conductance and water use efficiency of plants.

Photosynthesis is the most basic physiological process of plants, and the effect of long-term O_3 environment on plants is also expressed in photosynthetic properties. The decrease in stomatal conductance (G_s) leads to an increase in stomatal resistance, making it difficult for CO_2 and H_2O to enter the plant, which further affects changes in transpiration rate (E_t) and water consumption (WUE). Chlorophyll content (CHL) is an important indicator of the photosynthetic capacity of trees and has an impact on plant photosynthetic rate and primary productivity[24], and it was found that the CHL of *Pinus bungeana* decreased with the increase of O_3 concentration because O_3 can damage the structure and components of chloroplasts[25-27]. The experimental results showed that increasing O_3 concentration led to a significant decrease in G_s, $E_t$and WUE of *Pinus bungeana*. Photosynthetic rate reflects the photosynthesis ability of the plant under certain environment, and the study showed that the net photosynthetic rate (P_n) of *Pinus bungeana* decreased by 11.71% and 18.81% under O_3 treatment with NF40 and NF80 concentrations, respectively. In contrast, the intercellular CO_2 concentration (C_i) of *Pinus bungeana* increased with the increase of O_3 concentration in the experiment, indicating that the factors causing the decrease in photosynthetic capacity of *Pinus bungeana* were mainly non-stomatal factors. The Photosynthetic physiological indicators (P_n, WUE, E_t, G_s, C_i, CHL, F_v/F_m, *L*) of *Pinus bungeana* were higher in correlation with growth indicators (ΔH, ΔDBH), stomatal characteristics (*K*, *M*, *S*). In contrast, the intercellular CO_2 concentration increased significantly with the increase of O_3 concentration in this experiment, indicating that the factors causing the reduction of photosynthetic indexes such as photosynthetic rate in *Pinus bungeana* are not only stomatal factors, but may be caused by non-stomatal factors such as reduced assimilation capacity of leaf pulp cells[28]. In addition, it has been shown that O_3 elevation blocks the photosynthetic electron transport chain[29] and reduces the chlorophyll fluorescence parameter F_v/F_m (maximum photochemical quantum yield), which is consistent with the findings in this experiment on *Pinus bungeana*, where chlorophyll decomposition under O_3, a strong oxidant, leads to an impairment of plant photosynthesis, which also further contributes to a decrease in maximum photochemical rates (F_v/F_m) etc. The magnitude of relative conductivity (*L*) reflects the degree of plant cell membrane damage, and the degree of injury to the membrane system of plants can be understood by measuring the value of the relative conductivity change in plants[30]. This study showed that the *L* value of *Pinus bungeana* gradually increased with the increase of O_3 concentration, which is because O_3 is a strong oxidant that can change membrane permeability, and O_3 entered the leaves through the stomata, the cell membrane was damaged, and the relative conductivity (*L*) then increased, indicating that the cell membrane of *Pinus bungeana* leaves had been significantly damaged. Compared with the NF concentration, the water use efficiency (WUE) decreased by 2.62% and 6.70% under NF40 and NF80, respectively, indicating that the increased O_3 concentration inhibited the water consumption of *Pinus bungeana*. The reduced photosynthetic capacity then made it difficult to maintain the nutrients required for normal plant growth, further leading to

slower plant growth.

By comparing the growth of *Pinus bungeana* in different air chambers, it was found that the differences in all indicators of *Pinus bungeana* under O_3 treatment of NF and NF80 were significant ($P < 0.05$), indicating that *Pinus bungeana* would respond more significantly to a significant increase in O_3 concentration. Some indicators (ΔH, ΔDBH, M, CHL, P_n, G_s, W and F_{O_3}) showed a more pronounced response when the O_3 concentration was increased to NF40, and showed less significant differences in the higher concentration treatments, indicating that the NF40 concentration gradient affected more the growth and O_3 uptake of *Pinus bungeana* and stomatal density and part of the photosynthetic capacity. While some indicators (K, S, WUE, F_v/F_m, E_t, C_i, L) showed more significant differences under NF40 and NF80 treatments, and relatively less significant differences under NF and NF40 treatments, on the one hand, suggesting that *Pinus bungeana* has a certain resistance to O_3, because NF40 concentration is already close to the O_3-induced; on the one hand, it indicates that *Pinus bungeana* has some resistance to O_3, because NF40 concentration is already close to the threshold of O_3-induced plant injury, and even NF80 already exceeds the threshold of causing plant injury[31]; on the other hand, it indicates that the increase of O_3 concentration to NF80 will have a greater effect on the physiological characteristics, stomatal characteristics and some photosynthesis ability of *Pinus bungeana*.

In this study, only two O_3 concentration gradients were selected for control tests with normal ambient atmospheric O_3 concentrations, and the thresholds were floating values, influenced by the atmospheric O_3 concentrations in the normal environment; only the correlations between growth, photosynthesis, some physiological indicators and absorption characteristics under O_3 stress were studied, and no tests and measurements were performed for their resistance indicators. Pre-treatment of normal ambient O_3 in open-topchambers to achieve relatively consistent and stable concentrations; refinement of the O_3 concentration gradient to study and compare the thresholds of changes in each index, and incorporation of quantitative analysis of resistance (antioxidant system) of *Pinus bungeana* under O_3 stress will be the next research direction.

5. Conclusion

In this study, the functional traits of *Pinus bungeana* were analyzed in response to different concentrations of O_3 stress, and the following conclusions were drawn.

(1) The plant height growth (ΔH), diameter growth at 50 cm (ΔDBH), stomatal size (S), stomatal density (M) stomatal opening (K), stomatal conductance (G_s), net photosynthetic rate (P_n), transpiration rate (E_t), water use efficiency (WUE), maximum photochemical efficiency (F_v/F_m)), chlorophyll content (CHL), whole-tree water consumption (W), and O_3 uptake rate (F_{O_3}) all decreased with the increase of O_3 concentration, while intercellular CO_2 concentration (C_i) and relative conductivity increased with the increase of O_3 concentration.

(2) The correlation between growth indicators (ΔH, ΔDBH) and O_3 uptake (F_{O_3}, W) was highest in *Pinus bungeana* under O_3 stress, followed by photosynthetic indicators (P_n, WUE, E_t, G_s, C_i) and growth indicators (ΔH, ΔDBH) and stomatal characteristics (K, M, S), and some physiological indicators (L, F_v/F_m) were relatively weakly correlated with photosynthesis (P_n, WUE, E_t, G_s, C_i) and stomata (K, M, S).

(3) There was a close relationship between O_3 and functional traits of *Pinus bungeana* plants. Compared to NF concentration, *Pinus bungeana* growth (ΔH, ΔDBH) and O_3 uptake (W and F_{O_3}), as well as stomatal density (M) and some photosynthetic capacity (P_n ,G_s) indicators were significantly reduced at NF40 concentration compared to NF concentration; the physiological properties (F_v/F_m, L), stomatal properties (K, S) and some photosynthetic properties (WUE, E_t, C_i) of *Pinus bungeana* produced more significant differences at NF80 concentration compared to NF40 concentration.

(4) During the experimental period, *Pi-*

nus bungeana did not stop growing even under NF80 concentration, nor did it show delayed or dysregulated stomatal response, indicating that it could still maintain the balance between its own growth and internal material cycle by adjusting leaf functional traits under O_3 stress conditions, which also tentatively proved its certain resistance to O_3.

Acknowledgement

Supported by the National Natural Science Foundation of China (31500352); the Dean's Fund of Beijing Academy of Forestry and Fruit Tree Science (201903); the Youth Fund of Beijing Academy of Agriculture and Forestry (QNJJ202017).

Conflict of interest

The authors declare that they have no conflict of interest.

References

1. Ainsworth EA, Lemonnier P, Wedow JM. The influence of rising tropospheric carbon dioxide and ozone on plant productivity. Plant Biology 2020; 22(Suppl.1): 5–11.
2. Wang T, Xue L, Brimblecombe P, *et al*. Ozone pollution in China: A review of concentrations, meteorological influences, chemical precursors, and effects. Science of the Total Environment 2017; 575: 1582–1596.
3. Ma J, Chu B, Liu J, *et al*. NOx promotion of SO_2 conversion to sulfate: An important mechanism for the occurrence of heavy haze during winter in Beijing. Environmental Pollution 2018; 233: 662–669.
4. Yang Y, Liu X, Qu Y, *et al*. Formation mechanism of continuous extreme haze episodes in the megacity Beijing, China, in January 2013. Atmospheric Research 2015; 155: 192–203.
5. Ministry of Ecology and Environment of the People's Republic of China. Report on the state of the ecology and environment in China 2019. Beijing: Ministry of Ecology and Environment of the People's Republic of China; 2020.
6. Li K, Jacob DJ, Liao H, *et Al*. Anthropogenic drivers of 2013–2017 trends in summer surface ozone in China. Proceedings of the National Academy of Sciences 2019; 116(2): 422–427.
7. Beijing Municipal Ecological and Environment Bureau. Beijing Environmental Statement 2013. Beijing: Beijing Municipal Ecological and Environment Bureau; 2014.
8. Beijing Municipal Ecological and Environment Bureau. Beijing Environmental Statement 2015. Beijing: Beijing Municipal Ecological and Environment Bureau; 2016.
9. Beijing Municipal Ecological and Environment Bureau. Beijing Ecology and Environment Statement 2019. Beijing: Beijing Municipal Ecological and Environment Bureau; 2020.
10. Galant A, Koester RP, Ainsworth EA, *et al*. From climate change to molecular response: Redox proteomics of ozone-induced responses in soybean. New Phytologist 2012; 194(1): 220–229.
11. Wilkinson S, Mills G, Illidge R, *et al*. How is ozone pollution reducing our food supply. Journal of Experimental Botany 2012; 63(2): 527–536.
12. Yamaguchi M, Watanabe M, Matsumura H, *et al*. Experimental studies on the effects of ozone on growth and photosynthetic activity of Japanese forest tree species. Asian Journal of Atmospheric Environment 2011; 5(2): 65–78.
13. Agathokleous E, Saitanis CJ, Wang XN, *et al*. A review study on past 40 years of research on effects of tropospheric O_3 on belowground structure, functioning, and processes of trees: A linkage with potential ecological implications. Water, Air & Soil Pollution 2016; 227(1): 1–28.
14. Schaub M, Skelly JM, Zhang JW, *et al*. Physiological and foliar symptom response in the crowns of Prunus serotina, Fraxinus americana and Acer rubrum canopy trees to ambient ozone under forest conditions. Environmental Pollution 2005; 133(3): 553–567.
15. Wan W, Xia Y, Zhang H, *et al*. The ambient ozone pollution and foliar injury of the sensitive woody plants in Beijing exurban region. Acta Ecologica Sinica 2013; 33(4): 1098–1105.
16. Galloway JN, Townsend AR, Erisman JW, *et al*. Transformation of the nitrogen cycle: Recent trends, questions, and potential solutions. Science 2008; 320(5878): 889–892.
17. Li P, Feng Z, Shang B, *et al*. Stomatal characteristics and ozone dose-response relationships for six greening tree species. Acta Ecologica Sinica 2018; 38(8): 2710–2721.
18. Chen B, Li S, Lu S. Ozone uptake characteristics in different dominance hierarchies of poplar plantation. Journal of Beijing Forestry University 2015; 37(7): 29–36.
19. Niu J. Effects of elevated ozone and nitrogen deposition on the growth and physiology of *Cinnamomum camphora* seedlings [PhD thesis]. Beijing: Chinese Academy of Sciences; 2012.
20. Zhu J, Xu C, Qin G, *et al*. Responses of leaf functional characters of three typical greening plants to air pollution and leaf economic spectrum analysis: A Beijing city as the study case. Journal of Central South University of Forestry & Technology 2019; 39(3): 91–98.
21. Hoshika Y, Carriero G, Feng ZZ, *et al*. Determinants of stomatal sluggishness in ozone-exposed deciduous tree species. Science of the Total Environment 2014; 481: 453–458.
22. Hoshika Y, Omasa K, Paoletti E. Both ozone expo-

sure and soil water stress are able to induce stomatal sluggishness. Environmental and Experimental Botany 2013; 88 (Suppl.1): 19–23.
23. Paoletti E, Grulke NE. Ozone exposure and stomatal sluggishness in different plant physiognomic classes. Environmental Pollution 2010; 158(8): 2664–2671.
24. Cao X, Run L. The exploration of the purification of automobile exhausts contamination by plants. Journal of Central South University of Forestry & Technology 2007; 27(2): 133–136.
25. Pang J, Kobayashi K, Zhu JG. Yield and photosynthetic characteristics of flag leaves in Chinese rice (Oryza sativa) varieties subjected to free-air release of ozone. Agriculture, Ecosystems and Environment 2009; 132(3): 203–211.
26. Feng ZZ, Kobayashi K, Ainsworth E. Impact of elevated ozone concentration on growth, physiology, and yield of wheat (Triticum aestivum). Global Change Biology 2008; 14: 2696–2708.
27. Calatayud A, Barreno E. Response to ozone in two lettuce varieties on chlorophyll a fluorescence, photosynthetic pigments and lipid peroxidation. Plant Physiology and Biochemistry 2004; 42(6): 549–555.
28. Xin Y, Shang B, Chen X, *et al*. Effects of elevated ozone and nitrogen deposition on photosynthetic characteristics and biomass of *Populus cathayana*. Environmental Science 2016; 37(9): 3642–3649.
29. Feng Z, Li P, Yuan X, *et al*. Progress in ecological and environmental effects of ground-level O_3 in China. Acta Ecologica Sinica 2018; 38(5): 1530–1541.
30. Liu D, Zhao S, Wang X, *et al*. The effect of ozone on the leaf damages symptom and physiological characteristics of landscape plants. Zhang Q (editor). China Ornamental Horticulture Symposium 2015; 2015 Aug 18–20; Fujian, Xiamen. Beijing: China Forestry Publishing House; 2015. p. 507–512.
31. Zhang W. Effects of elevated O_3 level on the native tree species in subtropical China [PhD thesis]. Beijing: Research Center for Eco-Environmental Sciences, Chinese Academy of Sciences; 2011.

Sustainable Forestry (2022) Volume 5 Issue 1
doi:10.24294/sf.v5i1.1620

ORIGINAL RESEARCH ARTICLE

Effects of interplanting native species of *Eucalyptus* on stand growth and soil physicochemical properties under different interplanting intensities

Muyi Huang[1], Yanfang Liang[2], Fucong Su[2], Yuanli Zhu[2], Zhihui Li[1*], Liling Liu[1], Suya Zhao[1], Yingyun Gong[1]

[1] *College of Forestry, Central South University of Forestry & Technology, Changsha 410004, China. E-mail: lzh1957@126.com*

[2] *Guangxi Qipo State Forestry Farm, Nangning 530003, China.*

ABSTRACT

Objective: To study the growth, accumulation and soil nutrient content of each overseeded species under different interharvesting intensity treatments of *Eucalyptus*, and to explore the best re-cultivation method suitable for mixed overseeded species after *Eucalyptus* interharvesting. **Methods:** In Guangxi state-owned Qipo forest, *Eucalyptus* tailorii with different planting densities (DH32-29) were mixed with *Castanopsis hystrix*, *Mytilaria laosensis* and *Michelia macclurei*, and four different treatments (CK, LT, MT and HT) were established for re-cultivation of *Eucalyptus* near-mature forests with different logging intensities, and the differences in growth conditions and soil physicochemical properties of each species were analyzed. **Results:** (1) As the proportion of *Eucalyptus* allocation decreased, the growth of *Eucalyptus* diameter at breast height, tree height and individual wood volume could be promoted; the growth of the three parameters of HT and MT *Eucalyptus* were significantly different from LT and CK. (2) The average wood volume per plant of the set species in the CK and LT treatments was *Mytilaria laosensis* > *Michelia macclurei* > *Castanopsis hystrix*, while in the MT and HT treatments it was *Mytilaria laosensis* > *Castanopsis hystrix* > *Michelia macclurei*. (3) The differences in soil aeration, total saturated water holding capacity, capillary water holding capacity, and field water holding capacity in soil layers of different depth varied. In the same soil layer, soil aeration, total porosity and capillary porosity were HT > CK > LT > MT; saturated water holding capacity and capillary water holding capacity were HT > CK > LT > MT, while field water holding capacity was CK > HT > LT > MT. (4) Organic matter, pH, total nitrogen, total phosphorus, total potassium, fast-acting nitrogen, fast-acting phosphorus, and fast-acting potassium changed with varying soil depth in each treatment.

Keywords: *Eucalyptus urophylla×E. grandis DH32-29*; Interplanting Setts; Stand Growth; Stand Structure; Soil Physicochemical Properties

ARTICLE INFO

Received: 20 March 2022
Accepted: 3 May 2022
Available online: 15 May 2022

1. Introduction

Eucalyptus is an important fast-growing and productive tree species in the world, with characteristics such as high adaptability, fast growth rate, high resistance, excellent material and wide use[1]. In recent years, in order to solve the problems of soil acidification, reduced enzyme activity, reduced biodiversity and decreased productivity caused by continuous planting of *Eucalyptus*[2-6], pure or mixed forests of *Eucalyptus* have been established to suit the characteristics of southern forest lands in China. *Eucalyptus* artificial mixed forests can make full use of the forest land, improve the forest environment, enhance resistance to resistance, promote the growth of forest trees, and improve the ecological and economic benefits of forest stands[7-9]. The cultiva-

tion mode of *Eucalyptus* intercalation with mixed species is the best way to re-cultivate *Eucalyptus* pure forests, and improving stand structure and regulating interspecific relationships through intercalation is the key to management[10]. The interplanting of near mature eucalypts with high quality broadleaf species to form a heterogeneous complex mixed forest can improve the yield per unit area, target the cultivation of *Eucalyptus* large-diameter timber, and make full use of the forest space, which is an ideal *Eucalyptus* mixed cultivation mode.

Eucalyptus urophylla×*E. grandis DH32-29* is an excellent variety of *Eucalyptus tailorii*, which is fast-growing and productive with a straight and complete trunk, and is superior to *Eucalyptus* caudatum in terms of stand growth and economic benefits, and is commonly planted in Guangxi and Guangdong[11]. *Mytilaria laosensis*, *Castanopsis hystrix* and *Michelia macclurei* are excellent native species in Guangxi with strong adaptability and can also change the environment of the plantation site[12-15]. In order to explore the best mixed growth pattern of *Eucalyptus* near mature forests, transform *Eucalyptus* low-quality and inefficient forests, achieve precise quality improvement of *Eucalyptus* plantations and sustainable use of forest land in the future, and bring into play the multiple functions of *Eucalyptus* plantations. In this study, we selected *Mytilaria laosensis*, *Castanopsis hystrix* and *Michelia macclurei*, which have good shade tolerance in young age, as hybrid species to transform and cultivate *Eucalyptus* plantation hybrid forests, and explored the effects of different intercutting intensities of *Eucalyptus* on stand growth and soil quality in the conversion of *Eucalyptus* near mature forests in terms of the growth status, accumulation volume and soil nutrients of each species in different hybrid patterns, with a view to providing reference for the cultivation of *Eucalyptus* pure forests.

2. Materials and methods

2.1 Overview of the study area

The study area is located in the state-owned Qipo Forest Farm, Nanning City, Guangxi Zhuang Autonomous Region (22°41′–22°52′N, 108°02′–108°09′E). The area has a humid subtropical monsoon climate with sufficient sunshine, abundant precipitation, distinct dry and wet seasons, long summer rainfall, average annual precipitation of 1,300 mm, average annual relative humidity of 80%, and average annual temperature of 21.6 ℃. The soil type is mainly red loam with a thickness of 1 m or more; the surface vegetation is rich, It is mainly composed of *Verbenaceae*, *Araliaceae*, *Lauraceae*, *Moraceae*, *Dennstaedtiaceae*, *Euphorbiaceae*, and *Rutaceae*.

2.2 Sample plot setting and management design

The target of re-cultivation is near-mature *Eucalyptus urophylla*×*E. grandis clone DH32–29*. All the *Eucalyptus* plantations plot in the study area were planted in 2010 with a planting density of 1,667 plants /hm^2 and all the interplanting measures were carried out in 2012. The thinning method adopts the lower layer thinning method. According to the thinning intensity, the trees with poor growth and poor dry shape are preferentially felled, and at the same time, the uniformity of the space position of the reserved wood is taken into account. In October 2014, plots with the same elevation, slope and orientation were selected to investigate the species, diameter at breast height, height and crown width of each tree in the sample plots before the mixed forest conversion operation. Each sample plot was set up with an area of 20 m × 20 m. A total of 12 sample plots, including control plots, were set up. The sample plots were investigated for stand diameter at breast height, tree height, height under branches, crown width, stem shape quality, stand composition, stand structure, understory regeneration and its soil nutrients. The stands were divided into four different re-cultivation types for the re-cultivation operation in October 2015: HT (400–450 plants/hm^2 retained after thinning), MT (750–800 plants/hm^2 retained after thinning), LT (1,200–1,250 plants/hm^2 retained after thinning) and CK (1,500–1,550 plants/hm^2). After clearing the felling residue properly, blocks were prepared and then planted with high quality trees, such as *Mytilaria laosensis*, *Castanopsis hystrix* and *Michelia macclurei*, using

Table 1. General situation and management operation of each sample plot

Stand	Sample plot	Slope/(°)	Altitude/m	Pre-thinning density/(plant·hm^{-2})	Planed density/(plant·hm^{-2})	Post-thinning density/(plant·hm^{-2})	(2020) average DBH/cm	(2020) average tree height/m
HT	QP–1	15–20	140	1,061	400–450	411	24.75	30.30
MT	QP–2	15–20	160	1,042	750–800	731	24.53	28.91
LT	QP–3	15–20	170	1,326	1200–1250	1,224	20.53	25.65
CK	QP–4	15–20	155	1,512	1,512	1,512	17.46	24.10

1-year old live seedlings, and planting holes were dug in the planting zone with the specifications of 50 cm × 50 cm × 30 cm, where the planting density ratio of each treatment of *Mytilaria laosensis*, *Castanopsis hystrix* and *Michelia macclurei* was 1:1:1 for 375 plants/hm^2 per hectare. The sample plot setup and management design are shown in **Table 1**.

2.3 Data survey

2.3.1 Soil nutrient survey

Soil sampling and determination soil samples were selected by randomly laying 3 points in each sample plot diagonally from the lower to upper slope of the microtopography, digging the soil profile and taking soil samples at 3 levels: upper, middle and lower. 2 kg of soil samples were taken from each level at each point in plastic bags and brought back to the room. The samples were manually ground after 14 days of air-drying to remove plant residues and gravels, sieved, and mixed with the soil samples at the same level by the same weight. The mixed soil samples were divided by the method of quartering and sealed in a cool and ventilated place for storage. The physical properties of soil water holding capacity and aeration are determined by the ring knife method; the pH of soil is determined by the potentiometric method; the organic matter content is determined by the potassium dichromate volumetric method; the total nitrogen is determined by the selenium powder—potassium sulfate—sulfuric acid digestion distillation titration method; the total potassium is determined by the flame photometer method; the total phosphorus is determined by the sulfuric acid—perchloric acid digestion—molybdenum. The total phosphorus was determined by sulfuric acid—perchloric acid digestion—molybdenum antimony anti-colorimetric method; the fast-acting nitrogen was determined by alkaline solution diffusion boric acid absorption method; the fast-acting potassium was determined by flame photometer method; the effective phosphorus was determined by hydrochloric acid—sulfuric acid leaching method, and the determination method was referred to "Methods for Agricultural Chemical Analysis of Soil"[16].

2.3.2 Investigation of growth indicators

In June 2020, a random sampling method was used to conduct a per-wood survey in each *Eucalyptus* mixed forest sample plot separately, and the neighboring *Eucalyptus* trees with different sets of species in each row were tracked and recorded. The diameter at breast height of each individual plant was measured with a perimeter ruler with an accuracy of 0.1 cm, the height of the tree and the height under the branch were measured with a laser height meter (Nikon Rangefinder Ruihao 1000aS) with an accuracy of 0.1 m, and the crown width was measured in both east-west and north-south directions using a tape measure, and the average value was taken. Crown length = the height of the tree – the height under the branch. The wood volume was calculated as[17,18]:

$$V_{\text{eucalyptus}} = 0.0000628767 d^{1.821621} H^{0.96436}$$

$$V_{\text{Rice Lao Pai}} = 0.0000683297 d^{1.926256} H^{0.8840614}$$

$$V_{\text{red vertebra}} = 0.000052764 d^{1.88216} H^{1.00931}$$

$$V_{\text{Fire Nan}} = 0.000052764291 d^{1.8821611} H^{0.931923697}$$

2.4 Data processing

The experimental data were statistically and analytically analyzed using Excel 2007 and SPSS 23.0 software, and one-way ANOVA was performed for the main growth parameters and soil physical and chemical properties.

3. Results and analysis

3.1 Growth of *Eucalyptus* trees

We conducted variance analysis on growth indicators such as average tree height and average diameter at breast height of *Eucalyptus* after stand replanting, and the results showed that there was no significant difference in average diameter at breast height, average tree height and average volume per plant of *Eucalyptus* between HT and MT treatments., but the differences between HT and MT, LT and CK were significant and increased with decreasing density of *Eucalyptus* trees, which indicated that as the density of *Eucalyptus* trees decreased in the stand, the space for growth of *Eucalyptus* trees in the stand increased substantially. Sufficient light reduces soil nutrient pressure, which is conducive to the growth of *Eucalyptus* DBH and tree height; the mean branch height of *Eucalyptus* does not differ significantly between MT and LT treatments, but MT and LT differ significantly from HT and CK, and increases with the decrease of *Eucalyptus* density; the canopy width of *Eucalyptus* does not differ significantly between the stands in each treatment, which indicates that the change of *Eucalyptus* density has little effect on the growth of canopy width under the reasonable structure of stand level (**Table 2**).

Table 2. The effect of different cultivation methods on the growth of *Eucalyptus*†

Stand	DBH/cm	Tree height/m	Height under branches/m	Crown width/m	Individual volume/m^3
CK	17.46 ± 0.34 c	24.10 ± 0.36 c	16.71 ± 0.26 c	3.02 ± 0.04 a	0.2570 ± 0.0116 c
LT	20.53 ± 0.39 b	25.65 ± 0.39 b	17.98 ± 0.25 b	3.04 ± 0.09 a	0.3649 ± 0.0161 b
MT	24.53 ± 0.56 a	28.91 ± 0.55 a	18.99 ± 0.44 b	3.13 ± 0.06 a	0.5650 ± 0.0319 a
HT	24.75 ± 1.13 a	30.30 ± 1.04 a	20.66 ± 0.44 a	3.22 ± 0.10 a	0.6184 ± 0.0610 a

† The letters in each column indicate significant differences ($P < 0.05$).

Table 3. Effects of different cultivation methods on the growth of interplanting trees†

Stand	Varieties of trees	Existing density/(plant·hm^{-2})	Survival rate/%	Average DBH/cm	Average tree height/m	Average individual volume/m^3
CK	*Mytilaria laosensis*	323	86.1	7.67 ± 0.29 aC	7.44 ± 0.28 aC	0.0236 ± 0.0024 aC
	Castanopsis hystrix	302	80.5	3.21 ± 0.20 cC	4.32 ± 0.17 bD	0.0028 ± 0.0005 bC
	Michelia macclurei	332	88.4	3.95 ± 0.13 bC	4.28 ± 0.16 bB	0.0031 ± 0.0003 bC
LT	*Mytilaria laosensis*	335	89.3	8.32 ± 0.26 aC	8.12 ± 0.24 aC	0.0283 ± 0.0020 aC
	Castanopsis hystrix	316	84.3	3.79 ± 0.17 cC	4.92 ± 0.19 bC	0.0039 ± 0.0004 bC
	Michelia macclurei	345	92.0	5.19 ± 0.15 bB	4.68 ± 0.11 bB	0.0058 ± 0.0007 bB
MT	*Mytilaria laosensis*	340	90.7	9.12 ± 0.27 aB	9.13 ± 0.20 aB	0.0366 ± 0.0026 aB
	Castanopsis hystrix	345	92.0	5.51 ± 0.24 bB	6.39 ± 0.21 bB	0.0101 ± 0.0011 bB
	Michelia macclurei	342	91.3	6.01 ± 0.21 bA	5.86 ± 0.20 bA	0.0091 ± 0.0008 bA
HT	*Mytilaria laosensis*	344	91.7	10.11 ± 0.25 aA	10.95 ± 0.33 aA	0.0526 ± 0.0040 aA
	Castanopsis hystrix	349	93.0	9.46 ± 0.27 aA	9.41 ± 0.23 bA	0.0378 ± 0.0030 bA
	Michelia macclurei	346	92.3	6.48 ± 0.21 bA	6.07 ± 0.17 cA	0.0105 ± 0.0009 cA

† a: lowercase letters indicate significant differences ($P < 0.05$) among different tree species with the same treatment. b: capital letters indicate that there are significant differences ($P < 0.05$) among the same tree species with different treatments.

3.2 Growth of the crop species

3.2.1 Growth of diameter at breast height

As shown in **Table 3**, the diameter at breast height of each tree species increased as the density of *Eucalyptus* decreased. Among them, the diameter at breast height of *Mytilaria laosensis* and *Castanopsis hystrix* did not differ significantly between CK and LT, and differed significantly between LT, MT and HT; while the diameter at breast height of *Michelia macclurei* did not differ significantly between MT and HT, and differed significantly between CK, LT and MT. In CK and LT, the growth of diameter at breast height of each tree species showed *Mytilaria laosensis* > *Michelia macclurei* > *Castanopsis hystrix*, and in MT and HT, it showed *Mytilaria laosensis* > *Castanopsis hystri* > *Michelia macclurei*, which indicated that in this indicates that the diameter at breast height of *Mytilaria laosensis* is larger than that of the other two species in each

treatment, and as the density of the native species of *Eucalyptus* continues to decrease, the diameter at breast height of *Mytilaria laosensis* and *Castanopsis hystrix* changes more and more obviously, while the opposite is true for *Michelia macclurei*.

3.2.2 Growth of tree height

As seen in **Table 3**, the tree height of each set of tree species increased with decreasing density of *Eucalyptus* in different transformation treatments. The height of *Mytilaria laosensis* was higher than that of *Castanopsis hystrix* and *Michelia macclurei* in all treatments and the difference was significant; the height of *Castanopsis hystrix* and *Michelia macclurei* differed significantly only under HT treatment among treatments; the difference between CK and LT under different treatments of *Mytilaria laosensis* was not significant, while the difference between LT, MT and HT was significant, the height of *Castanopsis hystrix* trees differed significantly between CK, LT, MT and HT, the height of *Michelia macclurei* trees differed significantly between CK and LT, MT and HT treatments The differences between CK and LT, MT and HT treatments were not significant, but the differences between LT and MT treatments were significant, which indicated that the tree height of each species responded to the continuous reduction of *Eucalyptus* density, but the response rhythm of different species was different, with *Castanopsis hystrix* responding the most strongly, followed by *Mytilaria laosensis*, and *Michelia macclurei* the least.

3.2.3 Growth of wood volume and accumulation

Table 4 shows that the different transformation modes had significant effects on the three tree species; the accumulation volume of *Mytilaria laosensis* was the largest in all treatments, and its total accumulation volume was 2.54 times that of the total accumulation volume of *Castanopsis hystrix* and 4.87 times that of *Michelia macclurei*. As the proportion of *Eucalyptus* in the stand decreased, the increase in the accumulation of rice old row compared to the previous treatment was 0.24%, 31%, and 45%, respectively; 46%, 182%, and 279% for red spine; and 94%, 56%, and 17% for *Mytilaria laosensis*. This indicates that HT treatment is the best choice if the main purpose is to operate *Mytilaria laosensis*, *Castanopsis hystrix*, and *Michelia macclurei*r after *Eucalyptus* near maturity forest conversion.

Table 4. Average stand stock volume and total stand stock volume of different interplanting trees $m^3 \cdot hm^{-2}$†

Stand	*Mytilaria laosensis* stock volume	*Castanopsis hystrix* stock volume	*Michelia macclurei* stock volume	Total stock volume
CK	7.6228 d	0.8456 d	1.0292 d	9.4976 d
LT	9.4805 c	1.2324 c	2.0010 c	12.7139 c
MT	12.4440 b	3.4845 b	3.1122 b	19.0407 b
HT	18.0944 a	13.1922 a	3.6330 a	34.9196 a

†The letters in each column indicate significant differences ($P < 0.05$).

3.3 Stand structure and stand quality status

The distribution of stand diameter order can reflect the growth condition of the stand and the competition between stands, which is an important indicator of the stability of stand structure[19]. From **Table 5**, it can be seen that: the skewness of the diameter order frequency distribution plot of *Mytilaria laosensis* becomes smaller as the density of *Eucalyptus* in the stand decreases, and the diameter order distribution under HT and MT treatments is closest to normal distribution; the skewness of the diameter order frequency distribution plot of *Castanopsis hystrix* is significantly higher under CK and LT treatments than the other two types of trees, indicating that the stand growth is abnormal under these two treatments and the competition among trees is highly differentiated, and gradually tends to the skewness of the diameter distribution diagram of *Michelia macclurei*r was not significantly different among the treatments, but the kurtosis was significantly higher than the other two species in each treatment, indicating that the diameter distribution deviated from the normal distribution, and the main

feature was that there was greater differentiation between stands smaller than the mean diameter and stands larger than the mean diameter. The vertical and horizontal structure of the stand did not adversely affect the trees in each diameter class.

3.4 Effect of different re-cultivation treatments on changes in physical properties of soil in forest stands

Roots can improve physical properties such as soil structure, porosity and permeability and help the soil to form agglomerate structure[20]. Soil porosity and soil water content reflect the water holding and water supply capacity of the soil and are important indicators of soil structure; the larger the value, the stronger the ability of the soil to contain water and maintain water and soil. As can be seen from **Table 6**, soil venting quality, total porosity, capillary porosity, saturated water holding capacity, capillary water holding capacity, and field water holding capacity of 0–20 cm soil layer in each model were greater than those of 20–40 cm soil layer; in the same soil layer, soil aeration, total porosity, and capillary porosity all showed HT > CK > LT > MT; in 0–20 cm soil layer, saturated water holding capacity, capillary water holding capacity, and field water holding capacity showed HT > CK > LT > MT, but in 20–40 cm soil layer, saturated water holding capacity, capillary water holding capacity showed HT > CK > LT > MT, and field water holding capacity showed CK > HT > LT > MT. The differences between the groups were not significant, but in the 20–40 cm soil layer, the saturated water holding capacity and capillary water holding capacity were HT > CK > LT > MT, and the field water holding capacity was CK > HT > LT > MT, and the differences were significant. This indicates that in the 20–40 cm soil layer, the physical properties of soil in the mixed forests tended to decrease and then increase with the decreasing proportion of *Eucalyptus*. HT and CK were generally better than the LT and MT treatments. HT and CK were more advantageous than LT and MT in improving the internal soil structure and increasing soil permeability.

Table 5. Diameter class distribution of interplanting trees in different cultivation methods

Stand	Varieties of Trees	Number of plants	Average DBH/cm	Coefficient of variation/%	Skewness	Kurtosis	Minimum DBH/cm	Maximum DBH/cm
CK	*Castanopsis hystrix*	39	3.21 ± 0.196	40.94	0.850	0.505	1.3	6.7
	Mytilaria laosensis	36	7.67 ± 0.287	25.08	0.070	-0.421	3.1	11.3
	Michelia macclurei	40	3.95 ± 0.135	22.83	-0.107	-0.828	2.1	5.7
LT	*Castanopsis hystrix*	40	3.79 ± 0.167	29.58	0.329	0.153	1.6	6.8
	Mytilaria laosensis	38	8.32 ± 0.280	23.57	0.029	-0.278	4.1	12.6
	Michelia macclurei	41	5.19 ± 0.150	19.40	0.061	-0.722	3.2	7.2
MT	*Castanopsis hystrix*	41	5.51 ± 0.242	29.42	0.129	0.076	1.9	9.5
	Mytilaria laosensis	40	9.11 ± 0.265	9.51	-0.019	0.154	4.4	12.8
	Michelia macclurei	41	6.01 ± 0.219	24.42	0.196	-0.841	3.6	8.9
HT	*Castanopsis hystrix*	41	9.46 ± 0.270	19.14	0.088	0.066	5.0	13.5
	Mytilaria laosensis	42	10.11 ± 0.252	6.73	-0.020	0.097	6.3	13.8
	Michelia macclurei	42	6.48 ± 0.213	22.01	0.085	-0.844	3.8	9.1

Table 6. Soil physical properties of different soil layers in different cultivation methods

Soil layers/cm	Stand	Venting quality/%	Total porosity/%	Capillary porosity/%	Saturated water holding capacity/%	Capillary water holding capacity/%	Field water holding capacity/%
0–20	CK	24.61 ± 0.37 ab	24.78 ± 0.38 ab	23.85 ± 0.73 a	35.73 ± 1.14 a	34.36 ± 0.88 a	23.31 ± 0.37 a
	LT	24.04 ± 0.38 ab	24.17 ± 0.23 ab	22.60 ± 1.09 a	36.98 ± 1.50 a	34.52 ± 1.58 a	19.58 ± 0.61 a
	MT	23.07 ± 1.18 b	23.22 ± 1.19 b	22.43 ± 1.16 a	35.10 ± 3.96 a	33.92 ± 3.83 a	22.26 ± 2.01 a
	HT	26.44 ± 0.90 a	26.60 ± 0.90 a	25.27 ± 1.03 a	41.64 ± 3.61 a	39.67 ± 4.06 a	24.62 ± 3.79 a
20–40	CK	24.12 ± 1.21 ab	24.30 ± 1.21 ab	23.53 ± 0.67 ab	32.65 ± 2.74 ab	31.58 ± 2.03 ab	23.90 ± 1.65 a
	LT	23.01 ± 0.48 b	23.14 ± 0.82 b	22.12 ± 0.37 b	32.47 ± 0.52 ab	31.03 ± 0.37 ab	18.56 ± 1.77 b
	MT	22.30 ± 0.81 b	22.44 ± 1.39 b	21.20 ± 1.19 b	29.30 ± 1.24 b	27.69 ± 1.72 b	18.18 ± 0.06 b
	HT	26.46 ± 0.33a	26.62 ± 0.59 a	26.07 ± 1.06 a	37.02 ± 0.80 a	36.25 ± 1.64 a	21.72 ± 1.88 ab

†The letters in each column indicate that there are significant differences between different treatments in the same soil layer ($P < 0.05$).

3.5 Changes in soil nutrient content under different re-cultivation methods

3.5.1 Changes in soil ph and organic matter content under different cultivation methods

The pH of the soil can affect some chemical reactions in the soil and is a response to the different free ion ratios in the soil. As seen in **Table 6**, there were different degrees of differences in ph between different patterns of the same soil layer, which showed that HT > MT > LT > CK, indicating that the acidity of the soil in the stand diminished as the density of *Eucalyptus* in the stand decreased. Soil organic matter is one of the important indicators for evaluating soil properties and can improve the effectiveness of soil nutrients. As shown in Figure 1, the soil organic matter of 0–20 cm was significantly higher than that of 20–40 cm in each model. The differences in soil organic matter content among different treatments in the same soil layer all reached significant levels. It showed a trend of increasing and then decreasing with the decrease of *Eucalyptus* density, which showed MT > LT > HT > CK. It can be seen that the HT and LT models have higher soil organic matter content and better fertilizer retention and supply capacity, which may be related to the reasonable mix of stand structure, which can produce more dead leaves and higher fern cover in the forest understory.

3.5.2 Changes in soil total N, total P, and total K contents under different re-cultivation methods

The content of soil total N, total P and total K is an important indicator to respond to the long-term fertility level of soil. From **Figure 1**, it can be seen that the contents of total N, total P and total K per unit soil volume in the same soil layer differed to different degrees among different modes. The contents of total N, total P, and total K in the 0–20 cm soil layers were greater than those in the 20–40 cm soil layer in each model. In the 0–20 cm soil layer, the performance of soil total N was MT > LT > HT > CK, which was similar to the performance of organic matter content, while in the 20–40 cm soil layer, LT was better than other treatments, and there was no significant difference in total N content among other treatments; in terms of total P content, it was MT > HT > LT > CK in the 0–20 cm soil layer, and in the 20–40 cm In terms of total K content, CK > MT > LT > HT in the 0–20 cm soil layer and CK > LT > MT > HT in the 20–40 cm layer, and the total K content showed a trend of decreasing with decreasing density of *Eucalyptus* in the stand. The results of the analysis of the total N, P and K contents of different soil layers in different treatments showed that the conversion treatments with smaller *Eucalyptus* densities were favorable to the increase of total N and P nutrients, while the conversion treatments with higher *Eucalyptus* densities were favorable to the increase of total K nutrients.

3.5.3 Changes of soil fast-acting N, fast-acting P and fast-acting K contents under different cultivation treatments

Soil fast-acting nutrients are the guarantee of high crop yield and can be directly absorbed and used by crops. The results of **Figure 1** show that the content of fast-acting nutrients in the 0–20 cm soil layer of each model is higher than that in the 20–40 cm soil layer. In terms of fast-acting N, HT > LT > MT > CK in the 0–20 cm soil layer, LT was significantly higher than other treatments in the 20–40 cm soil layer, and there was no significant difference among other treatments; in terms of fast-acting P, the effect among soil layers was: HT > MT > LT > CK in the 0–20 cm, MT > HT > LT > CK in the 20–40 cm, and the fast-acting P content in all soil layers continued to increase with decreasing density of *Eucalyptus*. In terms of fast-acting K, the differences among soil layers were not significant, with LT significantly higher than other treatments in the 0–20 cm soil layer and no significant differences among other treatments. The results of the analysis showed that the effect of soil fast-acting nutrient content was better in the treatments with smaller *Eucalyptus* density.

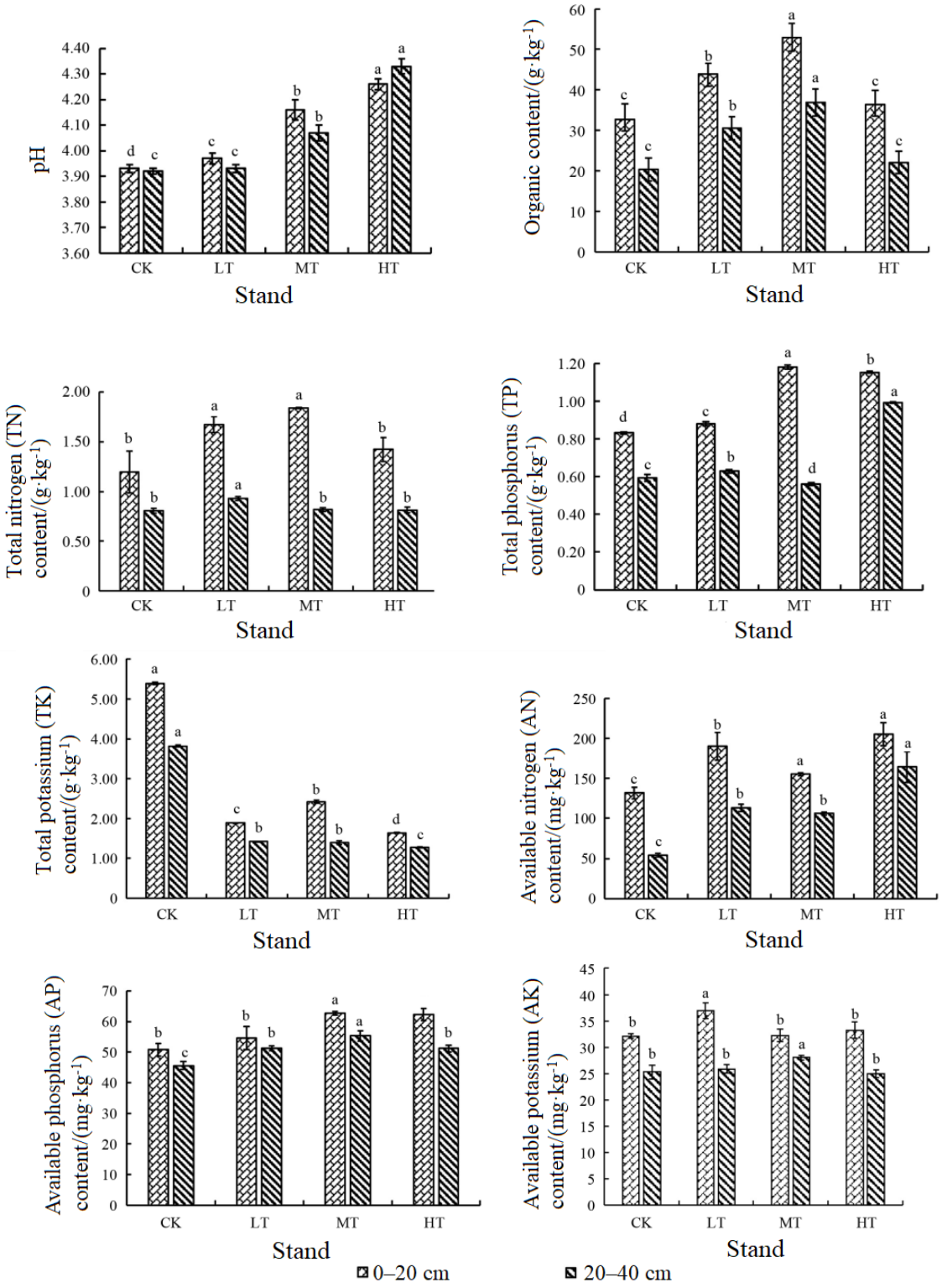

Figure 1. Soil chemical properties of different soil layers in different cultivation methods.
Note: The letters on the column indicate that there are significant differences ($P < 0.05$) between different treatments in the same soil layer.

4. Conclusion and discussion

The present study showed that the diameter at breast height, tree height and individual wood volume of *Eucalyptus* in mixed stands increased with decreasing density in mixed stands, which is similar to the results of previous studies[20]. *Eucalyptus* is a former silvicultural species, which has been above the canopy for a long time, and the reduced density of silviculture and reduced compe-

tition among individuals, together with the increased light penetration in the forest, lead to a great advantage in resource acquisition and thus changes in growth. The differences in diameter at breast height and tree height between MT and HT eucalypts are not significant, and the reasons for this are: first, after the eucalypts grow to a certain age, the respiratory consumption of the tree increases and the supply of nutrients required for tree height growth decreases; second, during the growth of *Eucalyptus* stands, the available soil nutrients are reduced due to the overgrowth of other mixed species, which eventually limits the growth of tree height; third, Chen mentioned in his study that understory ferns would Third, Chen mentioned in his study that understory ferns promote the growth of *Eucalyptus*[21], and it was observed that the greater depression of the stand at MT and the wetter soil surface layer than HT resulted in ferns being the dominant ground cover plant in its understory, which indicates that the growth of *Eucalyptus* near mature age is influenced by its biology.

After thinning of *Eucalyptus* trees, 3 kinds of broad-leaved trees, namely *Mytilaria laosensis*, *Castanopsis hystrix* and *Michelia macclurei*, were interplanted in a strip-like pattern of *Eucalyptus* and broadleaf. The three broad-leaved trees are shade-tolerant when young, neutral shade after middle age, prefer a warm and humid environment, and have high preservation rates in all treatments. Among them, *Mytilaria laosensis* has the best growth status and stand structure in all treatments. *Castanopsis hystrix* growth was significantly suppressed in CK and LT treatments, but improved in MT treatment and reached the optimum in HT treatment. *Michelia macclurei*, on the other hand, responded least to different density configurations of *Eucalyptus* in the stand. In terms of stocking volume of each tree species in the set, the treatments with different intercutting intensities of *Eucalyptus* did not significantly increase the woody growth of *Michelia macclurei*, but the treatments with smaller *Eucalyptus* densities had a significant effect on the woody growth of *Mytilaria laosensis* and *Castanopsis hystrix*. This indicates that to transform *Eucalyptus* near-mature forests into multi-species mixed forests and to cultivate *Eucalyptus* large-diameter timber at the same time, the small density of *Eucalyptus* in a stand can have better ecological and economic benefits.

Eucalyptus mixed with the above three broad-leaved trees can improve the nutrient content of soil in *Eucalyptus* succession stands to a certain extent, among which pH, organic matter, total phosphorus, total nitrogen, fast-acting phosphorus, fast-acting nitrogen, and fast-acting potassium perform better in the conversion stands with smaller *Eucalyptus* densities. However, in terms of soil physical properties, the MT and LT treatments performed significantly worse than the HT and CK treatments, which may be due to the poor root development caused by the growth inhibition of the overseeded native species in the CK treatment, which occupied less space horizontally and had less contact area with the root system of *Eucalyptus* and no obvious growth competition, resulting in a more reasonable horizontal distribution of the root system in the mixed forest. In contrast, in LT and MT treatments, the growth of the set species gradually tends to normalize, the root system is well developed, the horizontal occupation of space gradually increases, there is horizontal overlap, and the roots mostly cross each other, causing root fracture and division, distortion or even necrosis, and the soil subsurface structure is damaged to some extent, which is similar to Farooq's study[22]; Sarto and Sudmeyer, on the other hand, both found in their studies[23,24] that the number of *Eucalyptus* roots decreases significantly with increasing forest composition, while with the appearance of its lateral extent of roots and maximum root density within 0.5 m of the soil surface will be in fierce competition with other species, and because of these reasons dead and untimely decayed vegetation may cause short-term deterioration of soil physical properties. In the HT treatment, the soil structure was rationalized again and soil physical properties were significantly improved due to the significant reduction of *Eucalyptus* density in the stand, which led to an increase in the distance between the root system of *Eucalyptus* and the root system of the overgrown broadleaf forest. This aspect may also be

related to the chemosensory effect of plants, where mutual constraints between plants may switch to mutual facilitation with the decrease in the number of one of them[25,26].

The differences in growth and various indicators of soil physicochemical properties in the mixed forests with different conversion methods are mainly caused by different treatments of *Eucalyptus* intercalation intensity, while the ecological differences in the mixed forests are amplified by the biological ecological properties of *Mytilaria laosensis*, *Castanopsis hystrix* and *Michelia macclurei* themselves. For soil improvement, it is generally believed that mixed forests affect soil microbiological traits and root secretions through decomposition of apoplastic material[27]. It has been shown that *Castanopsis hystrix* with high amount of apoplastic material and short decomposition cycle of apoplastic material has a great effect on soil improvement and water conservation[28]. The results of this experiment showed that the physical properties of the soil in the HT treatment where *Castanopsis hystrix* grew better were significantly better than those in the other stands, which may be related to this reason. In the case of *Mytilaria laosensis*, some studies showed that its promotion of soil sucrase, protease and acid phosphatase were all significantly higher than that of *Eucalyptus*, *Castanopsis hystrix* and *Michelia macclurei*[29,30], as well as significant enhancement of soil microbial biomass carbon, nitrogen and phosphorus[12]. The strength of soil enzyme activity and the content of microbial biomass carbon, nitrogen and phosphorus will directly affect the soil nutrient content, which may lead to the results of this experiment in which LT, MT and HT soil nutrient content, except for total potassium, were significantly better than CK in the better growing *Mytilaria laosensis*.

In this paper, we conducted a study on the experiment of planting native species under different intercutting intensities, focusing on the selection of the best conversion treatment for the conversion of *Eucalyptus* near-mature forest to multi-species mixed forest, and we observed and analyzed the growth and accumulation of *Eucalyptus* and three native species, and measured and analyzed a series of soil physical properties and nutrient contents, which are of guiding significance for production. Throughout the paper, the HT treatment was evaluated highly in terms of the growth performance of each species, stand structural performance, and soil physical and chemical properties in the transition period of the conversion of *Eucalyptus* near-mature forests to multi-species mixed forests. However, due to the large number of tree species involved in this trial, there are limitations in the study of the specific effects of chemosensory effects and root distribution patterns among tree species on the growth and soil physicochemical properties of mixed forests. In addition, the experiment was conducted for a short period of time, and there was a lack of comparison between different years for each index, so further research is needed on the growth of mixed stands, changes in understory vegetation diversity, dynamic changes in soil physicochemical properties, and changes in soil enzyme activity and soil microbial diversity.

Acknowledgements

This work was supported by National “Thirteenth Five-Year Plan” key R&D project “Integration and Demonstration of *Eucalyptus* High Yield and Efficiency Technology” (2017YFD06010202).

Conflict of interest

The authors declared no conflict of interest.

References

1. Xie Y. The real *Eucalyptus*. Beijing: China Forestry Publishing House; 2015.
2. Wen Y, Liu S, Chen F. Effects of continuous cropping on understory species diversity in *Eucalyptus* plantations. Chinese Journal of Applied Ecology 2005; 16(9): 1667–1671.
3. Wang Z, Duan C, Qi L, *et al.* A preliminary investigation of ecological issues arising in the man-made forest of *Eucalyptus* in China. Chinese Journal of Ecology 1998; 17(6): 65–69.
4. Yu F, Huang X, Wang K, *et al.* An overview of ecological degradation and restoration of *Eucalyptus* plantation. Chinese Journal of Eco-Agriculture 2009; 17(2): 393–398.
5. Jurskis V. Eucalypt decline in Australia, and a general concept of tree decline and dieback. Forest Ecology and Management 2005; 215(1/2/3): 1–20.
6. Robinson N, Harper RJ, Smettem KRJ. Soil water

depletion by *Eucalyptus* spp. Integrated into dryland agricultural systems. Plant and Soil 2006; 286(1/2): 141–151.
7. Santos FM, Chaer GM, Diniz AR, *et al.* Nutrient cycling over five years of mixed-species plantations of *Eucalyptus* and Acacia on a sandy tropical soil. Forest Ecology and Management 2017; 384: 110–121.
8. Le Maire G, Nouvellon Y, Christina M, *et al.* Tree and stand light use efficiencies over a full rotation of single- and mixed- species *Eucalyptus* grandis and Acacia mangium plantations. Forest Ecology and Management 2013; 288: 31–42.
9. Bristow M, Vanclay JK, Brooks L, *et al.* Growth and species interactions of *Eucalyptus* pellita in a mixed and monoculture plantation in the humid tropics of north Queensland. Forest Ecology and Management 2006; 233(2/3): 285–294.
10. Important progress and results achieved in 2018 of the National Key R & D Program "Research on Efficient Cultivation Technology of *Eucalyptus*". Eucalypt Science & Technology 2018; 35(4): 33–60.
11. Lu D, Cai H, Zhang X, *et al.* Growth and economic evaluation of *Eucalyptus* clones plantation. Journal of Zhejiang A & F University 2008; 25(1): 65–68.
12. Li Z, Li B, Qi C, *et al.* Studies on the importance of valuable wood species resources and its development strategy. Journal of Central South University of Forestry & Technology 2012; 32(11): 1–8.
13. Wang T, Wan X, Cheng L, *et al.* Effects of broadleaf tree species on soil microbial stoichiometry in a reforested Cunninghamia lanceolata woodland. Chinese Journal of Applied Ecology 2020; 31(8): 1–9.
14. Pang S, Zhang P, Jia H, *et al.* Effects of different afforestation modes on diversity of undergrowth plants in *Eucalyptus* plantation. Journal of Northwest A & F University (Natural Science Edition) 2020; 48(9): 44–52.
15. Jiang Q, Li Q, Zhong C. The cultivation and comprehensive utilization of Michelia macclurei Dandy. Forest Science and Technology 2017; 63(8): 3–7.
16. Lu R. Methods for agricultural chemical analysis of soil. Beijing: China Agricultural Science and Technology Press; 2000.
17. Mo X, Yu X, Zhu C, *et al.* Theory and method of *Eucalyptus* plantation cultivation. Beijing: China Forestry Publishing House; 2005.
18. Liu Q. Chinese standing timber volume table. Beijing: China Forestry Publishing House; 2017.
19. Jiang J. Study on the effect of mixed afforestation of Castanopsis hystrix and Cunninghamia lanceolata. Journal of Forest and Environment 2002; 43(4): 329–333.
20. Wang Z. The research on monitoring and evaluation of ecological benefit of national non-commercial forest in Hunan Province [PhD thesis]. Changsha: Central South University of Forestry & Technology; 2013.
21. Chen J. The understory fern Dicranopteris dichotoma facilitates the overstory *Eucalyptus* trees in subtropical plantations. Ecosphere 2014; 5(5): 1–12.
22. Farooq T, Wu W, Tigabu M, *et al.* Growth, biomass production and root development of Chinese fir in relation to initial planting density. Forests 2019; 10(3): 1–15.
23. Sarto MVM, Borges WLB, Sarto JRW, *et al.* Root and shoot interactions in a tropical integrated crop-livestock-forest system. Agricultural Systems 2020; 181(6): 2–11.
24. Sudmeyer RA, Speijers J, Nicholas BD. Root distribution of *Pinus pinaster*, *P. Radiata*, *Eucalyptus globulus* and *E. Kochii* and associated soil chemistry in agricultural land adjacent to tree lines. Tree Physiology 2004; 24(12): 1333–1346.
25. Lin W, Zhan C, Chen H. Effects of allelopathy among tree species. World Forestry Research 2011; 24(5): 13–17.
26. Ping X, Wang T. Ecological significance of plant allelopathy and progress in allelopathy research in grassland ecosystems. Acta Prataculturae Sinica 2018; 27(8): 175–184.
27. Wu W. Plant diversity, soil microbial diversity and ecosystem multifunction in pure and mixed plantations [PhD thesis]. Nanning: Guangxi University; 2019.
28. Liu E, Wang H, Liu S. Characteristics of carbon storage and sequestration in different age beech (Castanopsis hystrix) plantations in south subtropical area of China. Chinese Journal of Applied Ecology 2012; 23(2): 335–340.
29. Zhu C. Soil fertility comprehensive evaluation of five broad-leaved trees plantations [PhD thesis]. Nanning: Guangxi University; 2015.
30. Huang H. Study on soil physical and chemical properties and enzyme activities of different species plantation in southwest Guangxi [PhD thesis]. Nanning: Guangxi University; 2017.

Sustainable Forestry (2022) Volume 5 Issue 1
doi:10.24294/sf.v5i1.1621

ORIGINAL RESEARCH ARTICLE

Composition, structure and ecological importance of Moraceae in a residual forest of Ucayali, Peru

Fred C. Ramírez[1*], Gumercindo A. Castillo[1], Ymber Flores[2], Octavio F. Galván[1], Luisa Riveros[1], Lyanna H. Sáenz[3]

[1] *Universidad Nacional Intercultural de la Amazonía (UNIA), Pucallpa, Peru. E-mail: fredc.ramirez.g@gmail.com*

[2] *Instituto Nacional de Innovación Agraria (INIA), Pucallpa, Peru.*

[3] *Universidade do Estado do Amazonas (UEA), Manaus, Brazil.*

ABSTRACT

Species of the Moraceae family are of great economic, medicinal and ecological importance in Amazonia. However, there are few studies on their diversity and population dynamics in residual forests. The objective was to determine the composition, structure and ecological importance of Moraceae in a residual forest. The applied method was descriptive and consisted of establishing 16 plots of 20 m × 50 m (0.10 ha), in a residual forest of the Alexánder von Humboldt substation of the National Institute of Agrarian Innovation-INIA, Pucallpa, department of Ucayali, where individuals of arboreal or hemi-epiphytic habit, with DBH ≥ 2.50 cm, were evaluated. The floristic composition was represented by 33 species, distributed in 12 genera; five species not recorded for Ucayali were found. Structurally, the family was represented by 138 individuals/ha with a horizontal distribution similar to an irregular inverted "J". However, there were different horizontal structures among species. It was determined that 85% of the species were in diameter class I (2.50 to 9.99 cm), being the most abundant *Pseudolmedia laevis* (Ruiz & Pav.) J.F. Macbr. (41.88 individuals/ha); and the most dominant were *Brosimum utile* (Kunth) Oken (1.71 m^2/ha) and *Brosimum alicastrum* subsp. *bolivarense* (Pittier) C.C.Berg (0.90 m^2/ha). Likewise, P. *laevis* and B. *utile* were the most ecologically important. The information from the present research will allow the establishment of a baseline, which can be used to propose the management of Moraceae in residual forests in the same study area.

Keywords: Residual Forest; Abundance; Dominance; IVI; New Records

ARTICLE INFO

Received: 4 April 2022
Accepted: 22 May 2022
Available online: 1 June 2022

1. Introduction

Peru has an arboreal richness of 4,618 species, grouped in 148 families[1], which represents an incomparable opportunity and an urgent priority for floristic research. In addition, it is considered one of the most biologically diverse countries in the world[2]. However, large forest areas remain unexplored[3], and records are still incomplete and fragmented[1,4]. Moraceae presents considerable abundance and species richness[5-7], which influences it to be considered ecologically important in the different forests of Amazonia[8-13]. Recent studies found that *Brosimum utile* (Kunth) Oken is the species with the greatest ecological weight, at 107 masl in Colombia[13]; while, in Ecuador, *Ficus cuatracasana* Dugand dominates the horizontal space, between 601 to 1,000 masl[14]. In Peru, the Moraceae family is represented by 19 genera, 128 species, with the genus Ficus being the most diverse with 102 species and 20 subspecies[1,15-17], which has been complemented by the discovery of new species and new reports for the Peruvian flora[18,19], which

together group all the names recognized to date; while, for the Ucayali region there are a total of 58 species and 6 subspecies[4].

The Moraceae are of economic importance mainly for the value of their wood[3,20,21], being the most used species, in primary processing, *Brosimum utile* subsp. ovatifolium (Ducke) C.C. Berg "Panguana", Maquira coriacea (H. Karst.) C.C. Berg "Capinurí" and Clarisia racemosa Ruiz & Pav. "Mashonaste, Tulpay"[22]. In addition, there are species with medicinal[20,23,24] and food use[25]. The fruits produced by several species are indispensable for numerous species of vertebrate frugivores, which significantly influences forest dynamics[26-28]. Other authors mention that Moraceae are among the top ten families, in terms of number of tree species[1], with *Pseudolmedia laevis* (Ruiz & Pav.) J.F. Macbr. being the fourth most abundant species in the Amazon[29]; however, Licona *et al.*[30] indicate that there are not many studies on the dynamics of Amazonian forests and the ecology of their species. Likewise, Calvi[6] points out that one of the main factors affecting the distribution and species richness of the Moraceae family in the Madidi National Park in Bolivia is the conservation status of the forests.

The objective of this study was to know the composition, structure and ecological importance of Moraceae in a residual forest of the Alexander von Humbolt substation of the National Institute of Agrarian Innovation Ucayali (Peru).

2. Materials and methods

2.1 Study area

The work was developed in a residual primary forest at the Alexander von Humboldt substation of INIA, Von Humboldt district, in the province of Padre Abad, department of Ucayali (Peru), between 8°49′31.7″S and 75°3′19.5″W. The study sector belongs to the lowland rainforest Ecozone[31] and is physiographically undulating (profile with regular waves of 5 to 10 m in height) with good drainage[32]. It has an estimated precipitation of 3,600 mm and the average temperature is 26 °C[33].

2.2 Species inventory

Based on topographic charts, the study area was preliminarily defined where, due to the degree of forest fragmentation, 16 sampling units of 0.10 ha (20 m × 50 m) were selectively located in an altitudinal range from 211 to 286 m following the methodology of Calvi[6] (**Figure 1**). Each woody individual of arboreal or hemi-epiphytic habit, belonging to the Moraceae family, with diameter at breast height (DBH) ≥ 2.50 cm was evaluated. The herborization protocol of Bridson and Forman[34] was used to collect and transfer the samples.

2.3 Taxonomic identification

A review was made of the Moraceae collections from the Alexander von Humboldt Experimental Annex, located in the Forest Herbarium of INIA-Pucallpa, as well as virtual catalogs, specialized bibliography and databases: The Plant List (http://www.theplantlist.org), Missouri Botanical Garden (http://www.tropicos.org), Global Biodiversity Information Facility-GBIF (https://www.gbif.org), NYBG Steere Herbarium (http://sweetgum.nybg.org) and the Field Museum (https://plantidtools.fieldmuseum.org). Subsequently, the identification was corroborated at the Herbarium Selva Central Oxapampa (HOXA), biological station of the Missouri Botanical Garden, located in Oxapampa. Finally, the exsiccatae were deposited in the Biological Depository of INIA-Pucallpa.

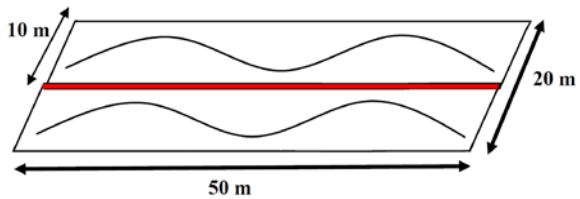

Figure 1. Diagram of the plot used for the study of Moraceae in a residual forest.

2.4 Data analysis

To represent the floristic composition, the species existing at the site were considered[35-37]. To calculate sampling efficiency, a species accumulation curve was elaborated using the non-parametric CHAO 2 estimator[38], which considers the distribution of species by sampling[39]. The analysis was performed using Estimates v.9.1.0[40].

The horizontal structure for the 16 plots (1.6 ha) was represented by the number of individuals per diameter class and the abundance of species; basal area was also calculated to know the distribution of the family and species dominance[36,37,41]. The data were grouped into the following diameter classes: I (2.50 to 9.99 cm), II (10 to 19.99 cm), III (20 to 29.99 cm), IV (30 to 39.99 cm), V (40 to 49.99 cm), VI (50 to 59.9 cm), VII (60 to 69.99 cm), VIII (70 to 79.99 cm), IX (80 to 89.99 cm), X (90 to 99.99 cm), XI (100 to 109.99 cm), XII (110 to 119.99 cm), XIII (120 to 120.99 cm) and XIV (130 to 139.99 cm).

Ecological importance was determined by calculating the species Importance Value Index (IVI) expressed as a percentage[42], the formula is shown below:

$$IVI = IVI_j = AbR_j + FR_j + DoR_j$$

Where:

Relative abundance: $AbR_j = 100 \times Ab_j / \Sigma Ab_j$

Relative Frequency: $FR_j = 100 \times F_j / \Sigma F_j$

Relative dominance: $DoR_j = 100 \times Do_j / \Sigma Do_j$

Being:

Ab_j: Total number of individuals of species j in all plots.

F_j: Number of plots where species j is present.

Do_j: Total basal area of species j in all plots.

3. Results

3.1 Floristic composition of the family Moraceae

In the 16 sampling plots (1.6 ha), 33 species were identified, while according to CHAO 2 the expected species were 44 (**Figure 2**). Accordingly, the richness (S) observed represented 75% of the species that constitute the residual forest.

The species composition was distributed in 12 genera: *Batocarpus*, *Brosimum*, *Clarisia*, *Ficus*, *Helicostylis*, *Maquira*, *Naucleopsis*, *Perebea*, *Poulsenia*, *Pseudolmedia*, *Sorocea* and *Trophis*. Three genera presented the highest richness: *Ficus* (8 species), *Brosimum* (6 species) and *Perebea* (4 species), grouping 54.55% of the total number of species (**Figure 3**).

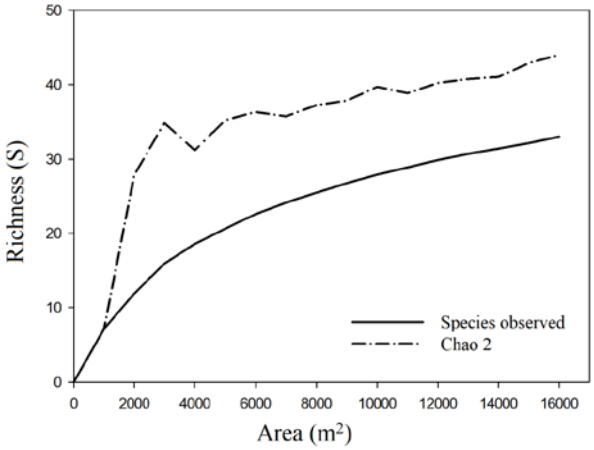

Figure 2. Accumulation curve of observed and expected species of the Moraceae family in a residual forest.

Five species are new records for the Ucayali region: *Ficus americana* subsp. *guianensis* (Desv. ex Ham.) C.C. Berg, *Ficus schultesii* Dugand, *Ficus ursina* Standl., *Ficus tonduzii* Standl. vel. sp. afí, and *Perebea guianensis* subsp. *hirsuta* C.C. Berg.

3.2 Horizontal structure of the family Moraceae

In 1.6 ha, 221 individuals were recorded and evaluated, 138 individuals/ha from 2.50 cm DBH; while from 10 cm DBH the density was 41.25 individuals/ha. The average DBH was 13.32 cm and the maximum was 136 cm. The individuals were grouped in 11 of the 14 diameter classes considered for the structural analysis, showing an irregular discetaneous diameter distribution similar to an inverted "J" (**Figure 4**).

Species with complete discetal structures were *Pseudolmedia laevis* (Ruiz & Pav.) J.F. Macbr. and *Poulsenia armata* (Miq.) Standl.; while *Brosimum lactescens* (S. Moore) C.C. Berg, *Clarisia biflora* Ruiz & Pav, *Clarisia racemosa* Ruiz & Pav., *Brosimum acutifolium* subsp. *obovatum* (Ducke) C.C. Berg, *Brosimum multinervium* C.C. Berg and *Brosimum utile* (Kunth) Oken showed irregular discetal structures. On the other hand, *Ficus maxima* Mill. vel. sp. aff., *F. americana* sbsp. *guianensis*, *Pseudolmedia macrophylla* Trécul, *Brosimum alicastrum* subsp. *bolivarense* (Pittier) C.C. Berg and *Perebea mollis* subsp. *mollis* showed bimodal structures (**Figure 5**).

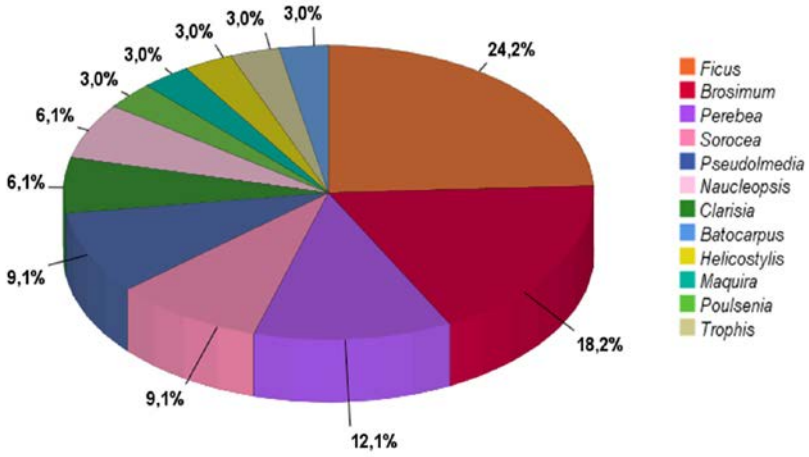

Figure 3. Richness of genera of the Moraceae family in a residual forest.

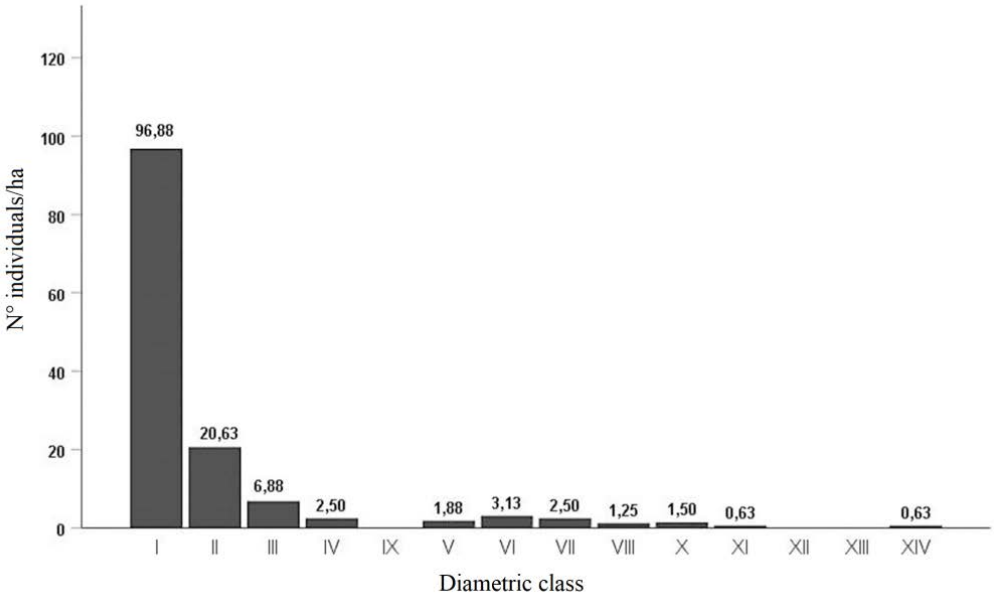

Figure 4. Irregular inverted horizontal structure of species of the Moraceae family in a residual forest.

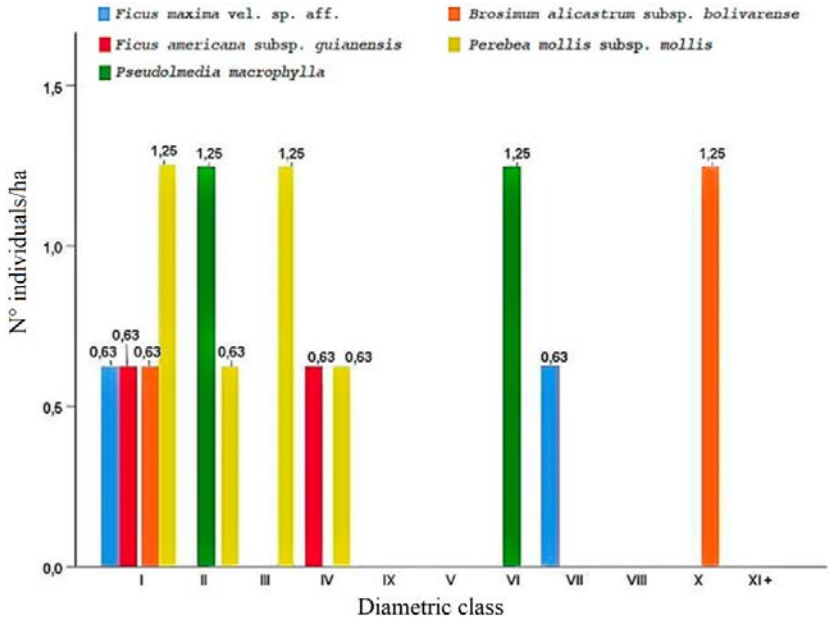

Figure 5. Species of the Moraceae family with bimodal horizontal structures in a residual forest.

Another group of species were distributed only in classes I and II. *Helicostylis tomentosa* (Poepp. & Endl.) Rusby, *Perebea angustifolia* (Poepp. & Endl.) C.C. Berg and *Pseudolmedia laevigata* Trécul presented horizontal structures of discetaneous appearances; while, *Brosimum guianense* (Aubl.) *Huber* and *Batocarpus costaricensis* Standl. & L.O. Williams showed horizontal structures with bimodal appearances.

3.3 Abundance of species

The six most abundant species were: *Pseudolmedia laevis* (41.88 individuals/ha), *Brosimum utile* (11.25 individuals/ha), *Clarisia biflora* (8.75 individuals/ha), *Poulsenia armata* (8.75 individuals/ha) and *C. racemosa* (6.25 individuals/ha), representing 55.7% of the total number of individuals.

The species that were present only in class I and were represented by only one individual (0.63 individual/ha) were: *Ficus tonduzii* vel. sp. aff., *Ficus paraensis* (Miq.) Miq, *Perebea guianensis* subsp. *hirsuta*, *Naucleopsis glabra* Spruce ex Pittier and *Sorocea briquetii* J.F. Macbr. While *Perebea longipedunculata* C.C. Berg, *Sorocea steinbachii* C.C. Berg, *Naucleopsis ulei* (Warb.) Ducke and *Maquira calophylla* (Poepp. & Endl.) C.C. Berg presented 1.88, 2.50, 4.38 and 5.63 individuals/ha in class I, respectively. On the other hand, *F. ursina* and *F. schultesii* were distributed in classes III and VI, with 0.63 individuals/ha each; on the other hand, *Ficus insipida* subsp. *insipida* and *Ficus popenoei* Standl. presented 0.63 individuals/ha each in class VII.

3.4 Basal area

The total basal area of the species evaluated was 5.81 m^2/ha. The distribution, by diameter class of the species, showed a discontinuous increase in the last classes (**Figure 6**). The genus *Brosimum* represented 61.1% of the total basal area (3.55 m^2/ha). A co-dominance of species was found, the first was *Brosimum utile* with 1.71 m^2/ha and the second was *B. alicastrum* subsp. *bolivarense* with 0.89 m^2/ha, despite being represented by only one individual in class I and another in class X. Both species represented 44.80% of the total basal area.

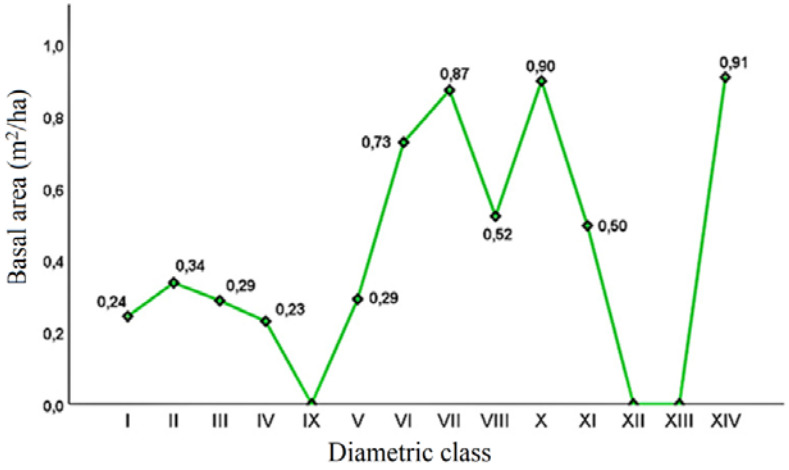

Figure 6. Cumulative distribution of basal areas by diameter class of the Moraceae family in a residual forest.

Table 1. Ecological importance of species of the Moraceae family in a residual forest

Species	AbA	AbR	FA	FR	DoA	DoR	IV (300%)	IVI (100%)
Pseudolmedia laevis (Ruiz & Pav.) J.F. Macbr.	67	30.32	0.88	12.50	0.71	7.62	50.44	16.81
Brosimum utile (Kunth) Oken	18	8.14	0.63	8.93	2.73	29.34	46.42	15.47
Brosimum alicastrum subsp *bolivarense* (Pittier) C.C. Berg	3	1.36	0.19	2.68	1.45	15.47	19.51	6.50
Brosimum acutifolium subsp. *obovatum* (Ducke) C.C. Berg	6	2.71	0.38	5.36	0.66	7.11	15.19	5.06
Clarisia racemosa Ruiz & Pav.	10	4.52	0.50	7.14	0.26	2.84	14.51	4.84
Ciarisia biflora Ruiz & Pav.	14	6.33	0.44	6.25	0.17	1.84	14.42	4.81

Table 1. (*Continued*)

Species	AbA	AbR	FA	FR	DoA	DoR	IV (300%)	IVI (100%)
Brosimum multinervium C.C. Berg	7	3.17	0.19	2.68	0.61	6.59	12.44	4.15
Poulsenia armata (Miq.) Standl.	14	6.33	0.31	4.46	0.12	1.32	12.12	4.04
Pseudolmedia macrophylla Trécul	4	1.81	0.19	2.68	0.51	5.44	9.92	3.31
Perebea mollis (Poepp. & Endl.) Huber subsp. *mollis*	6	2.71	0.31	4.46	0.19	2.02	9.20	3.07
Maquira calophylla (Poepp. & Endl.) C.C. Berg	9	4.07	0.31	4.46	0.03	0.34	8.88	2.96
Brosimum lactescens (S. Moore) C.C. Berg	6	2.71	0.25	3.57	0.20	2.13	8.41	2.80
Naucleopsis ulei (Warb.) Ducke	7	3.17	0.31	4.46	0.01	0.09	7.72	2.57
Helicostylis tomentosa (Poepp. & Endl.) Rusby	7	3.17	0.25	3.57	0.05	0.57	7.31	2.44
Ficus maxima Mill. vel. sp. aff.	2	0.90	0.13	1.79	0.34	3.66	6.35	2.12
Ficus insipida Willd. subsp. *insipida*	11	0.45	0.06	0.89	0.38	4.12	5.47	1.82
Perebea angustifolia (Poepp. & Endl.) C.C. Berg	55	2.26	0.19	2.68	0.05	0.51	5.45	1.82
Trophis cancana (Pittier) C.C. Berg	9	4.07	0.06	0.89	0.02	0.22	5.18	1.73
Ficus popenoei Standl.	1	0.45	0.06	0.89	0.32	3.48	4.83	1.61
Sorocea steinbachii C.C. Berg	4	1.81	0.19	2.68	0.01	0.08	4.57	1.52
Pseudolmedia laevigata Trécul	3	1.36	0.19	2.68	0.01	0.12	4.16	1.39
Ficus americana subsp. guianensis (Desv. ex Ham.) C.C. Berg	2	0.90	0.13	1.79	0.12	1.32	4.01	1.34
Ficus schultesii Dugand	1	0.45	0.06	0.89	0.21	2.31	3.66	1.22
Perebea longipedunculata C.C. Berg	3	1.36	0.13	1.79	0.00	0.02	3.17	1.06
Brosimum guianense (Aubl.) Huber	2	0.90	0.13	1.79	0.03	0.37	3.06	1.02
Batocarpus costaricensis Standl. & L.O. Williams	2	0.90	0.13	1.79	0.01	0.15	2.84	0.95
Sorocea guilleminiana Gaudich.	2	0.90	0.06	0.89	0.03	0.31	2.11	0.70
Ficus ursina Standl.	1	0.45	0.06	0.89	0.03	0.37	1.72	0.57
Perebea guianensis Aubl. subsp. *hirsuta*	1	0.45	0.06	0.89	0.01	0.08	1.42	0.47
Naucleopsis glabra Spruce ex Pittier	1	0.45	0.06	0.89	0.00	0.04	1.39	0.46
Ficus tonduzii Standl. vel. sp. aff.	1	0.45	0.06	0.89	0.00	0.04	1.38	0.46
Sorocea briquette J.F. Macbr.	1	0.45	0.06	0.89	0.00	0.04	1.38	0.46
Ficus paraensis (Miq.) Miq.	1	0.45	0.06	0.89	0.00	0.03	1.38	0.46
Total	221	100.00	7.00	100.00	9.31	100.00	300.00	100.00

Note: AbA (Absolute abundance), AbR (Relative abundance), FA (Absolute frequency), FR (Relative frequency), DoA (Absolute dominance), DoR (Relative dominance), IVI (Importance Value Index = AbR + FR + DoR).

3.5 Ecological importance of the species of the Moraceae family

The ecological weight of the first six species represented 53.49% of the IVI. The most important were *Pseudolmedia laevis* and *Brosimum utile*, the former due to its abundance (30.32) and frequency (12.50); while, the latter due to its abundance (8.14) and dominance (29.34). The species *B. alicastrum* subsp. *bolivarense* and *B. acutifolium* subsp. *obovatum* were also important, but due to their dominance (15.47) and (7.11), respectively; while *Clarisia racemosa* and *C. biflora* were important due to their abundance (4.52) and frequency (6.25) (**Table 1**).

4. Discussion

4.1 Floristic composition

When studying the composition of Moraceae, in the Madidi forest in Bolivia, between 100 to 250 m altitude, using plots of 20 m × 50 m and 10 m × 100 m, with a sampling area of 4.9 ha, 24 species and 11 genera were found[6], being this richness lower than that obtained in the present study, 33 species and 12 genera in 1.6 ha in a residual primary forest. As in the investigations of Calvi[6] and Marcelo-Peña and Reynel[12], Ficus was the genus that reported the highest floristic richness.

4.2 Horizontal structure

According to Louman *et al*.[41], this occurs because some diameter classes have few or many individuals. However, this type of distribution showed that the forest has a good reserve of small individuals, at the family level, in class I, 70% of the total number of individuals and 85% of the species, which is abundant enough to replace large individuals. Lam-Precht[35] mentions that the aforementioned distribution guarantees the sustainable yield of humid tropical forests, so it can be affirmed that the harvesting of all or most of the species of the Moraceae family in the forest under study could be carried out in compliance with the ecological dimension of sustainable forest management. *Pseudolmedia laevis* was the most abundant species, thus agreeing with ter Steege *et al*.[29].

The complete discetaneous structures of *Pseudolmedia laevis* and *Poulsenia armata* indicate that these species will not present problems to regenerate; whereas, species with irregular discetaneous structures (such as *Brosimum lactescens*, *Clarisia biflora*, *C. racemosa*, *B. acutifolium* subsp. *obovatum*, *B. multinervium* and *B. utile*) and with bimodal structures (such as *Ficus maxima* vel. sp. afí, *F. americana* sbsp. *guianensis*, *Pseudolmedia macrophylla*, *Brosimum alicastrum* subsp. *bolivarense* and *Perebea mollis* subsp. *mollis*) will need large clearings to regenerate[41].

The discontinuous increase in the basal area of Moraceae in the last classes reflects the degree of intervention in the study area. According to Louman *et al*.[41], undisturbed forests generally show an accumulation of basal area in the last class. Orozco and Brumér[43] explain that if a species has the largest basal area of a site, it is dominating, even if it is not abundant, as was the case of *Brosimum utile* and *B. alicastrum* subsp. *bolivarense*.

4.3 Ecological importance

Brosimum utile was the second species with the greatest ecological weight, after *Pseudolmedia laevis*, obtaining a similar result to the study conducted by Mena-Mosquera *et al*.[13]. Licona *et al*.[30] point out that there is not much information on the dynamics of Amazonian forests and the ecology of their species. On the other hand, we do not know other biological processes associated with richness and diversity, such as the effects caused by dispersers and competition between plants, which could help to understand many concepts.

5. Conclusions

The residual forest of the Alexander von Humboldt substation of INIA harbors an important richness of species of the Moraceae family, with five new reports for Ucayali.

There are different horizontal structures between species belonging to the same family, with notorious implications for the identification and planning of silvicultural interventions; suggesting for this type of forest, that management be diversified (or multiple use) in terms of species utilization and the generation of timber and non-timber goods.

The differences in structure and ecological importance are a manifestation of the individuality of each species; however, *Pseudolmedia laevis* and *Brosimum utile* are noteworthy because they presented the highest ecological weights.

Conflict of interest

The authors declared no conflict of interest.

References

1. Vásquez R, Rojas R, Monteagudo A, *et al*. Catalog of Peruvian trees. Revista Qeuña 2018; 9(1): 1–167.
2. MINAM (Ministerio del Ambiente, Perú). Plan/Estrategia: Estrategia Nacional de Diversidad Biológica al 2021 (Plan de Acción 2014–2018)

(Spanish) [Plan/Strategy: National Biodiversity Strategy to 2021 (Action Plan 2014–2018)]. Lima, Peru: Ministerio del Ambiente; 2014. p. 114.
3. Honorio E, Reynel C. Vacíos en la colección de la flora de los bosques húmedos del Perú (Spanish) [Gaps in the collection of the flora of Peruvian rainforests]. Lima: Universidad Nacional Agraria la Molina, Herbario de la Facultad de Ciencias Forestales; 2003. p. 87.
4. Flores Y. Árboles nativos de la region Ucayali, Perú (Spanish) [Native trees of the Ucayali region, Peru]. 1st ed. Pucallpa, Peru: Instituto Nacional de Innovación Agraria; 2018. p. 354.
5. Mostacedo B; Balcazar J, Montero JC. Tipos de bosque, diversidad y composición florística en la Amazonia sudoeste de Bolivia (Spanish) [Forest types, diversity and floristic composition in the southwestern Amazon of Bolivia]. Ecología en Bolivia 2006; 41(2): 99–116.
6. Calvi SP. Diversidad y distribución de la familia Moraceae en los bosques de la Región Madidi, La Paz, Bolivia (Spanish) [Diversity and distribution of the Moraceae family in the forests of the Madidi Region, La Paz, Bolivia] [PhD thesis]. La Paz: Universidad Mayor de San Andrés; 2013. p. 67.
7. García C, Marín H, Moriones D, *et al*. Structure, composition and diversity of the natural forests of Smurfit kappa cardboard of Colombia: Popayán and cajibío. Biotecnología en el Sector Agropecuario y Agroindustrial 2014; 12(1): 10–19.
8. Neill D, Killeen T. Curso de dendrología tropical en la Amazonía Boliviana, Valle de Sacta (Spanish) [Tropical dendrology course in the Bolivian Amazon, Sacta Valley]. La Paz: Herbario Nacional de Bolivia; 1991. p. 60.
9. Nebel G, Dragsted J, Vanclay JK. Estructura y composición florística del bosque de la llanura aluvial inundable de la Amazonía Peruana: II El sotobosque de la resting (Spanish) [Structure and floristic composition of the alluvial floodplain forest of the Peruvian Amazon: II The understory of the resting forest]. Folia Amazónica 2000; 10(1–2): 151–181. doi: 10.24841/fa.v10i1-2.246.
10. Cardona V, Fuentes A; Cayola L. Las moráceas de la región de Madidi, Bolivia (Spanish) [The moraceae of the Madidi region, Bolivia]. Ecología en Bolivia 2005; 40(3): 212–264.
11. Araujo-Murakami A, Bascopé F, Cardona V, *et al*. Composición florística y estructura del bosque amazónico preandino en el sector del Arroyo Negro, Parque Nacional Madidi, Bolivia (Spanish) [Floristic composition and structure of the pre-Andean Amazonian forest in the Arroyo Negro sector, Madidi National Park, Bolivia]. Ecología en Bolivia 2005; 40(3): 281–303.
12. Marcelo-Peña JL, Reynel C. Diversity patterns and floristic composition of permanent evaluative plots in the peruvian central forest. Rodriguésia 2014; 65(1): 35–47. doi: 10.1590/S2175-78602014000100003.
13. Mena-Mosquera VE, Andrade HJ, TorresTorre JJ. Floristic composition, structure and diversity of the tropical pluvial forest of the sub-basin of the Munguidó River, Quibdó, Chocó, Colombia. Entramado 2020; 16(1): 204–215. doi: 10.18041/1900-3803/entramado.1.6109.
14. Torres Navarrete B, Garcia WO. Composición florística de la familia Moraceae, como fuente de carbon aéreo en la gradiente altitudinal de un bosque siempreverde, piemontano de la Amazonia Ecuatoriana, año 2018 (Spanish) [Floristic composition of the Moraceae family, as a source of aerial carbon in the altitudinal gradient of an evergreen, piedmont forest of the Ecuadorian Amazon, year 2018] [Master's thesis]. Quevedo, Ecuador: Universidad Tecnica Estatal de Quevedo; 2019. p. 95.
15. Brako L, Zarucchi JL. Catálogo de las Angiospermas y Gimnospermas del Perú (Spanish) [Catalog of the Angiosperms and Gymnosperms of Peru]. Missouri: Missouri Botanical Garden; 1993. p. 1–1286.
16. Ulloa Ulloa C, Zarucchi JL, León B. Diez años de Adiciones a la Flora del Perú: 1993–2003 (Spanish) [Ten Years of Additions to the Flora of Peru: 1993–2003]. Arnaldoa 2004; Sp. Ed.: 1–242.
17. Ulloa Ulloa C, Acevedo-Rodríguez P, Beck S, *et al*. 2017. An integrated assessment of the Vascular plant species of the Americas. Science 2017; 358(6370): 1614–1617. doi: 10.1126/science.aao0398.
18. Berg C, Homeier J. Three new species of South American Moraceae. Blumea-biodiversity, evolution and biogeography of plants 2010; 55(2): 196–200. doi: 10.3767/000651910X527707.
19. Mitidieri N, Cardoso L, Damián A, *et al*. A new species and a new record of Ficus sect. Pharmacosycea (Moraceae) from Peru. Systematic Botany 2020; 45(1): 91–95. doi: 10.1600/0363636464420X15801369352342.
20. Reynel C, Pennington TD, Pennington RT, *et al*. Árboles del Perú (Spanish) [Trees of Peru]. Lima: Jesús Bellido M.; 2016. p. 1047.
21. SERFOR (Servicio Nacional Forestal y de Fauna Silvestre, Perú). Anuario forestal y de fauna silvestre 2019 (Spanish) [Forestry and wildlife yearbook 2019]. Lima: SERFOR; 2000. p. 132.
22. FAO (Organización de las Naciones Unidas para la Alimentación y la Agricultura). La Industria de la Madera en el Perú: Identificación de las barreras y oportunidades para el comercio interno de productos responsables de madera, provenientes de fuentes sostenibles y legales, en las MIPYMEs del Perú (Spanish) [The timber industry in Peru: Identification of barriers and opportunities for domestic trade of responsible wood products from sustainable and legal sources in Peruvian MSMEs]. Lima: FAO; 2018. p. 178.
23. Mejía K, Rengifo E. Plantas medicinales de uso popular en la Amazonía peruana (Spanish) [Medicinal plants for popular use in the Peruvian Amazon]. 2nd ed. Lima, Peru: IIAP (Instituto de Investi-

gaciones de la Amazonía Peruana); 2000. p. 286.
24. Mass W, Campera M. Árboles medicinales: Conocimientos y usos en la cuenca baja del río Marañón, zona de amortiguamiento de la Reserva Nacional Pacaya Samiria (Spanish) [Medicinal trees: Knowledge and uses in the lower basin of the Marañón River, buffer zone of the Pacaya Samiria National Reserve]. Iquitos: MINAM; 2011. p. 81.
25. Spichiger R, Méroz J, Loizeau P, *et al*. Contribución a la flora en la Amazonía peruana: Los árboles del Arboretum de Jenaro Herrera. Volumen II: Linaceae a Palmae (Spanish) [Contribution to the flora in the Peruvian Amazon: The trees of the Jenaro Herrera Arboretum. Volume II: Linaceae to Palmae]. Geneva, Switzerland: IIAP (Instituto de Investigaciones de la Amazonía Peruana); 1990. p. 359.
26. Shanahan M, Samson SO, Estephen SG, *et al*. Fig-eating by vertebrate frugivores: A global review. Biological Reviews 2001; 76(4): 529–572. doi: 10.1017/S146479310100576010.
27. Kanashiro LJ. Etología de Forrajeo de Ateles belzebuth chamek (Atelidae: Atelinae) en el Parque Nacional del Manu durante la temporada seca 2005 (Spanish) [Foraging ethology of Ateles belzebuth chamek (Atelidae: Atelinae) in Manu National Park during the 2005 dry season.] [PhD thesis]. Lima: Universidad Nacional Agraria La Molina; 2009.
28. Alegria DO. Influencia de la disponibilidad de frutos (familia Moraceae) en las dinámicas de fisión-fusión de Ateles chamek (Humboldt, 1812) en el Parque Nacional de Manu (Spanish) [Influence of fruit availability (Moraceae family) on fission-fusion dynamics of Ateles chamek (Humboldt, 1812) in Manu National Park] [PhD thesis]. Lima: Universidad Nacional Agraria La Molina; 2019. p. 75.
29. ter Steege H, Pitman N, Sabatier D, *et al*. 2013. Hyperdominance in the Amazonian tree flora. Science 2013; 342(6156): 245–337. doi: 10.1126/science.1243092.
30. Licona JC, Peña M, Mostacedo B. Composición florística, estructura y dinámica de un bosque amazónico aprovechado a diferentes intensidades en Pando, Bolivia (Spanish) [Floristic composition, structure and dynamics of an Amazonian forest harvested at different intensities in Pando, Bolivia]. Santa Cruz, Bolivia: Instituto Boliviano de Investigación Forestal; 2007. p. 60.
31. FAO (Naciones Unidas para la Alimentación y la Agricultura, Italia); SERFOR (Servicio Nacional Forestal y de Fauna Silvestre, Perú). Nuestros bosques en números: Primer reporte del Inventario Nacional Forestal y de Fauna Silvestre (Spanish) [Our forests in numbers: First report of the National Forest and Wildlife Inventory] [Internet]. Lima: FAO, SERFOR; 2017. Available from: https://sinia.minam.gob.pe/documentos/nuestros-bosques-numeros.
32. Vidaurre HE. Balance of silvicultural experience with cedrelinga catenaeformis Ducke in the Pucallpa region in the Peruvian Amazone [Master's thesis]. Turrialba, Costa Rica: CATIE; 1994. p. 165.
33. Angulo W, Fasabi H. Fenología de 10 especies forestales para determinar la influencia del cambio climático por efecto del calentamiento global: cinco años de estudio (2012–2016) (Spanish) [Phenology of 10 forest species to determine the influence of climate change due to the effect of global warming: Five years of study (2012–2016)]. Pucallpa: INIA; 2016. p. 31.
34. Bridson D, Forman L. The herbarium handbook. Kew: Royal Botanic Gardens; 1992. p. 93.
35. Lamprecht H. Silvicultura en los trópicos. Los ecosistemas forestales en los bosques tropicales y sus especies arbóreas. Posibilidades para un aprovechamiento sostenido (Spanish) [Silviculture in the tropics. Forest ecosystems in tropical forests and their tree species. Possibilities for a sustainable use]. Carrillo A (translator). Eschborn, Federal Republic of Germany: GTZ; 1990. p. 335.
36. Finegan B. El potencial de manejo de los bosques húmedos secundarios neotropicales de las tierras bajas (Spanish) [The management potential of lowland neotropical secondary moist forests]. Luján R (translator). Turrialba: CATIE; 1992. p. 37.
37. Mostacedo B, Fredericksen T. Manual de métodos básicos de muestreo y análisis en ecología vegetal (Spanish) [Manual of basic methods of sampling and analysis in plant ecology]. Santa Cruz de la Sierra: BOLFOR; 2000. p. 87.
38. Colwell RK, Chang XM, Jing C. Interpolando, extrapolando y comparando las curvas de acumulación de especies basadas en su incidencia (Spanish) [Interpolating, extrapolating and comparing species accumulation curves based on their occurrence]. Ecology 2005; 85(10): 2717–2727.
39. Magurran EA. Measuring biological diversity. Oxford: Blackwell Publishing; 2004. p. 256.
40. Colwell RK. Estimates 9.1.0 user's guide: Statistical estimation of species richness and shared species from samples. Connectitut: University of Connecticut; 2013.
41. Louman B, Quirós D, Nilsson M. Silvicultura de bosques latifoliados húmedos con énfasis en América Central (Spanish) [Silviculture of moist broadleaf forests with emphasis on Central America]. Turrialba: CaTIE; 2001. p. 265.
42. Curtis JT, McIntosh RP. An upland forest continuum in the prairieforest border region of Wisconsin. Ecological Society of America 1951; 32(3): 476–496. doi: 10.2307/1931725.
43. Orozco L, Brumér L. Inventarios forestales para bosques latifoliados en América Central (Spanish) [Forest inventories for broadleaved forests in Central America]. Turrialba: CATIE; 2002. p. 264.

Sustainable Forestry (2022) Volume 5 Issue 1
doi:10.24294/sf.v5i1.1121

ORIGINAL RESEARCH ARTICLE

Biological resistance of elm (*Ulmus carpinifolia* var. *Umbelifera*) trees against fungal endophytes and white rot decay fungi

Huijun Dong[1], Mina Raiesi[2], Mohsen Bahmani[2*], Ali Jafari[2], Hamed Aghajani[3]

[1] *College of Material Science and Engineering, Nanjing Forestry University, Nanjing, China.*

[2] *Department of Natural Resources and Earth Sciences, Shahrekord University, Shahrekord, Iran. E-mail: mohsen.bahmani@sku.ac.ir*

[3] *Department of Forestry, Sari Agricultural Sciences and Natural Resources University, Sari, Iran.*

ABSTRACT

Urban trees are one of the valuable storages in metropolitan areas. Nowadays, a particular attention is paid to the trees and spends million dollars per year to their maintenance. Trees are often subjected to abiotic factors, such as fungi, bacteria, and insects, which lead to decline mechanical strength and wood properties. The objective of this study was to determine the potential degradation of Elm tree wood by *Phellinus pomaceus* fungi, and *Biscogniauxia mediterranae* endophyte. Biological decay tests were done according to EN 113 standard and impact bending test in accordance with ASTM-D256-04 standard. The results indicated that with longer incubation time, weight loss increased for both sapwood and heartwood. Fungal deterioration leads to changes in the impact bending. In order to manage street trees, knowing tree characteristics is very important and should be regularly monitored and evaluated in order to identify defects in the trees.

Keywords: Wood Decay; Impact Bending; Endophytes; Elm Tree; Urban Forestry

ARTICLE INFO

Received: 14 April 2022
Accepted: 27 May 2022
Available online: 7 June 2022

1. Introduction

Urban trees are one of the valuable storages in metropolitan regions. However, trees are exposed to wood decay fungi. Most of the fungi are able to degrade the chemical composition of woody structure of the trees, decreasing their mechanical stability that can cause serious damage to people, particularly during severe weather events[1,2]. Certain bio- logical agents can naturally deteriorate wood in the presence of a favorable environment. In nature, wood can be rapidly colonized by microorganisms[3,4]. In the forest, most of the wood decay fungi present were reported in association with sings and fallen, dead wood[5,6].

Fungi, bacteria, and insects are able to attack wood and consume the cell wall components. In fungi, wood cell wall decomposition is classified as white, brown, or soft rot[2,3,7,8]. If they consume cellulose and hemicellulose, a brown rot will be created; when lignin is break down, a white rot will be produced. White rot is divided into simultaneous white rot and selective delignification[9,10]. Decay fungi enter standing trees through wounds or breaks in the bark. Wounds can result from a variety of incidents including storms, pruning, or root cutting. Once the decay fungus breaches the bark, it enters the sapwood and can eventually affect the heartwood. Members of white-rot fungi are able to decompose all structural components in wood cell walls, i.e. the cellulose,

hemicellulose, and lignin[2,3,11,12]. In the simultaneous rot, carbohydrates and lignin are almost uniformly degraded at the same time and similar rate[2,13]. In the selective delignification, lignin is preferentially degraded, particularly in the compound middle lamella region (CML) with a separation of individual cells. Cellulose is consumed at the late stage of attack[14-17].

Fungal attack is responsible for significant decreases in mechanical and physical wood properties, influencing moisture content, electrical conduction, acoustics, convection, elasticity and plasticity in wood[2,18]. The changes cause significant losses in mechanical properties even before measurable weight loss[19,20]. Former studies have already shown a close relationship between the degradation of hemicellulose components and losses in mechanical propertie[21,22].

Endophytes are bacterial or fungal microorganisms that colonize healthy plant tissue intercellularly and/or intra- cellularly without causing any apparent symptoms of disease[23]. The objective of this study was to examine the role of white rot fungi and endophyte fungi in the wood degradation and their relationship in the wood of *Ulmus carpinifolia* var. *umbelifera* in in urban forestry. According to field survey, this fungus was the most frequently in the trees and therefore considered for this study.

2. Materials and methods

2.1 Site study

The study area in this research is located in Shahid-Rajaie Park, Isfahan, Iran, between 30 degrees and 43 minutes to 34 degrees and 27 minutes north latitude, 49 degrees and 36 minutes to 55 degrees, and 31 minutes east of the Cas- pian Sea from Greenwich (**Figure 1**).

2.2 Tree wood species

This research was conducted on elm (*Ulmus carpinifolia* var. *umbelifera*) species. One infected and living tree selected from green spaces. *Ulmus carpinifolia* var. *umbelifera* was originally cultivated in Iran, where it was widely planted as an ornamental and occasionally grew to a great size, being known there as "*Nalband*" *Persian*.

2.3 Wood samples

Wood samples were achieved from (*Ulmus carpinifolia* var. *umbelifera*) trees at breast height and air-dried to reach 23 ± 2% moisture content. Samples of $25_l \times 20_r \times 15_t$ mm according to the EN113[24] were used for determination of mass loss (ML), and $60_l \times 20_r \times 6_t$ mm according to ASTM-D256-04[25] for testing impact bending strength. The specimens used to assess impact bending strength were cut in cross section. 10 replicate specimens were prepared from different disks for each test. They were kept in a conditioning chamber (25 ℃, and 40 ± 3% RH) for 4 weeks before testing.

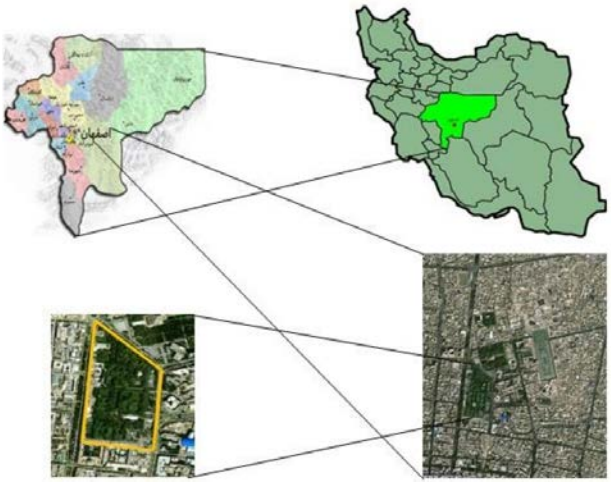

Figure 1. Study area map.

2.4 Decay test

In order to evaluate the degradation capabilities of fungi and endophytes, *Ulmus* wood blocks were cut according to EN113[24] and then they were initially oven dried at 103 ± 2 ℃ and weighed prior to fungal exposure. The wood blocks were then sterilized at 121 ℃ for 20 min and exposed to fungi grown in Petrie dish according to EN113. Both heartwood and sapwood were incubated at 25 ℃ and 65% relative humidity until the samples were acclimatized by the P. *pomaceus* fungi, and were then transferred to an incubator for 4 and 8 weeks (under the same conditions). The samples were removed from the incubator and fungal mycelia were removed from the surface of the specimens. The samples were then placed in an oven at 103 ± 2 ℃ for 24 hours to reach to constant weight and to

determine weight loss for each individual sample to EN113[24], as follows:

Weight loss (Mass loss) = $[(M_2-M_1)/M_1] \times 100$

Where, M_1 is the oven-dry weight of sample prior to exposure, and M_2 is the oven-dry weight of sample after exposure to fungus.

2.5 Mechanical tests

The compression strength and unnotched impact bending tests were carried out according ASTM-D256-04[25] standard and calculated by the following formula:

Unnotched impact bending (J × m) = F_{max}/A

Where, F_{max} = force (J), A = cross section area (m^2).

2.6 Statistical analysis

To compare mechanical properties, weight loss and a student t-test was performed (95% confidence level) between decayed and un-decayed samples. Statistical analysis was performed using the SPSS software program, version 23.

3. Results and discussion

The results of decay and mechanical tests on sapwood and heartwood after 4 and 8 weeks are summarized in **Table 1**. Statistical analysis indicated that there is a significant difference between mass loss and impact bending of sapwood and heartwood after incubation ($P < 0.05$).

Average mass losses were 10.74%, 4.02% after 8 weeks incubation for *P. pomaceus* in sapwood and heartwood, respectively, and 12.48%, 4.36% for *P. pomaceus*+ *B. mediteranae* endophyte for sapwood and heartwood, and 6.37%, 4.91% for *P. pomaceus* + *B. nummularia* endophyte sapwood and heartwood, and 11.04% for *B. mediteranae* endophyte, sapwood, and 3.59% for *B. nummularia*, endophyte sapwood.

Table 1. Average ML and IB for Elm wood samples exposed to P. pomaceus fungi, B. mediteranae endophyte P. pomaceus + B. *mediteranae* endophyte, *B. nummularia* endophyte, *P. pomaceus* + *B. nummularia* endophyte for 4 and 8 weeks (%) (n = 10).

Test Samples	Mass loss (%)		Impact bending		F*	Sig**
	4 weeks	8 weeks	4 weeks	8 weeks		
Heartwood (control)	0.0		5.87			
Decayed heartwood (*P. pomaceus*)	2.28	4.02	3.17	2.77	14.70	0.010
Decayed heartwood (*P. pomaceus* With *B. mediteranae*)	0.64	4.36	3.08	2.78	17.09	0.000
Decayed heartwood (*P. pomaceus* With *B. nummularia*)	0.59	4.91	3.75	3.12	12.51	0.010
Sapwood (control)	0.0		6.17			
Decayed Sapwood (*P. pomaceus*)	2.56	10.74	3.10	2.55	32.71	0.000
Decayed Sapwood (*P. pomaceus* With *B. mediteranae*)	5.16	12.48	3.15	2.87	28.59	0.000
Decayed Sapwood (*P. pomaceus* With *B. nummularia*)	1.46	6.37	4.62	2.57	10.30	0.020
Decayed Sapwood (B. *mediteranae*) Accession number: MF358883[26]	1.12	11.04	3.77	2.60	33.92	0.000
Decayed Sapwood (B. *nummularia*) Accession number: MF358880[26]	2.04	3.59	4.03	2.85	17.04	0.000

*F indicated that the means between two groups are significantly different.
** Sig. indicated that the differences between some of the means are statistically significant.

The results of the T-test **Table 2** indicated that the mentioned white-rot fungus had a significant effect on the weight loss of sapwood and heartwood samples ($p < 0.05$). Because the mean weight loss of decayed. Average mass losses were 4.46%, 3.25% after 8 weeks incubation for *P. pomaceus* (*Pp*), sapwood and heartwood, respectively, and 9.02%, 3.62% for *P. pomaceus*+ *B. mediteranae* endophyte sapwood and heartwood, and 5.01%, 1.87% for *P. pomaceus* + *B. nummularia* endophyte sapwood and heartwood, and 9.89% for *B. mediteranae* endophyte (*Bm*), sapwood, and 2.90% for *B.*

nummularia endophyte (*Bn*), sapwood. Results also indicated that mass loss of sapwood samples exposed to endophyte *B. mediteranae* was higher than other and then *P. pomaceus* and endophyte *B. mediteranae* had highest reduction, respectively.

Table 2. T-test analysis for average mass loss and impact bending

Tests	Test Samples	Mean	Number	StD	DF	Sig.
Mass Loss (%)	Decayed heartwood (*P. pomaceus*)	3.25	18	2.77	34	0.383
	Decayed Sapwood (*P. pomaceus*)	4.46	18	3.43		
	Decayed heartwood (*P. pomaceus* With *B. mediteranae*)	3.62	18	1.96	34	0.011
	Decayed Sapwood (*P. pomaceus* With *B. mediteranae*)	9.02	18	3.42		
	Decayed heartwood (*P. pomaceus* With *B. nummular- ia*)	1.87	18	0.98	34	0.001
	Decayed Sapwood *(P. pomaceus* With *B. nummularia*)	5.01	18	2.73		
	Decayed Sapwood (*B. mediteranae*)	9.89	18	5.59	34	0.000
	Decayed Sapwood (*B. nummularia*)	2.90	18	1.69		
Impact bending	Decayed heartwood (*P. pomaceus*)	4.02	10	1.99	10	0.050
	Decayed Sapwood *(P. pomaceus*)	10.74	10	5.71		
	Decayed heartwood (*P. pomaceus* With *B. mediteranae*)	4.36	10	4.52	10	0.058
	Decayed Sapwood (*P. pomaceus* With *B. mediteranae*)	12.48	10	2.21		
	Decayed heartwood (*P. pomaceus* With *B. nummularia*)	4.91	10	9.80	10	0.092
	Decayed Sapwood (*P. pomaceus* With *B. nummularia*)	6.37	10	2.21		
	Decayed Sapwood (*B. mediteranae*)	11.04	10	4.25	10	0.464
	Decayed Sapwood (*B. nummularia*)	3.59	10	2.78		

Figures 2 and **3** display the effects of the cell wall degradation on the impact bending strength after exposure to the white-rot fungi and endophytes. Average decrease of impact bending strength by the fungi was 10.74%, 4.02% (*Pp*), sapwood and heartwood, and 12.48%, 4.36% for (*Pp*) + (*Bm*) endophyte sapwood and heartwood, and 6.37%, 4.91% for (*Pp*) + (*Bn*) endophyte sapwood and heartwood, and 11.04% for (*Bm*) endophyte sapwood, and 3.59% for (*Bn*) endophyte sapwood, respectively, while it was 6.17% sapwood and 5.87% heartwood, for the control sample. Impact strength is the ability of wood to absorb the force of impact bending and characterizes the ability of material to with- stand impact loads. Impact strength is expressed as the energy spent while breaking wood with defined dimensions.

This mechanical property is most sensitive to decay and unlike other strength properties that decrease gradually as decay progresses, impact strength declines rapidly during incipient wood decay[27]. Trees are vital constituents with a lot of benefits. However, the fracture and falling of the trees due to high loading, especially during storms and severe winds, lead to serious economic and even life-threatening damage, particularly in urban green areas. Trees are always considered as one of the most important indicators in urban planning and management. Therefore, for sustainable management and development, it is very important to learn information regarding the street trees[28].

In nature, wood undergoes biological decay, primarily by white, brown and soft-rot fungi[2,3,7,29]. Basidiomycetes are responsible for the majority of wood decay. Soft-rot fungi (ascomycetes and deuteromycetes) degrade wood under wet conditions[30-32]. *Phellinus* is a genus of fungi in the family Hymenochaetaceae. Many of them cause white rot. It should be noted that any decrease in compression parallel to grain was a result of fungal attack and

changes in the chemical components of the cell walls, especially decrease in lignin content[2,11] resulting in a reduction in wood density that can also affect strength properties[32]. Impact bending of the wood samples was also reduced following exposure to *P. pomaceus* fungi, *B. mediteranae* endophyton and *P. pomaceus*+ *B. mediteranae* endophyton (**Table 1**). However, the loss exposure to *P. pomaceus* fungi approximately half of the loss exposure to *B. mediteranae* endophyton and *P.pomaceus*+*B. mediteranae* endophyton, but B. nummularia endophyton and *P. pomaceus*+*B. nummularia* endophyton had less weight compared to *P.pomaceus* fungi. According to previous reports[19,20], decrease in hardness could be due to loss of hemicellulose.

In general, hemicelluloses are responsible for the compression strength perpendicular to grain. The arabinan and galactan are side chain elements of xylan and mannan, the two main hemicellulose polymers[33] and may be either more vulnerable to degradation or may have to be removed before the main chain of the polymer can be attacked[20]. Reduction in hemicellulose affects integrity of the cell wall polymers and decreases the strength against mechanical loads. As shown in **Tables 1** and **2**, *P. pomaceus* fungi, *B. mediteranae* endonphyton and *P. pomaceus* + *B. mediteranae* endophyton could reduce the impact load resistance. Cleaved ether bonds in cellulose are responsible for reduction in impact load resistan[12]. It is also reported that cell wall thinning, bore holes and appearance of micro-cracks in the cell walls due to fungal degradation are other reasons for strength losses; especially impact load resistance[11,32], indicated that simultaneous white-rot leads to a brittle fracture of the infected wood because of the progressive degradation of the cellulose-rich secondary wall[11].

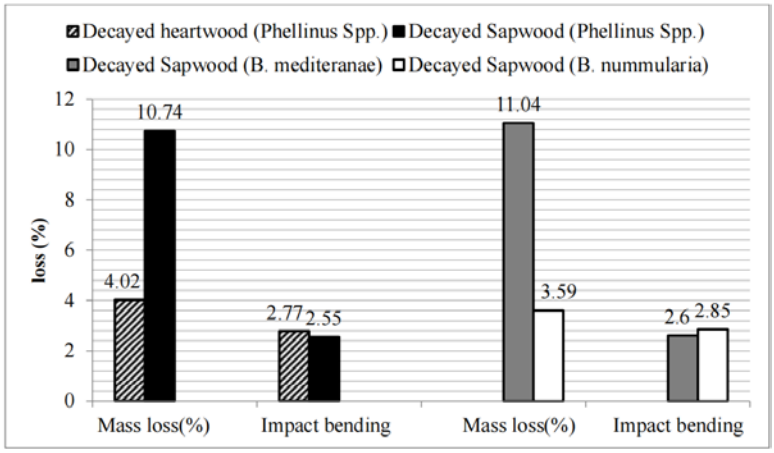

Figure 2. Mean mass loss and mechanical strength.

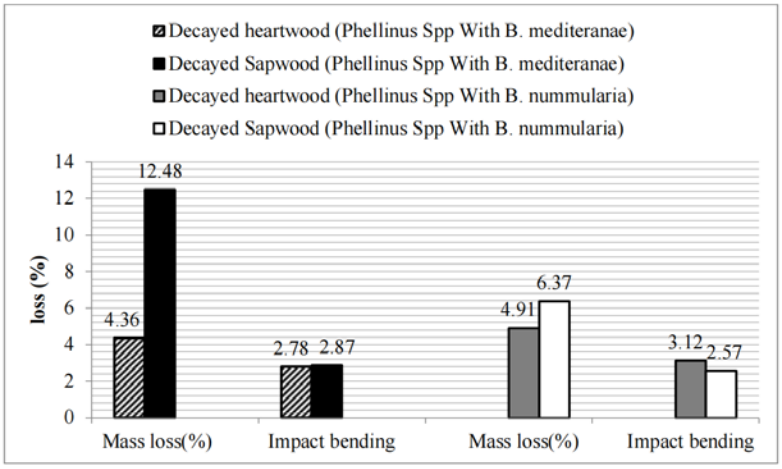

Figure 3. Average mass loss and impact bending.

4. Conclusion

Elm wood subjected to white-rot fungi and endophytes for 4 and 8 weeks of incubation by investigation of mass loss and mechanical properties. Results indicated that *phellinus* and entophytes lead to a significant mass loss which was along with losses in mechanical properties. Overall, under the conditions of the present research, it was concluded that the decay capacity of *phellinus* and was more aggressive than that of endophytes in some test cases.

Conflict of interest

The authors declare that there is no conflict of interest.

References

1. Weber K, Mattheck C. Manual of wood decays in trees. Gloucestershire: Arboricultural Association; 2003. p. 127.
2. Schmidt O. Wood and tree fungi: Biology, damage, protection, and use. Berlin: Springer Berlin Heidelberg; 2006. p. 336.
3. Eriksson KE, Blanchette RA, Ander P. Microbial and enzymatic of wood and wood components. Berlin: Springer Berlin Heidelberg; 1990. p. 407.
4. Stokland JN, Siitonen J, Jonsson BG. Biodiversity in dead wood. Cambridge: Cambridge University Press; 2012.
5. Aghajani H. Study on the oak (*Quercus castaneifolia*) and Hornbeam (*Carpinus betulus*) decaying macro fungi in mixed Oak-Hornbeam forest community in Kheyroud Forest, North of Iran [MSc thesis]. Tehran: University of Tehran; 2012. p. 95.
6. Aghajani H, Mohadjer M, Asef MR, *et al*. The relationship between abundance of wood macrofungi on chest- nut-leave Oak (*Quercus castaneifolia* C.A.M.) and hornbeam (*Carpinus betulus* L.) and physiographic factors (Case study: Kheyroud forest, Noshahr) (in Persian). Journal of Natural Environment, Iranian Journal of Natural Resources 2013; 66(1): 1–12.
7. Zabel RA, Morrell JJ. Wood microbiology: Decay and its prevention. San Diego: Academic Press; 1992. p. 764.
8. Eaton RA, Hale MDC. Decay pests and protection. New York: Chapman and Hall; 1993. p. 546.
9. Liese W. Ultrastructural aspects of woody tissue disintegration. Ann Rev Phytopath 1970; 8: 231–258.
10. Nilsson T, Daniel G. Micromorphology of the decay caused by Chonrostereum purpureum (Pers.: Fr.) Pouzar and Flammulina velutipes (Curt., Fr.). International Research Group on Wood Preservatives 1988; 1358.
11. Schwarze FWMR, Engels J, Mattheck C. Fungal strategies of wood decay in trees. 2nd ed. New York: Springer-Berlin Heidelberg; 2004. p. 218.
12. Kubicek CP. Fungi and lignocellulosic biomass. Wiley-Blackwell; 2013.
13. Rayner ADM, Boddy L. Fungal decomposition of wood. Its biology and ecology. John Wiley & Sons Ltd.; 1988.
14. Blanchette RA. Screening wood decayed white rot fungi for preferential lignin degradation. Applied and Environmental Microbiology 1984; 48: 647–653.
15. Blanchette RA. Selective delignification of eastern hemlock by Ganoderma tsugae. Phytopathology 1984; 74: 153–160.
16. Azimi Y, Bahmani M, Jafari A, *et al*. Anatomical, chemical and mechanical characteristics of beech wood degraded by two Pleurotus species. Drvna Industrija 2020; 71(1): 47–53.
17. Bahmani M, Schmidt O. Plant essential oils for environment-friendly protection of wood objects against fungi. Maderas. Ciencia y Tecnología 2018; 20(3): 325–332.
18. Cowling EB. Comparative biochemistry of the decay of sweetgum sapwood by white-rot and brown-rot fungi. US Department of Agriculture; 1961.
19. Curling SF, Winandy JE, Clausen CA. An experimental method to simulate, incipient decay of wood by basidiomycete fungi. The International Research Group on Wood Preservation. Section 2, Test Methodology and Assessment: 31st annual meeting; 2000 May 14–19; Kona, Hawaii, USA. Stockholm, Sweden: IRG Secretariat; 2000.
20. Curling SF, Clausen CA, Winandy JE. Relationships between mechanical properties, weight loss, and chemical composition of wood during incipient brown-rot decay. Forest Products Journal 2002; 52: 34–39.
21. Wilcox WW. Review of literature on the effects of early stages of decay on wood strength. Wood Fiber 1978; 9: 252–257.
22. Winandy JE, Morrell JJ. Relationship between incipient decay, strength, and chemical composition of Douglas-Fir heartwood. Wood Fiber Science 1993; 25: 278–288.
23. Wilson D. Endophyte: The evolution of a term, and clarification of its use and definition. Oikos 1995; 73(2): 274–276.
24. EN 113. Wood preservatives test method for determining the protective effectiveness against wood destroying basidiomycetes—Determination of the toxic values. 1996.
25. ASTM-D256. Standard test methods for determining the Izod pendulum impact resistance of plastics.
26. Ataei TA. Isolation and identification of fungal endophytes from Sari forests [Master's thesis]. Sari: Sari Agriculture and Natural Resources University; 2019.
27. Williams RS. Weathering of wood. In: Rowell RM (editor). Handbook of wood chemistry and wood

composites. Madison: USDA, Forest Service, Forest Products Laboratory; 2005.
28. Bahmani M, Raiesi M, Jafari A. Study of the environmental risk of Ulmus carpinifolia var. umbelifferain green spaces of Shahid-Rajaie Park Isfahan. The Second National Conference and the Fourth Specialized Exhibition of Environmental Education, Iran. Iran: Payame Noor University; 2018. p. 1–8.
29. Mohebby B. Biological attack of acetylated wood [PhD thesis]. Göttingen: Göttingen University; 2003.
30. Findlay WPK, Savory JG. Moderfäule. Die Zersetzung von Holz durch niedere Pilze (German) [Soft rot. The decomposition of wood by lower fungi]. Holz als Roh-und Werkstoff 1954; 12: 293–296.
31. Liese W. On the decomposition of the cell wall by micro-organisms. British Wood Preserving Association Record 1955; 159–160.
32. Kollmann FFP, Cote JRWA. Principles of wood science and technology. Solid Wood 1975; 1.
33. Timell TE. Recent progress in the chemistry of wood hemicelluloses. Wood Science and Technology 1967; 1: 45–70.

Sustainable Forestry (2022) Volume 5 Issue 1
doi:10.24294/sf.v5i1.1622

ORIGINAL RESEARCH ARTICLE

Cedrela odorata L. seed yield variation at two sites in Veracruz, Mexico

Juan Márquez Ramírez*, Héctor Cruz-Jiménez, Juan Alba-Landa, Lilia Del Carmen Mendizábal-Hernández, Elba Olivia Ramírez-Garcia

Instituto de Investigaciones Forestales, Universidad Veracruzana, Xalapa 91050, Mexico. E-mail: jumarquez@uv.mx

ABSTRACT

With the purpose of identifying the characteristics of variation in fruit size and seed production (potential and efficiency) of *Cedrela odorata* L. between sites and progenies established in the ejido La Balsa, municipality of Emiliano Zapata, Veracruz, fruits were harvested from 20 trees in February 2013, preserving the identity of each one. Fruit length and width were measured, seed was extracted and developed and aborted seeds were counted to calculate Seed Production Potential (SPP) and Seed Efficiency (SE). The results showed significant differences between sites and between progenies and for fruit length between sites. The mean values found were: 32.52 mm (fruit length), 18.73 mm (fruit width), 39.9 seeds per fruit (SPP) and 57.51% (SE). The seed of this species for its use should be selected taking into account the production characteristics of crops and outstanding individual trees, in addition, due to the current regulatory restrictions on seed collection, the establishment of trials and plantations for germplasm production is a viable option for forest management of the species.

Keywords: *Cedrela Odorata*; Fruits; Seeds; SPP; SE

ARTICLE INFO

Received: 15 April 2022
Accepted: 27 May 2022
Available online: 7 June 2022

1. Introduction

The renewability of forest resources and the establishment of plantations are directly proportional to their reproductive capacity and adequate management of the species that comprise them[1], so the correct application of regeneration methods in the management of natural forests and the production of sufficient and high quality seedlings in commercial plantations are vital in this productive process[2-5].

Seed production in a given site—rodal, area or seed orchard—depends on the processes that affect the production of male and female stromata, the biological and ecological conditions of the population and the potential losses during the maturation process of the reproductive structures until seed production[6-8].

To compensate for years of low production and improve the quality of the seed and forest products, seed orchards were designed[9], which are currently the most intensively managed and controlled plantations available. One of the best sources of information for orchard management is cone analysis[10]. The main objective of this analysis is to determine the potential seed production per cone, the effective seed production and to find the probable causes of losses in order to adjust management practices[11,12]. However, each component of the forestry production chain, such as seed collection and management, plant production, plantation establishment and field monitoring[13], must be precisely addressed, taking into account that each step is the basis for the

success of the next, so that the quantity and quality of the seed used has an impact on the entire process and its final result.

Cedrela odorata L. is a species with a wide ecological distribution, but of low local abundance[14,15], which, due to its use and commercial value, makes it a species in high demand in the warm zones of Mexico[16].

Due to the importance and demand of the species, two provenance/progeny trials were established in La Balsa, municipality of Emiliano Zapata, Veracruz, Mexico in September 2000, including three provenances and twenty-two progenies distributed in six blocks with four replications. In order to identify the variation in fruit size and seed production characteristics (Potential and Efficiency) of *Cedrela odorata* L. between sites and progenies, the present study was conducted.

2. Material and methods

Fruits were collected in February 2013 from 20 trees from two provenance/progeny trials located in the ejido La Balsa municipality of Emiliano Zapata, Veracruz. The first is located at 19°20′46.63″ North and 96°38′59.65″ West, at an altitude of 414 masl, the second at 19°20′59.27″ North and 96°38′43.58″ West, at an altitude of 404 masl with a mean annual temperature of 25.1 °C and a total annual precipitation of 912.1 mm[17].

Of these 20 parents, those numbered one to six are half-siblings present at both sites and eight (7 to 14) only showed seed at site one, with a total of 14 progenies being compared.

Most of the fruits were collected from each tree and then a random sample of 28 fruits per tree was taken, when the quantity was sufficient, otherwise all the fruits collected were taken, based on the methodology proposed by Bramlett *et al.*[10]. The length and width of the fruit were measured with a Mitutoyo brand digital vernier to the nearest tenth of a millimeter and placed individually in paper bags, noting the tree number and fruit number on each bag. Once the fruits were opened, the seeds were extracted for analysis.

Seed production potential refers to the maximum number of both developed and underdeveloped seeds contained in a given fruit. The value of this potential depends directly on the number of ovules in the ovary and indicates the biological limit of the fruit to produce a certain amount of seeds. By its nature, seed production potential is a characteristic subject to a strong genetic control and its value was calculated by adding the number of developed and underdeveloped seeds found in each fruit[18].

Seed production efficiency refers to the ratio of developed seeds in a given fruit to its seed production potential. This characteristic is subject to a strong environmental control and its value varies from 0 to 100%, indicating the failure or success of the fruit to produce a certain number of seeds with an embryo potentially capable of germinating and giving rise to a new plant. The value of this index was calculated by dividing the number of seeds developed by the seed production potential by 100.

The values obtained were captured in a database in the Statistica program[19], where graphs, analysis of variance with the GLM procedure and comparison of means by Tukey's method were performed. The fixed effects model used was as follows:

$$Y_{ijk} = \mu + S_i + F_j + E_{ijk}$$

Where:

Y_{ijk} = Observed value of the variable

μ = Effect of the overall mean

S_i = Effect of the i-th site

F_j = Effect of the j-th progeny

E_{ijk} = Experimental error

3. Results

The results for fruit characteristics and seed production of *Cedrela odorata* L. established at La Balsa are shown in **Table 1**, with an average SPP of 39.94 seeds per fruit and an SE of 57.51%, which indicates an average production of 23 seeds per cone.

Table 1. Descriptive characteristics of fruit and seed production of *Cedrela odorata* L. in two provenance/progeny trials established at La Balsa Emiliano Zapata, Veracruz

Variable	N	Media	Minimum	Maximum	Variance	Des. Est.
Length	458	32.52085	20.27000	47.92000	17.5415	4.18826
Width	458	18.73568	12.70000	32.93000	4.1522	2.03770
SPP	458	39.34323	20.00000	54.00000	35.3666	5.94698
SE	458	57.51353	16.66667	93.75000	285.2359	16.88893

3.1 Length of the fruit

Site one presented an average of 32.83 mm and site two 31.53 mm. The analysis of variance showed that between sites there were no significant differences ($P \leq 0.05$), but between progenies there was a significant difference (**Table 2**).

Tukey's test showed the formation of three homogeneous groups, progenies 7, 9, 8 and 5, which presented the lowest values, were completely separated from progenies 11 and 12 with the highest means (**Table 3**).

Table 2. Analysis of variance of fruit length of *Cedrela odorata*

Length	G. L.	S. C.	C. M.	F	p
Site	1	21.7	21.7	1.06	0.161959
Progeny	13	2,971.5	228.6	20.64	0.000000
Error	443	4,9054	11.1		
Total	457	8,016.5			

Table 3. Comparison of means for fruit length of *C. Odorata*

Progeny	Average (mm)	1	2	3
7	29.78143	a		
9	29.09450	a		
8	3027143	a		
5	30.68950	a		
14	31.01125	a	b	
13	31.58455	a	b	
3	31.88316	a	b	
6	32.18786	a	b	
2	32.33636	a	b	
1	33.83500		b	
10	34.07143		b	
4	34.14059		b	
11	38.18750			c
12	41.51313			c

3.2 Width of fruit

At site one the fruits were less wide (average 18.51 mm) than at site two (average 19.48 mm). Analysis of variance showed statistically significant differences ($P \leq 0.05$) between sites and between progenies (**Table 4**).

Tukey's test showed the conformation of seven homogeneous groups, progenies 1, 9, 14 and 11 separated from progenies 3, 10, 8, 12 and 4, showing a continuous but overlapping variation among all progenies, except progenies 1, 9 and 4 (**Table 5**).

Table 4. Analysis of variance of fruit width of *C. Odorata*

Width	G. L.	S. C.	C. M.	F	P
Site	1	52.74	52.74	17.55	0.000034
Progeny	13	487.91	37.53	12.49	0.000000
Error	443	1,330.99	3.00		
Total	457	1,897.57			

Table 5. Comparison of means for fruit width of *C. odorata*

Progeny	Average (mm)	1	2	3	4	5	6	7
1	16.67571	a						
9	16.82200	a						
14	17.51437	a	b					
11	17.86357	a	b	c				
6	18.46571		b	c	d			
5	18.58400		b	c	d	e		
7	18.61571		b	c	d	e	f	
2	18.65545		b	c	d	e	f	
13	18.73945		b	c	d	e	f	
3	19.12053			c	d	e	f	
10	19.64643				d	e	f	
8	19.97036					e	f	g
12	20.34937						f	g
4	21.72824							g

3.3 Seed Production Potential

The SPP for site one was 40.67 seeds per fruit, while for site two it was lower, 37.59 seeds per fruit. The analysis of variance presented significant differences ($P \leq 0.05$) both between sites and between progenies (**Table 6**).

Tukey's test showed the formation of four homogeneous groups, where progenies 5 and 11 were completely separated from the rest, and progenies 3, 1, 2, 4, 10, 7 and 12, which were above the general mean, formed a separate group (**Table 7**).

Table 6. Analysis of variance of SPP of *C. odorata*

SPP	G. L.	S. C.	C.M.	F	_P
Site	1	534.9	534.9	30.93	0.000000
Progeny	13	7,721.9	594.0	34.35	0.000000
Error	443	7,659.7	17.3		
Total	457	16,162.5			

Table 7. Comparison of means for PPS of *C. odorata*

Progeny	Average (S/F)	1	2	3	4
5	32.67500	a			
11	33.50000	a			
14	35.25000	a	b		
9	35.90000	a	b	c	
6	37.03571		b	c	
8	39.10714		b	c	
13	39.41818			c	
3	42.92105				d
1	43.53571				d
2	43.68182				d
4	43.88235				d
10	44.42857				d
7	44.89286				d
12	46.31250				d

3.4 Efficiency of seed production

Seed production efficiency presented an overall mean at site one of 56.32%, while for site two it was higher (61.40%); the analysis of variance shows significant differences ($P \leq 0.05$), between sites and between progenies (**Table 8**).

Tukey's test showed five homogeneous groups, with progenies 10, 7 and 3 being the least efficient, while progeny 11 showed the highest efficiency (**Table 9**).

Table 8. Analysis of variance of SE of *C. Odorata*

EN	G. L.	S. C.	C. M.	F	P
Site	1	3411.0	3411.0	17.455	0.000035
Progeny	13	41652.3	3204.0	16.396	0.000000
Error	443	86568.7	195.4		
Total	457	130352.8			

Table 9. Comparison of means for ES of *C. odorata*

Progeny	Mean(%)	1	2	3	4	5
10	42.15492	a				
7	45.06216	a				
3	46.44347	a				
14	53.66295	a	b			
4	54.04801	a	b			
2	54.70346	a	b			
6	59.07851		b	c	d	
1	59.44750		b	c	d	
8	60.46395		b	c	d	
13	62.51414		b	c	d	
12	64.04179		b	c	d	e
5	68.95260			c	d	e
9	69.95462			c	d	e
11	75.07415					e

4. Discussion

Rodríguez[20] found for trees from three provenances in Veracruz, a mean of 32.79 mm in length and 17.89 mm in width in fruits of *Cedrela odorata*, results similar to those of the present study; Alderete[21] reported 3.40 cm in length and 1.96 cm in width for 22 families of this same species from the state of Campeche, slightly larger than those found in this study, perhaps due to differences in environmental conditions, genotypes and soil characteristics.

Studies have been carried out on seed production potential and efficiency in hardwood species, Niembro[22] found a SPP between 54 and 89 seeds per fruit for trees in the China Experimental Field, Campeche, while De la Cruz Landero and Hernández[23] obtained potentials of 57 to 70 seeds per fruit in 20 trees located in the state of Campeche, both for mahogany (*Swietennia macropbylla* King).

Chávez and Ramírez[24] obtained a SPP between 34 and 47 seeds per fruit in 22 trees distributed in the state of Campeche; while Rodríguez *et al*.[18] obtained an average SPP of 43 seeds per fruit in a population located in La Antigua, Veracruz, the seed production efficiency was 53.83%; both studies were conducted with cedar (*Cedrela odorata* L.) and provide results similar to the present one. Mendizábal-Hernández *et al*.[25], found for a previous harvest (2011) at the same site a SPP of 46.6 s/f, higher than that found in 2013 and an SE of 50.3% lower than the 57.5 of this study.

Viveros *et al*.[26] report an average potential of 57 seeds per fruit, finding significant differences among thirty guazamo trees (*Guazuma ulmifolia* Lambert) from a coastal population in central Veracruz.

5. Conclusions

Thirteen years after the trials were established, fruit and seed production appear to be reaching the mature stand parameters of this species for the sites. Site one presented a higher Seed Production Potential but the fruits of site two were wider and presented higher Seed Efficiency. Regarding progeny, regardless of site, family four had the largest fruits and was in the group with the highest SPP but presented a low ES.

Seed of this species for nursery use should be selected taking into account the production characteristics of the crops and individual trees, in addition, due to current regulatory restrictions, the establishment of trials and plantations for seed

production is a viable option for the management of the species.

Conflict of interest

The authors declare that they have no conflict of interest.

References

1. Bazzaz FA, Ackerly DD, Reekie EG. Reproductive allocation in plants. In: Fenner M (editor). Seeds the ecology of regeneration in plant communities. 2nd ed. New York, USA: CABI Publishing; 2000. p. 1–30.
2. Grayson KJ, Wittwer RF, Shelton MG. Cone characteristics and seed quality 10 years after an uneven-age regeneration cut in shortleaf pine stands. In: Outcalt KW (editor). Ashville, North Carolina: US Department of Agriculture, Forestry Service, Southern Research Station; 2002. p. 310–314.
3. Shelton MG, Cain MD. Do cones in tops of harvested shortleaf pines contribute to the stand's seed supply? Asheville, North Carolina: US Department of Agriculture, Forest Service, Southern Research Station; 2002. p. 315–319.
4. Landa JA, Hernández LCM, Ramírez JM. Comparación del potencial de producción de semillas de Pinus oaxacana Mirov de dos cosechas en los molinos, Veracruz, México (Spanish) [Comparison of seed production potential of Pinus oaxacana Mirov from two harvests in Los Molinos, Veracruz, Mexico]. Foresta Veracruzana 2001; 3(1): 35–38.
5. Owens JN. Constraints to seed production: Temperate and tropical forest trees. Tree Physiology 1995; 15(7–8): 477–484.
6. Barnett JP. Guidelines for estimating cone and seed yields of southern pines. In: Brown M, Stine M (editors). Proceedings of the 25th Biennial Southern Forest Tree Improvement Conference; 1999 Jul 11–14; New Orleans, LA. Louisiana State University; 1999. p. 31–35.
7. Barnett JP, Haugen RO. Producing seed crops to naturally regenerate southern pines: Forest Service research paper. New Orleans, LA: USDA, Forest Service. Southern Forest Experimental Station; 1995. p. 10.
8. Baldwin HI. Forest tree seed of the north temperate regions. Delhi, India: Periodical Experts Book Agency; 1942. p. 240.
9. Zobel B, Talbert J. Técnicas de mejoramiento genético de árboles forestales (Spanish) [Genetic improvement techniques for forest trees]. Mexico: LIMUSA; 1988. p. 545.
10. Bramlett DL, Belcher Jr EW, DeBarr GL, *et al.* Cone analysis of southern pines: A guidebook. Asheville, North Carolina: USDA Forest Service, Southeastern Forest Experiment Station; 1977.
11. Karrfalt RP. Seed orchard seed evaluation testing (SOSET) and cone analysis service (CAS) at the Eastern Tree Seed Laboratory [Pinus]. Proceedings of the Fourteenth Southern Forest Tree Improvement Conference; 1977 Jun 14–16; Gainesville, Florida. Gainesville, Florida; 1977. p. 122–129.
12. Karrfalt RP, Belcher EW. Evaluation of seed production by cone analysis. Proceedings of the 24th Northeastern Forest Tree Improvement Conference; 1976 Jul 26–29; Maryland. University of Maryland; 1976. p. 84.
13. PrietoR JA, López UJ. Colecta de semillas forestales en el género Pinus (Spanish) [Collection of forest seeds in the genus Pinus]. Folleto Técnico 2006; 28: 13–20.
14. Pennington TD, Sarukhán J. Árboles tropicales de México: manual para la identificación de las principales especies (Spanish) [Tropical trees of Mexico: Manual for the identification of the main species]. Universidad Nacional Autónoma de México (UNAM); 2005. p. 521.
15. Cintron BB. *Cedrela odorata* L. In: Francis JK, Lowe CA (editors). Bioecología de arboles nativos y exóticos de Puerto Rico y las Indias Occidentales. Rios Piedras, Puerto Rico: USDA Forest Service; 2000. p. 128–134.
16. COMISIÓN NACIONAL FORESTAL. 2012 Precios de productos forestales maderables (Spanish) [Prices of timber forest products]. Available from: http://www.mexicoforestal.gob.mx/files/120417%20sipre%20precios%20madera%20negros.pdf.
17. Cruz VG. Estudio de variación de dos pruebas de procedencias/progenie de *Cedrela odorata* L. (cedro rojo) en La Balsa, municipio de Emiliano Zapata, Veracruz (Spanish) [Variation study of two provenance/progeny tests of *Cedrela odorata* L. (red cedar) in La Balsa, municipality of Emiliano Zapata, Veracruz]. Xalapa, Veracruz, México: Universidad Veracruzana; 2009. p. 55.
18. Rodríguez RG, Márquez RJ, Rebolledo CV. Determinación del potencial y eficiencia de producción de semillas de *Cedrela odorata* L. y su relación con caracteres morfométricos del fruto (Spanish) [Determination of the potential and efficiency of seed production of *Cedrela odorata* L. and its relationship with morphometric characters of the fruit]. Foresta Veracruzana 2001; 3(1): 23–26.
19. Statsoft Inc. Electronic statistics textbook. Tulsa, Oklahoma: StatSoft; 2013. Available from: WEB: http://www.statsoft.com/textbook/.
20. Rodríguez RG. Estudios de variación en frutos y semillas de *Cedrela odorata* L. de tres procedencias del estado de Veracruz, México (Spanish) [Studies of variation in fruits and seeds of *Cedrela odorata* L. from three provenances in the state of Veracruz, Mexico] [MSc thesis]. Xalapa, Veracruz, Mexico: Universidad Veracruzana, Instituto de Genética Forestal; 2007. p. 65.
21. Alderete A. Variación de frutos, semillas y plántulas de *Cedrela odorata* L. de Campeche y Tabasco y establecimiento de una prueba de progenie (Spanish)

[Variation in fruits, seeds and seedlings of *Cedrela odorata* L. from Campeche and Tabasco and establishment of a progeny test] [MSc thesis]. Xalapa: Instituto de Genética Forestal; 2004. p. 60.
22. Niembro RA. Estudios sobre la producción de semillas, germinación y crecimiento inicial de la caoba *Swietenia macrophylla* King (Spanish) [Studies on seed production, germination and early growth of mahogany *Swietenia macrophylla* King]. Sager. Inifap, Campeche, México: Centro de Investigación Regional del Sureste, Campo Experimental Chiná, División Forestal Campeche; 1998. p. 125.
23. de la Cruz Landero N, Hernández LCM. Variación en frutos de *Swietennia macrophylla* King y determinación de su potencial y eficiencia de producción de semillas en el Estado de Campeche, México (Spanish) [Variation in fruits of *Swietennia macrophylla* King and determination of its potential and efficiency of seed production in the State of Campeche, Mexico]. Foresta Veracruzana 2004; 6(1): 1–5
24. Chávez ÁA, Ramírez JM. Variación en frutos de *Cedrela odorata* L. y determinación de su potencial y eficiencia de producción de semillas en el Estado Campeche, México (Spanish) [Variation in fruits of *Cedrela odorata* L. and determination of its potential and efficiency of seed production in the State of Campeche, Mexico]. Foresta Veracruzana 2004; 6(1): 5–8.
25. Mendizábal-Hernández LC, Ramírez JM, Alba-Landa J, *et al.* Potencial y eficiencia de producción de semillas de *Cedrela odorata* L (Spanish) [Potential and efficiency of seed production of *Cedrela odorata* L.]. Foresta Veracruzana 2012; 14(2): 31–36.
26. Viveros CC, Márquez RJ, Ocampo V. Variación de frutos y semillas de *Guazuma ulmifolia* Lambert en una población costera del centro de Veracruz, México (Spanish) [Variation of fruits and seeds of *Guazuma ulmifolia* Lambert in a coastal population of central Veracruz, Mexico]. Foresta Veracruzana 2000; 2(2): 21–28.

EnPress Publisher, LLC

Add: 9650 Telstar Avenue, Unit A, Suit 121, El Monte, CA 91731

Tel: +1 (949) 299 0192

Email: contact@enpress-publisher.com

Web: https://enpress-publisher.com